Investigating cestode modulation of host neuronal excitability and cell-type-specific gene expression in an *ex vivo* mouse model of neurocysticercosis

by

Teresa Steyn

Submitted in fulfilment of the requirements of
MSc(Med) degree with specialisation in Neuroscience (Physiology)

Supervisors: Dr Joseph Raimondo and Dr Rachael Dangarembizi

Faculty of Health Sciences
Division of Cell Biology
Department of Human Biology
University of Cape Town

THE OPPENHEIMER MEMORIAL TRUST
National Research Foundation
UNIVERSITY OF CAPE TOWN
IYUNIVESITHI YASEKAPA • UNIVERSITEIT VAN KAAPSTAD

Plagiarism Declaration

I, Teresa Steyn, confirm that the work described in this thesis is my own (except where it has been acknowledged otherwise) and that neither the whole work nor any part of it has been, is being, or will be submitted for another degree at this or any other educational institution.

I empower the university to reproduce, for the purpose of research, the whole work or any part thereof.

Signature: Signed by candidate

Date: 18 May 2023

Abstract

Neurocysticercosis (NCC), caused by *Taenia solium* larvae, is the leading helminthic brain infection in humans, with epilepsy as its most common manifestation. Interestingly, seizures are rare during early stages when viable larvae are thought to suppress host inflammation. Seizures tend to occur when larvae die and immune suppression ceases, which has led to the hypothesis that the host's immune response contributes to seizures in NCC. Further research is required to better understand the effects that immune activation and *Taenia* larvae have in the brain. In this thesis, I exposed mouse hippocampal organotypic brain slice cultures (OBSCs) to lipopolysaccharide (LPS) and a *Taenia crassiceps* homogenate and used single-nucleus RNA sequencing and whole-cell patch-clamp electrophysiology to investigate potential links between inflammation and network excitability at a transcriptomic and electrophysiological level. In the first part of the thesis, I found that while LPS significantly affected cell-type specific gene expression associated with inflammatory pathways, it had little impact on genes modulating neuronal excitability. This was corroborated by whole-cell patch-clamp data demonstrating no LPS-induced changes in the intrinsic electrical properties of pyramidal neurons.

In the second part of the thesis, I exposed mouse hippocampal OBSCs to a *T. crassiceps* homogenate alone or in combination with LPS to evaluate its immunomodulatory activity. The *T. crassiceps* homogenate blocked the induction of pro-inflammatory transcriptional activity across different cell types when added to LPS. This suggested that it likely acts up-stream of the toll-like receptor 4 proinflammatory cascade. The homogenate had minimal influence on the expression of neuronal excitability genes, and whole-cell patch-clamp experiments confirmed no significant differences in pyramidal neuron electrical properties among the treatment groups. My data indicate that both LPS and a homogenate made from viable *Taenia* larvae drive cell-type-specific immunomodulatory changes but have limited effects on basic neuronal excitability, at least over a relatively short period of exposure and in the absence of an adaptive immune response. My findings are relevant for understanding how *Taenia* larvae and inflammatory responses relate to the emergence of seizures in NCC.

Acknowledgements

Thank you firstly to Joe (Joseph Raimondo) for the most incredible opportunity you have given me to do a master's under your supervision. I have learnt so much over the course of this project and felt a jump in my understanding in terms of ways to approach science and think critically about things. Thank you for all the things you have taught me, and the time and attention you have invested to help me collect, analyse, and interpret the snRNAseq, whole-cell patch-clamp, and HCR data. You have also created such a supportive environment where I feel encouraged and inspired to work hard and discover new things while also living a balanced life. It has been amazing being part of a lab with such a culture of fun, care, and a feeling that we are all in this together. There are not enough words to thank you for this time.

I would also like to thank Rachael Dangarembizi and Dorit Hockman for all the direct and indirect input you both have given towards this project. It has been so great to bounce ideas off you both and just have a chat now and then which has really helped me to get new ideas for the project as well as gain more perspective about a career as a neuroscientist.

Additionally, I would like to give a huge thank you to Josh, Rachael, Amalia, Anja, and Emily for your massive contributions towards generating the snRNAseq datasets. It was truly a team effort and could not have been done without all of your help. Many thanks as well to Andrew Lewis and UCT's high-performance computing team! This project would not have been possible without your world-class assistance and facilities. Thank you as well to Ruvi for all your time and help showing me how to do the HCRs. You were so patient and such a good teacher, and it was wonderful getting to hang out together during that time.

Thank you Anja for the many hours of time you dedicated to helping me plan and carry out various organo and ELISA experiments, and for being so supportive when things were difficult. I have cherished all our conversations about science, life, mental health, and ethics, and I have learnt so much from you about doing good science (such as keeping a thorough record of what I have done!)

To Christy, I can't thank you enough for the all the time, advice, and investment you have put into showing me the ropes with the snRNAseq analysis, helping to troubleshoot and solve coding errors when I was really struggling, and spending hours sharing ideas and discussing various aspects of the project. I am constantly blown away by your knowledge and skills and feel most fortunate to have you as my partner in crime.

To everyone in the Raimondo lab thank you for helping me with various aspects of this project and teaching me so much during my time in the lab. We have had some moments of shock, panic, frustration, and disappointment together but also some of the best laughs, conversations, and shared excitement that hopefully made the challenges all worthwhile. A shout out to Hayley and Sasha as well for all the help teaching me new techniques at the start of the master's and to Maahir and Emily for all the collaboration on various shared projects.

To Mom, Dad, Em, Liam, Dan, Christy, and my wonderful friends and family, thank you for all of the support, encouragement, patience, kindness, and love you have shown me. A two-year master's can be quite the undertaking, and I have gained so much energy, motivation, and perspective from all of you. Thank you.

Contents

List of Figures

Chapter 1

Chapter 3

Chapter 4

Supplementary data

Supplementary 1
Summary of snRNAseq sample metadata

Supplementary 2
2.1 FindAllMarkers output
2.2 User-defined SCSA reference databases curated from Mousebrain.org
2.3 SCSA output for different reference databases

Supplementary 3
HCR RNA-FISH - negative probe and negative hairpin slices

Supplementary 4
ELISA raw data and statistical analyses

Supplementary 5 snRNAseq data processing
5.1 Summary of nuclei counts across filtering steps
Number of nuclei filtered and remaining per sample for each of the filtering steps
Total nuclei filtered and remaining per sample across all filtering steps
Total nuclei filtered and remaining for all samples across all filtering steps

5.2 QC threshold processing steps
5.2.1 QC threshold graphs before filtering
Cell complexity (genes per UMI)
Distribution of the number of genes in each sample
Distribution of the number of UMIs in each sample
Genes vs UMIs per sample
Mito-ratio distribution in each sample
Number of nuclei per sample

5.2.2 QC threshold graphs after filtering
Cell complexity (genes per UMI)
Distribution of the number of genes in each sample
Distribution of the number of UMIs in each sample
Genes vs UMIs per sample
Mito-ratio distribution in each sample
Number of nuclei per sample

5.3 Summary of doublet processing.
Number of doublets identified by each tool for each sample
Table summary of doublets called by each tool per sample

Supplementary 6 PCA plots averaged per sample
PCA_plot_batch
PCA_plot_groupid
PCA_plot_sampleid
PCA_plot_cell_cycle_phase

Supplementary 7
UMAP of numbered clusters at res 0.4

Supplementary 8
Percentage of nuclei per cluster per treatment group
Summary number of nuclei per cluster per treatment group
Summary percentage of nuclei per cluster per treatment group

Supplementary 9
DE analysis results for LPS vs Ctrl - sig DEGs per cluster coarse

Supplementary 10
LPS vs control all downregulated DEGs EnrichR results
LPS vs control all upregulated DEGs EnrichR results

Supplementary 11
Expression of LPS receptors and binding proteins
Expression of Substance P receptor and precursor

Supplementary 12
LPS vs control individual cell type downregulated DEGs EnrichR results
LPS vs control individual cell type upregulated DEGs EnrichR results

Supplementary 13
Excitability_genes_and_description
Excitability genes_EnrichR results txt
Excitability genes_EnrichR results csv

Supplementary 14
DE results for LPS vs control excitability DEGs coarse neuronal clusters
LPS vs control EnrichR results 5 excitability DEGs

Supplementary 15
DE analysis results for Hom vs Ctrl - sig DEGs per cluster nuanced

Supplementary 16
Hom vs control all downregulated DEGs EnrichR results
Hom vs control all upregulated DEGs EnrichR results

Supplementary 17
DE analysis results for Hom vs Ctrl – sig DEGs per cluster coarse

Supplementary 18
DE analysis results for LPS+Hom vs LPS- sig DEGs per cluster coarse

Supplementary 19
LPSplusHom vs LPS all downregulated DEGs EnrichR results
LPSplusHom vs LPS all upregulated DEGs EnrichR results

Supplementary 20
DE analysis results for LPS+Hom vs control - sig DEGs per cluster coarse

Supplementary 21
LPSplusHom vs control all downregulated DEGs EnrichR results
LPSplusHom vs control all upregulated DEGs EnrichR results

Supplementary 22
LPSplusHom vs LPS individual cell type downregulated DEGs EnrichR results
LPSplusHom vs LPS individual cell type upregulated DEGs EnrichR results

Supplementary 23
DE results for LPSplusHom vs LPS excitability DEGs coarse neuronal clusters
LPSplusHom vs LPS downregulated EnrichR results 9 excitability DEGs
LPSplusHom vs LPS upregulated EnrichR results 9 excitability DEGs

Supplementary 24
DE results for LPSplusHom vs control excitability DEGs coarse neuronal clusters

Supplementary 25
Whole-cell patch-clamp raw data and statistical analyses

List of Abbreviations

Symbol	Description
ACh	Acetylcholine
AChE	Acetylcholinesterase
aCSF	Artificial cerebro-spinal fluid
ANOVA	Analysis of variance
AMPA	α-Amino-3-hydroxy-5-methyl-4-isoxazolepropionic acid
APs	Action potentials
BBB	Blood-brain barrier
Ca^{2+}	Calcium
Cl^-	Chloride
CNS	Central nervous sytem
COX-2	Cyclooxygenase-2
CO_2	Carbon dioxide
Ctrl	Control
DE	Differential expression
DEGs	Differentially expressed genes
ELISAs	Enzyme-linked immunosorbent assays
EPSCs	Excitatory post-synaptic currents
eEPSCs	Evoked excitatory post-synaptic currents
eIPSCs	Evoked inhibitory post-synaptic currents
GABA	γ-aminobutyric acid
HCR	Hybridisation Chain Reaction
Hom	Homogenate
IL-1	Interleukin-1
IL-1β	Interleukin-1β
IL-4	Interleukin-4
IL-6	Interleukin-6
IL-10	Interleukin-10
IL-18	Interleukin-18
IPSCs	Inhibitory post-synaptic currents
IQR	Interquartile range
K^+	Potassium
Lamp5	Lysosomal Associated Membrane Protein Family Member 5
LPS	Lipopolysaccharide
Mg^{2+}	Magnesium
Na^+	Sodium
NCC	Neurocysticercosis
NMDA	N-methyl-D-aspartate

OBSCs	Organotypic brain slice cultures
OPCs	Oligodendrocyte Precursor Cells
O_2	Oxygen
PBS	Phosphate buffered saline
PCA	Principal Component Analysis
PFA	Paraformaldehyde
Pvalb	Parvalbumin
RNA-FISH	RNA-Fluorescence In Situ Hybridisation
RNAseq	RNA sequencing
SEM	Standard error of the mean
scRNAseq	Single-cell RNAseq
Sncg	Synuclein-Gamma
snRNAseq	Single-nucleus RNAseq
Sst	Somatostatin
T. crassiceps.	*Taenia crassiceps*
T. solium	*Taenia solium*
TNF-α	Tumor necrosis factor-α
TLR4	Toll-like receptor 4
UMAP	Uniform Manifold Approximation and Projection
VLMCs	Vascular leptomeningeal cells
Vip	Vasoactive intestinal polypeptide
4-AP	4-aminopyridine

CHAPTER 1

Introduction

1.1 A background on neurocysticercosis

Neurocysticercosis (NCC) is the leading helminthic central nervous system (CNS) infection in humans and is caused by larvae of the pork tapeworm, *Taenia solium* (*T. solium*)[1,2]. In endemic countries such as South Africa, NCC is a major cause of acquired neurological disability and accounts for up to 30% of all recorded epilepsy cases[3,4]. Seizures and epilepsy are the most common and severe clinical manifestation of the disease, followed by elevated intracranial pressure, cognitive decline, headaches, hydrocephalus, and meningitis[1,2,5].

NCC is most prevalent in low- and middle-income countries but is steadily becoming more common in other parts of the world due to increasing migration to and from endemic countries[6]. The World Health Organisation (WHO) estimates that between 2.56 and 8.3 million people worldwide have either symptomatic or non-symptomatic NCC each year[7]. Furthermore, approximately 70 – 90% of symptomatic NCC patients will experience seizures[5,8]. This represents a serious global concern for several reasons. Firstly, NCC is associated with debilitating impacts on a patient's health and is estimated to result in approximately 50000 deaths annually[7,9]. Furthermore, the impact on health and quality of life is considerable for patients with epilepsy who are at an increased risk of injury, hospitalisation, and mortality as well as anxiety, depression, and cognitive impairment[10]. Unfortunately, in many parts of the world patients with seizures are also subject to heavy discrimination and stigmatisation[11]. Aside from its impact on health and quality of life, NCC places a heavy burden on the economic and medical resources of endemic countries, owing to the costs of drugs and other medical resources used to treat the disease, as well as lost human work hours[12,13]. It is evident that this disease warrants attention, and that both prevention and treatment strategies are necessary to alleviate the severe burden that NCC places on patients, families, and economies. Moreover, as an important cause of epilepsy, NCC may constitute a valuable disease system for investigating the pathophysiology of seizures more generally.

1.1.1 The life cycle of *Taenia solium*

Humans first become infected with *T. solium* after ingestion of the cestode larvae in contaminated pork meat[8,14] (Figure 1). After being ingested, *T. solium* larvae mature into adult tapeworms within the intestines of the definitive human host. Adult tapeworms then release segments of their body known as proglottids which contain the eggs of the cestode and are passed out in human faeces. Importantly, neither the adult tapeworms nor the eggs they

produce at this stage of the lifecycle can enter the bloodstream and cause cysticercosis, likely because of an absence of gastric elements required for their activation[8,15]. Cysticercosis occurs when humans become intermediate hosts of the parasite. This results from the accidental ingestion of *T. solium* eggs contained in small amounts of human faecal matter on hands, surfaces, food, or water usually by members of the same household or from autoinfection[16,17]. Humans are considered 'accidental' intermediate hosts to *T. solium* because the cestode can complete its life cycle without infecting human hosts intermediately. Once ingested, *T. solium* eggs become activated by gastric salts and produce enzymes that enable them to invade the intestinal wall[17]. The activated oncospheres enter the bloodstream and migrate to different tissues but tend to lodge preferentially in the brain[8,14]. Once in the brain, oncospheres enlarge over a period of weeks to months and develop into cysts.

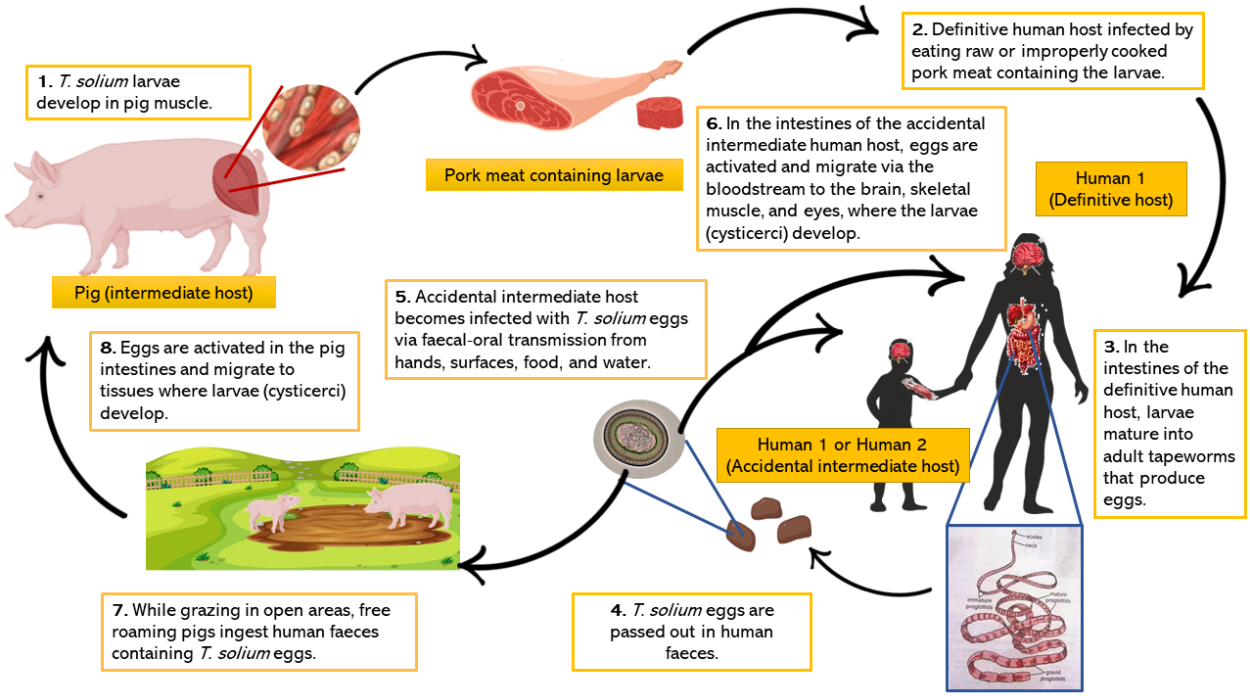

Figure 1. The life cycle of *Taenia solium* (Taken from Steyn *et al*. 2022[18])

1.1.2 Stages of neurocysticercosis and their association with seizures

A hallmark of NCC is its heterogeneity in disease severity and clinical presentation which are correlated with the location and number of cysts as well as the stage of cysts and associated changes in the host's inflammatory response[2,8,19,20]. There are four main stages of parenchymal *T. solium* cysts that have been characterised according to their viability as well as distinct clinical, molecular, and immune changes to the cyst and surrounding tissue[8].

The first stage is referred to as the vesicular stage and involves the presence of one or more viable cysts in the brain. These viable cysts are believed to be adapted to survive in the CNS by suppressing the host immune response and evading immune detection by masking themselves with a variety of host molecules on their surface[8,21–23]. Interestingly, the vesicular stage is associated with very few clinical symptoms including few or no seizures, and as a result, patients with NCC often live for years without showing any signs of the disease[14,24–26].

Over time, cysts eventually begin to degenerate and lose their ability to suppress the host immune response. This shift from a viable cyst state to a degenerating state is classified as the transitional stage. The transitional stage comprises the colloidal and granular-nodular phases and is generally accompanied with an invasion of the cyst wall and fluid by inflammatory cells and molecules, followed by the cyst cavity collapsing and starting to become fibrotic[8,14]. The main characteristics of the transitional stage, namely, the degeneration of cysts and accompanying host immune activation, appear to go hand in hand, and might be understood as follows: 1) over time, cysts either start to degenerate on their own accord or the host's immune response gradually results in the deterioration of the cyst; 2) as cysts degenerate, they lose their ability to suppress the host immune response, allowing for increased invasion of the cyst by inflammatory cells and molecules; 3) the increased host inflammatory response around the cyst leads to further collapse and degeneration of the cyst; 4) further degeneration of the cyst is associated with the release of damage-associated antigens which exacerbate inflammation around the cyst.

Following the transitional stage, cysts progress to the final inactive or calcified stage in which the entire cyst is completely replaced by fibrosis and becomes calcified[14,27,28]. Reportedly, a higher proportion of NCC patients with inactive lesions have seizures/epilepsy (>88%) compared to patients with active/viable lesions (60–63%)[5]. Furthermore, vesicular stage cysts are more prevalent in asymptomatic NCC patients than in symptomatic patients[24,25] and asymptomatic patients tend to have higher serum levels of anti-inflammatory cytokines while symptomatic patients have been found to have higher serum levels of pro-inflammatory cytokines[29,30]. These findings have led to the hypothesis that the host immune and inflammatory response may play an important role in eliciting seizures in patients with parenchymal NCC[4,8,31]. This hypothesis is corroborated by several clinical studies that have provided support for an involvement of neuroinflammation in the pathology of NCC[24,25,29,30,32,33].

Some mechanisms have been proposed for how inflammation can contribute to seizures in NCC. As cysts start to degenerate, they provoke a Th1 inflammatory response which involves

the release of pro-inflammatory cytokines and increased expression of adhesion molecules such as ICAM-1 in peripheral leukocytes and in endothelial cells making up the blood-brain barrier (BBB)[30]. Upregulation of pro-inflammatory cytokines and adhesion molecules can influence BBB permeability[34]. There is evidence for disruption of the BBB around larval cysts in both mouse and pig models of NCC[35,36], as well as increased serum levels of matrix metalloproteinases in symptomatic NCC patients compared to asymptomatic patients which is correlated with BBB breakdown[37]. Increased BBB leakage can increase vascular permeability to serum albumin which has previously been shown to facilitate epileptiform activity by compromising ion buffering and the glutamate reuptake capacity of astrocytes and enhancing excitatory synaptogenesis[38–40]. Of note, the NCC study in pigs demonstrated that treatment with the anti-parasitic drug praziquantel significantly increases BBB leakage around cystic lesions compared to brains from pigs that had not been treated with praziquantel[36], providing a possible mechanism by which treatment with cysticidal therapies could increase the risk of seizure occurrence initially. In addition to BBB leakage, there is some evidence that certain genetic polymorphisms of inflammatory genes such as Toll-like receptor 4 (TLR4) may confer greater risk of developing epilepsy in NCC patients[33], and this is hypothesised to be linked to TLR4's mediation of the Th1/Th2 axis.

Notably, calcified stage seizures are associated with increased inflammation, gliosis, and perilesional oedema around the calcified cysts[41]. Gliosis is a reactive change of glial cells following some form of damage to the CNS and involves glial hypertrophy and proliferation[42,43], while perilesional oedema refers to fluid retention in the intracellular or extracellular space surrounding a lesion[44]. In NCC, both gliosis and perilesional oedema are thought to reflect inflammatory reactions to calcified granulomas and have been strongly correlated with seizures and seizure recurrence[41,45]. However, it remains unclear whether oedema and gliosis are causes or consequences of seizures, or whether these processes tend to coincide with seizures due to the same underlying pathophysiology[46]. Understandings of causal relationships between these pathologies and seizures can potentially be gained from looking at other conditions in which they co-occur such as in traumatic brain injury and models of temporal lobe epilepsy[47–50]. For example, seizures have been shown to preferentially stimulate proliferation of radial glia-like astrocytes[51] and likewise, microglia-macrophage cells proliferate following exposure to status-inducing chemoconvulsants[52]. While this suggests that gliosis may occur secondary to seizures, it is also theorised that chronic astrogliosis and microgliosis can promote network hyperexcitability by compromising K^+ and glutamate buffering as well as neuronal survival, and thereby facilitating epileptogenesis[38,48,53,54]. Additionally, kainic acid induced seizures have been found to be accompanied by astroglial swelling and oedema and

it has been suggested that this oedema is elicited by the ionic imbalance following continual neuronal excitation[49].

1.1.3 Other theories about the cause of seizures in neurocysticercosis

While there is evidence in support of an association between the inflammatory stages of NCC and the presence of seizures, it is worth considering that seizures have also been reported to occur, albeit less commonly, during the vesicular stages of the disease when the immune response is generally suppressed[28]. Furthermore, patients with non-inflamed cysts or non-inflamed calcified scars can also present with seizures[28]. While this would imply that the host's inflammatory response alone cannot account for all seizures in the disease, some researchers have maintained that these seizures are still the result of episodic increases in the host inflammatory response that are not easily detectable[8]. In contrast, others have argued that there must be another explanation for at least a subgroup of seizures that are not associated with inflammation in NCC. One hypothesis is that the larval cysts and/or their associated granulomas may release molecules into the surrounding brain tissue which alter neuronal network excitability[28]. Some evidence for this has come from experimental work showing that intracranial injection of early-stage granuloma extracts from dead or dying *Taenia crassiceps* (*T. crassiceps*) cysticerci of WT mice induces seizures in mice and rats[55–57], and that the severity of seizures was correlated with the levels of Substance P contained in the granulomas [57,58]. Moreover, granulomas from mice that were deficient in the Substance P precursor did not contain Substance P and did not trigger epileptogenic activity[57]. Finally, seizures only occurred in response to the intrahippocampal injection of the granuloma extracts in mice that had receptors for Substance P, whereas mice that were deficient for the Substance P receptor did not have seizures in response to cysticercosis granuloma extracts[57]. Together, this work provides support for Substance P being a contributor to seizure activity in NCC. Moreover, immunohistochemical analysis of brain tissue specimens from patients with NCC found Substance P to be expressed in cells adjacent to remnants of dying cysts but not in regions distant from larval cysts nor in brain tissue from patients without NCC[57]. It is worth noting that Substance P has both immune- and neuro-modulatory properties[59], and it possible that its mechanism of action in eliciting epileptiform activity is via the regulation of inflammatory pathways. In addition to the research on Substance P, work by de Lange et al. showed that larval extracts from both *T. solium* and *T. crassiceps* have substantial Acetylcholine Esterase (AChE) activity. Moreover, AChEs derived from heat-activated secretory/excretory extracts of *Taenia* larvae were able to breakdown acetylcholine (ACh) at a concentration that is sufficient to induce changes in neuronal signalling[60]. While this did not result in seizure activity, it does

provide an example of how products released directly by *Taenia* larvae could potentially modulate neurotransmission.

Calcifications have also been associated with hippocampal sclerosis[61,62] which is a known contributor to medically intractable temporal lobe epilepsy and is thought to arise from structural and network changes due to neuron loss and gliosis[63]. This provides another possible mechanism for epileptogenesis in NCC. A different hypothesis for how seizures arise in NCC is that the high levels of calcium associated with calcified lesions is neurotoxic which may facilitate seizure activity due to high levels of glutamate released by damaged or dying neurons[61]. Studies in which lesions associated with calcified cysts are surgically removed have found that most patients who received a lesionectomy for calcified cysts had favourable outcomes and became seizure-free[64,65]. However, these studies had very small sample sizes, lacked control groups, and had large variability in clinical presentation of the patients undergoing these surgeries as well as variability in surgery procedures[66]. This leaves it unclear whether it was the removal of the calcified lesions or other factors responsible for seizure remediation in these patients. In most cases of intraparenchymal NCC, surgeries for the removal of cysts are not indicated as it is argued that risks of surgery outweigh the potential benefits for which there is not yet definite evidence[67–69].

A slightly more provocative theory of NCC-associated seizures is that their pathophysiology may be comparable to seizures in patients with cancerous brain gliomas. Both *T. solium* larval cysts and gliomas are space-occupying lesions requiring a blood supply to grow and survive in the brain[70]. Gliomas tend to develop a close association with brain vasculature leading to a breakdown of the BBB[70]. They have also been shown to release high levels of glutamate into the surrounding tissue which serves both as a growth factor as well as a neural excitotoxin to make space for the tumour's growth[70]. High levels of extracellular glutamate around gliomas have been shown to result in neuronal hyperexcitability in cortical networks, leading to epileptiform activity[70]. Based on certain similarities between the characteristics of gliomas and *T. solium* larval cysts, it is intriguing to hypothesise that similar seizure mechanisms could be at play in these two conditions[18].

Notably, some have argued that a distinction should be made between transitional stage seizures and viable stage seizures or seizures that occur when there are only remnants of a calcified scar remaining[2,71]. This has been proposed because transitional stage seizures appear to better reflect acute symptomatic seizures secondary to an inflammatory response, whereas seizures occurring during non-inflammatory stages are understood to represent "true" epileptogenic seizures that arise from epileptogenic foci in the brain. It follows from this

that seizures occurring outside of the inflammatory stages may require chronic anti-epileptic drug treatment to manage as these are seizures that would have become self-generating.

Further research is required to delineate the exact molecular and cellular pathways implicated in the occurrence of seizures in NCC. What does seem clear, however, is that there is an increased risk for seizures during the pro-inflammatory stages of the disease, and a reduced risk for seizures during the early stages of the disease when the host inflammatory response is often suppressed. This association between inflammatory changes and the presence or absence of seizures will be discussed further in section 1.2.

1.1.4 Current treatments for neurocysticercosis

Current treatments for NCC usually focus on targeting viable tapeworm larvae with two cysticidal drugs, albendazole and praziquantel[28,67,72–75], as well as treating seizures with antiepileptic drugs (AEDs)[2,71,76]. There is evidence that cysticidal regimens and AEDs can improve patient prognosis by resolving larval cysts and reducing the risk of seizure recurrence in the long term[68,71,74,76–80]. However, there are some important limitations of these drugs. Firstly, cysticidal drug regimens are often accompanied with an increase in perilesional oedema, brain swelling, raised intracranial pressure, and seizures[1,41,67,74,81]. These common side-effects are believed to follow from an increase in inflammation in the brain as the larval cysts beginning to degenerate, thereby losing their immunosuppressive function and releasing antigens which stimulate a local inflammatory response[1,41,67]. While this increase in acute provoked seizures and other symptoms is a contraindication of anti-helminthic therapy, these drugs are still prescribed in most cases to treat NCC, given their ability to resolve viable cysts and reduce the risk of seizure relapses in the long term[68,71]. Furthermore, corticosteroids and AEDs are generally prescribed in conjunction with the cysticidal drugs, and have been shown to reduce neuroinflammation, raised intracranial pressure, and seizures associated with the cysticidal drugs[1,67,80,82,83]. However, AEDs are often accompanied with harsh side-effects on general health and cognitive function[84], and so it is recommended that they are eventually withdrawn in patients who meet the following conditions 1) few seizures prior to antiparasitic therapy, 2) resolved cystic lesions, and 3) have had no seizures for 24 consecutive months[68]. An important consideration is that approximately half of all NCC patients will continue to experience seizure relapses despite receiving these treatments[71,85,86]. This is an important finding as it suggests that a considerable subgroup of symptomatic NCC patients have treatment-resistant epilepsy.

Based on the abovementioned treatment limitations, there is reason to identify more effective and specific therapeutic targets for treating and preventing seizures in patients with NCC.

Thus far, the burden of disease falls largely within developing countries and, as a result, limited resources have been dedicated to investigating how cestode infection of the brain results in the development of epilepsy. Moreover, owing to its significant inflammatory component, NCC represents a compelling model for investigating the relationship between inflammation and seizures more generally, and to deepen our understanding of the cellular, molecular, and electrophysiological changes that occur in the brain in response to both cestode infections as well as inflammatory challenges.

1.2 Epilepsy and what we know so far about the relationship between inflammation and seizures.

Epilepsy is a brain disorder characterised by recurrent seizures and associated emotional and cognitive dysfunction. It is estimated that up to 50 million people worldwide have this disorder[87], making it one of the most common neurological conditions. While there are numerous AEDs available, more than half of patients with epilepsy who receive one of these medications will still suffer one or more seizures a year after beginning the AED[88]. Extensive research has been dedicated towards investigating the mechanisms underlying this severe and complex condition. A large body of clinical and experimental evidence has emerged which supports a link between inflammation and seizures (for comprehensive reviews on the topic see[89–91]). This section will serve to summarise the main findings regarding the relationship between inflammation and seizures and discuss some important gaps that remain to be addressed in the literature.

1.2.1 Clinical evidence for an association between inflammation and seizures

The first inferences about a possible contribution of inflammation towards seizures came from studies showing that steroids and other anti-inflammatory drugs appeared to reduce seizure likelihood in patients with certain epilepsies that were resistant to conventional AEDs[92–94]. Further evidence for an association between inflammation and epilepsy emerged from studies in patients with autoimmune conditions who were at an increased risk for seizures as well as the finding that patients with seizure disorders often showed increased immune activation[95–98]. Additionally, several studies have demonstrated that resected hippocampi from patients with temporal lobe epilepsy tends to have higher levels of proinflammatory molecules, reactive astrocytosis, activated microglia, and other inflammatory biomarkers that are not present in brain tissue obtained from healthy control patients[99–104].

1.2.2 Experimental evidence for a bi-directional causal relationship between inflammation and seizures

When exploring the relationship between inflammation and seizures, it is useful to understand what electrophysiological changes occur within neurons and neuronal networks which underly

seizure activity. The classical understanding of a seizure is brain activity characterised by an imbalance between neural excitation and inhibition which results in neuronal hyperexcitability and hypersynchronous firing[105]. Markedly, while a single neuron can be in a hyperexcitable state and fire rapidly and repeatedly, a seizure is innately a network event that involves almost all neurons in a particular brain area or region firing concurrently (i.e., hypersynchronous firing)[105].

Some of the major ways that the balance between neural excitation and inhibition becomes disrupted to result in neuronal hyperexcitability include 1) any physiological condition that increases glutamatergic synaptic activity (e.g., seizure-induced sprouting or increased connectivity between excitatory pyramidal neurons); 2) increased ion currents mediating membrane depolarization (e.g., inward Na+ or Ca2+ flux); 3) any conditions that decrease the effect of gamma-aminobutyric acid (GABA)-ergic inhibitory synaptic activity; 4) any conditions that increase GABA-ergic depolarising activity (e.g., changes to the GABAa receptor reversal potential due to Cl- loading); and 5) decreased ion currents mediating membrane hyperpolarization (e.g., decreased outward K+ or decreased inward Cl- flux)[105,106]. Seizures also require excess energy to sustain themselves, and as a result metabolic activity has also been identified as playing a key role in hyperexcitability of neurons and seizures[107]. Additionally, there is a large body of clinical and experimental data providing support for a bi-directional relationship between inflammation and seizures. This will be outlined below.

Seizures as a cause of inflammation

While clinical studies have pointed to important associations between inflammation and epilepsy, experimental research has taken this further to suggest that inflammation may be both a consequence and a cause of epilepsy. *In vivo* studies in adult rats and mice have demonstrated that an increase in inflammatory mediators occurs following the induction of recurrent seizures or single prolonged seizures (i.e., status epilepticus) with the use of convulsant agents or electrical stimulation[101,108–113]. The increase in inflammation appears to occur irrespective of the method used to induce seizures[114], supporting the idea that seizure activity *itself* contributes to neuroinflammation[108,110,111,115–126]

Epileptogenicity can be understood as the sets of changes that underly the onset and persistence of spontaneous seizures after an initial precipitating event[127]. The induction of status epilepticus is one example of an event that can initiate epileptogenesis[127]. Interestingly, studies in rodent brains have demonstrated that the induction of status epilepticus is followed by waves of inflammation that occur over a period of days to weeks, coinciding with the epileptogenic process[114]. These prolonged inflammatory changes begin with the release of pro-inflammatory cytokines from microglia, astrocytes, and neurons, followed by the

upregulation of cytokine receptors, cyclooxygenase-2 (COX-2), prostaglandins, and components of the complement system in microglia, astrocytes, and neurons (See Vezzani et al.[114] and references therein). Additionally, inflammatory cytokines, chemokines and their receptors tend to be upregulated in neurons and activated astrocytes following a seizure[128,129], and this is thought to attract peripheral immune cells including leukocytes and lymphocytes into the brain[121]. Studies in the *ex vivo* isolated guinea pig brain have also demonstrated that seizures induce glial activation, vascular inflammation and accompanying damage to the blood-brain barrier which was dependent on IL-1β and interleukin 1 receptor type I[125,130,131]. Importantly, these seizure-induced inflammatory changes occur independently of peripheral leukocytes or inflammatory molecules. Taken together, these findings show that brain inflammation occurs acutely following the induction of a seizure and appears to develop over time in conjunction with the epileptogenic process.

Inflammation as a cause of seizures

As discussed above, numerous studies have demonstrated that the induction of seizures using electrical stimulation or proconvulsant agents such as kainic acid, pilocarpine, or bicuculine results in downstream inflammatory cascades. Likewise, there are several lines of evidence that inflammation can in turn elicit and exacerbate seizure activity[128,132]. Notably, numerous papers have shown that blocking inflammatory molecules and their receptors following induced seizures can reduce the threshold for seizures as well as the incidence, frequency, and duration of seizures[108,110,111,115–126]. In addition, the blockade of various inflammatory pathways in rodent brains results in a reduction in the occurrence of spontaneous and kindled seizures in models of epileptogenesis[121,122,133,134]. These results suggest that seizure-induced inflammation can perpetuate and exacerbate seizures.

Likewise, the addition of an inflammatory stimulus prior to the induction of seizures has been shown to reduce the threshold for seizure activity[135–139]. One study modelled febrile seizures by injecting rats intraperitoneally with both Lipopolysaccharide (LPS) and a sub-convulsant dose of kainic acid[137]. LPS is a well-known bacterial endotoxin and proinflammatory mediator that is often used to model the effect of an inflammatory challenge[140]. The study found that animals that developed febrile convulsions following the exposure to LPS and kainic acid had higher levels of the pro-inflammatory cytokine IL-1beta (IL-1β) in the hypothalamus and hippocampus[137]. In addition, intracerebroventricular injections of IL-1β resulted in a dose-dependent increase in the proportion of animals that experienced febrile convulsions, whereas administration of the IL-1a receptor antagonist appeared to have an anticonvulsant effect, reducing the proportion of rats with febrile convulsions, and prolonging the time to onset of febrile seizures[137]. Another research group exposed postnatal day 14 rat pups to LPS and observed an increase in adult seizure susceptibility in response to different chemoconvulsants

in rats that had received early LPS exposure compared to controls that had not[123]. This increase in seizure susceptibility was defined by a faster time to first seizure or a significantly lower dose of the convulsant required to induce generalised clonus (i.e., reduced seizure threshold) compared to controls that received saline injections postnatally[123]. In addition, systemic exposure to LPS postnatally resulted in increased hippocampal excitability following electrical stimulation of Schaffer collaterals in the CA1 area as well as a higher frequency of spontaneous epileptiform discharges following bath application of 4-aminopyridine (4-AP) in adult rats[123]. Several similar studies have corroborated these findings by showing that systemic exposure to LPS during specific developmental stages in neonatal rats results in lasting changes in neuronal excitability associated with increases in stress-related gene expression changes[118,123,141–144], as well as an increase in the number and duration of kindled seizures[142]. Taken together, these studies demonstrate that inflammatory challenges contribute to the incidence and severity of acute seizures, as well as to the epileptogenic process itself which results in the generation of recurrent spontaneous seizures.

Thus far, the evidence reviewed has shown that inflammation can reduce the threshold for seizures, as well as contribute towards epileptogenesis. However, these studies involved experimental models of epilepsy in which seizures were facilitated using either electrical stimulation or chemoconvulsants. Therefore, one may ask to what extent the immune response can independently elicit seizures, without the addition of a proconvulsant stimulus. One research group sought to answer this question by exploring how a pro-inflammatory stimulus affects seizure activity without the addition of any other stimuli[145]. They reported that cortical injections of LPS in adult rats resulted in a marked increase in evoked field potential amplitudes over 5-10 mins as well as the production of focal epileptiform discharges although no generalised seizures were observed[145]. This effect was blocked by the addition of TLR4 or interleukin-1 (IL-1) receptor antagonists, indicating a capacity for the innate immune response to participate independently in increasing excitability and possibly seizures[145].

Experimental work in rats has also demonstrated a role for another major component of the innate immune system, known as the complement system, in seizure induction[146]. The main end-product of the complement pathway is known as the membrane attack complex which promotes inflammation and enhances the ability of antibodies and phagocytes to attack and clear pathogens and damaged cells[147]. Seizures were found to occur in rats shortly after the sequential hippocampal infusion of 5 major proteins required to form the membrane attack complex. Importantly, seizures only occurred after all 5 proteins were added in the correct order *in vivo*[146]. In contrast, when all five proteins were premixed *in vitro* and then infused into the hippocampus, there was no formation of the membrane attack complex and no seizures[146].

These studies indicate that specific components of the immune system can directly trigger seizures when activated.

In addition, a well-established model system of a viral infection leading to epilepsy is the Theiler's murine encephalomyelitis virus (TMEV) model in which intracerebral inoculation of mice with TMEV leads to spontaneous recurrent epileptic seizures in approximately 50% of affected mice[148,149]. Markedly, seizure occurrence in this model system has been found to be partially dependent on specific components of the innate immune response including Interleukin-6 (IL-6), tumor-necrosis factor receptor 1, and complement component 3[148,150].

In addition to this *in vivo* work, several electrophysiological *in vitro* and *ex vivo* studies have explored the effect of LPS on neuronal network excitability and seizure susceptibility. Two such papers were able to demonstrate an independent role of LPS in triggering epileptiform discharges and long-duration burst events resembling epileptic seizures[151,152]. On the other hand, similar studies using LPS supported a role of inflammation in increasing excitatory neurotransmission but not seizure activity *per se*[60,153]*.* Thus, in some cases, inflammation may increase the propensity towards seizures but not actually elicit seizures independently.

Evidence against a causal relationship between inflammation and seizures

It is also worth acknowledging that several published studies appear to negate the seizure-inducing effects of inflammation, and in certain instances, even support an antiepileptogenic or inhibitory effect of pro-inflammatory molecules[154–162]. For example, the depletion of microglia and T-lymphocytes in rat hippocampal organotypic brain slice cultures (OBSCs) was observed to have no effect on the rate of development or severity of epileptic activity when compared to control brain slices in which these cell types were present, suggesting that neither of these key inflammatory cell types are necessary for epileptogenesis, at least in the OBSC model system[162]. In addition, one research group carried out various experiments showing that the intracerebral or intrahippocampal infusion of pro-inflammatory mediators such as IL-1B or LPS had an anticonvulsant effect and impeded the acquisition of kindled behavioural seizures in rats[154–156]. In accordance, exposure of rat hippocampal OBSCs to LPS over seven days has been observed to increase inhibitory neurotransmission as noted by CA1 pyramidal neurons having a significantly lower frequency of action potential (AP) discharges in response to a series of 4-second-long depolarizing steps[163]. This effect was inferred to be a result of at least two factors, including a lower membrane resistance and a more depolarised AP threshold[163]. Moreover, the amplitude of monosynaptic inhibitory post-synaptic potentials increased following the several-day LPS exposure, and this was abolished by the co-incubation with an IL-1 receptor antagonist[163].

In accordance, despite its known pro-inflammatory activity, murine recombinant tumor-necrosis factor alpha (TNF-α) which binds to neuronal p75 receptors has been reported to inhibit seizures in mice, while human recombinant TNF-α which shows strong specificity for mouse p55 receptors had no effect on seizure activity[164]. This stands in contrast to another publication which reported that TNF-α enhances voltage-gated sodium currents in primary cultures of mouse cortical neurons[165]. Therefore, there appears to be some disagreement about whether pro-inflammatory mediators such as LPS or TNF-α exacerbate, alleviate, or have no effect on neuronal excitability and seizure activity.

Other studies have found that Cox-2 inhibitors, which are a subclass of nonsteroidal anti-inflammatory drugs, may have a pro-convulsant effect[158,159,166]. This contradicts studies showing that Cox-2 inhibitors and their accompanying reduction in prostaglandins has an anticonvulsant effect[119,122,143]. All in all, this mix of findings implies that the relationship between inflammation and seizures is not necessarily as straightforward as seizures inciting inflammation and inflammation in turn augmenting seizure activity. This does not preclude the possibility, however, that under certain conditions inflammation does play a role in either triggering or exacerbating seizures or contributing to epileptogenic processes. Nonetheless, the question remains as to why a considerable subset of studies have found either no effect of pro- or anti-inflammatory mediators on seizure activity or in some cases even an anticonvulsant effect of pro-inflammatory agents. One consideration is that it is likely only specific components of the immune system that may provoke seizures or increase seizure susceptibility. Consequently, certain pro- or anti-inflammatory targets, such as the mouse TNF p55 receptors may fail to affect seizure activity. Another explanation is that a combination of factors may work to drive brain tissue beyond the seizure threshold. As a result, the variation in experimental designs across different studies such as the age of experimental animals used, brain regions being studied, *in vivo* versus *in vitro* or *ex vivo* conditions (and consequently the presence or absence of an adaptive immune response), duration and severity of pro-inflammatory challenges, and timing of anti-inflammatory therapies relative to kindled seizures could influence whether immunomodulation has any effect on network excitability and seizures. Further research is required to better understand the set of conditions that increases the risk and severity of seizures in the presence of neuroinflammation, especially in more complex diseases states such as neurocysticercosis.

1.3 Experimentally investigating neurocysticercosis

As discussed in the earlier sections, much of our understanding of the pathophysiological changes in NCC have emerged from clinical studies that have either conducted computer tomography and magnetic resonance imaging scans in NCC patients or have analysed human tissue samples such as cerebrospinal fluid, blood, or brain tissue samples from patients with

NCC. Additionally, experimental research has been conducted to elucidate a more complete mechanistic picture of the cellular, molecular, and electrophysiological changes underlying NCC. Several studies have utilised healthy cell culture lines of human nervous system immune cells or cultured immune cells from patients with NCC in conjunction with *T. solium* extracts to study immune responses to the parasite[24,25,29,30,32,33].

In addition to work in human cell lines, various animal models have been developed to try and study exact disease processes in NCC. These models have varied in the combination of chosen parasites as well as host organisms to model the disease (See review by de Lange et al.[14]). Naturally, the gold-standard parasite to work with is *T. solium* as this is the parasite which causes NCC in humans. Some studies have infected rodents, pigs, or monkeys with activated *T. solium* oncospheres and have, to varying degrees, succeeded in reproducing the disease phenotype, with at least a proportion of animals experiencing seizures post-infection[167–170]. However, using *T. solium* comes with certain challenges. Firstly, it is infectious to humans and therefore requires significant biosafety measures to work with[171]. Secondly, maintaining a steady supply of *T. solium* is difficult as it entails either harvesting them from naturally infected pigs in endemic areas or feeding oncospheres to a host and allowing them to become activated *in vivo* and develop into cysticerci[170,172]. Alternatively, oncospheres can be activated *in vitro* and then injected into the brain of a model host organism to develop into cysts[167,173].

Based on these limitations, several other cestodes have been used to try model NCC including *Taenia crassiceps (T. crassiceps)*, *Mesocestoides corti*, and *Taenia taeniaeformis*. Of these different cestodes, *T. crassiceps* has been most commonly used to model NCC for several reasons. Firstly, *T. solium* and *T. crassiceps* belong to the same genus, have significant antigenic similarity[174–177], similar secretory/excretory profiles, and comparable gene expression of microRNA (miRNAs)[178,179]. Another reason for its use is that *T. crassiceps* rarely infects humans, making it safer to work with[180]. This is especially the case with the ORF strain of *T. crassiceps* which has completely lost its capacity to infect a definitive host and mature into adult tapeworms, and therefore does not pose an infection risk to humans[181]. Thus, *T. crassiceps* is less resource-intensive to work with compared to *T. solium* and does not necessitate the same biosafety measures as *T. solium*[181]. *T. crassiceps* larvae also naturally infect small rodents and moles[182,183], making it appropriate to work with in rodent models of NCC. Moreover, an important advantage of this parasite is that *T. crassiceps* larvae can divide rapidly via asexual reproduction which makes it relatively easy and cost-effective to keep a supply of viable *Taenia* cestodes for research by maintaining a colony of the parasites in the peritoneum of an intermediate host (usually mice)[56,181].

There are, however, some limitations of *T. crassiceps* as a model organism for human NCC. The life cycle of *T. crassiceps* comprises foxes, dogs, and other wild canines as the definitive hosts of the adult tapeworm[183,184], while the intermediate hosts of the parasite include small mammals such as mice, rabbits, and other rodents[182,183]. This differs to *T. solium* which naturally survives in humans in its adult form and in either pigs or humans during the larval stage of the tapeworm[185]. It follows from this that *T. crassiceps and T. solium* must have evolved genetic differences including species-specific differences in antigen expression that allows them to induce distinct immune responses to survive within their respective hosts. The genetic variation between the two parasites is further supported by clear differences in characteristics such as the morphology and size of the two parasites. This implies that disease models which utilise *T. crassiceps* may present with important differences in their pathophysiology compared to models using *T. solium*[180,183]. Moreover, there is some evidence that genetic and morphological changes may occur in certain *T. crassiceps* strains that have been maintained intraperitoneally in mice and this could potentially augment differences between the two tapeworms[181,186]. Nonetheless, considering the benefits of working with *T. crassiceps* as an alternative cestode to model the effect of *T. solium* as well as the relative similarity of the two species, there is arguably still a benefit in carrying out research with *T. crassiceps* to gain insight into NCC pathophysiology.

The main way that *T. crassiceps* has been studied has been via intracranial injection of cestode larvae or larval extracts into the brains of mice or rats[56,57,187]. Notably, it is not ideal to infect small mammals such as rodents with *T. crassiceps* as the parasite takes up a large amount of space in the cerebrum, causing brain tissue to be displaced[188]. One way around this problem is to harvest *T. crassiceps* larvae from a mouse intraperitoneal colony, homogenise the larvae, and then expose brain tissue from the chosen host organism to the homogenate containing the *T. crassiceps* products[56]. Exposing brain tissue to *T. crassiceps* can be carried out *in vivo* or *ex vivo*. Arguably, *in vivo* work may recapitulate certain aspects of injury or disease more accurately as it allows for an examination of how variables such as the infiltration of peripheral leukocytes as well as alterations to the blood-brain barrier may be involved in the pathogenesis of NCC[189,190]. On the other hand, *ex vivo* models enable easy molecular and electrophysiological access to live brain tissue[191], which is often more difficult or expensive to carry out *in vivo*[192,193]. Another advantage of *ex vivo* work is its alignment to the principle of reduction and refinement in animal research as described by The National Centre for the Replacement, Refinement & Reduction of Animals Research (NC3Rs) in the United Kingdom[193,194]. For example, brain slice cultures make it possible to use fewer animals and to minimise the suffering of the animals being used by modelling the disease state in culture rather than in the animal while it is alive[195].

The Raimondo lab has established an *ex vivo* model of NCC by utilising a mouse hippocampal organotypic brain slice culture (OBSC) preparation[196]. The experimental setup maintains an *in vivo* component as mice are intraperitoneally injected with *T. crassiceps* larvae and serve as host organisms to maintain a living *T. crassiceps* colony. The brain is then exposed to a *Taenia* material *ex vivo* via the mouse hippocampal OBSCs which are a well-established preparation to gain molecular and electrophysiological access to brain tissue[197–200] and are also a well-characterised system for studying epileptogenesis (See Park et al. 2015[162]). As with other *ex vivo* or *in vitro* systems, the organotypic preparation allows for easy and precise pharmacological interventions without the costs and challenges associated with *in vivo* work[201]. However, it has an advantage over *in vitro* systems used to study the brain such as cultured dissociated neurons in that it preserves synaptic organisation, network architecture and the presence of all resident brain cell types, thereby enabling a more ecologically valid environment for studying neurophysiological phenomena[201].

To model cestode infection, *T. crassiceps* larvae of the ORF strain are homogenised and the growth media used to feed the mouse hippocampal OBSCs is treated with thawed aliquots of the homogenate. This setup allows for brain tissue to be exposed to the same antigens and factors that make up the *T. crassiceps* larvae. A key preliminary finding from the Raimondo lab using this model was that the *T. crassiceps* larval homogenate was able to abolish the release of pro-inflammatory cytokines induced by the potent pro-inflammatory mediator, LPS. This demonstrated a capacity of *T. crassiceps* larvae to block the induction of inflammation by a pro-inflammatory stimulant, and it has been hypothesised that this effect may mimic the immune suppression seen during the viable cyst stage of NCC. This is not improbable considering that the homogenate is made from *T. crassiceps* larvae that are mostly viable upon freezing.

Further exploration is required to improve our understanding about the immunosuppressive activity of the *T. crassiceps* homogenate as well as other cellular and molecular pathways it may be modulating. Furthermore, the effect of *Taenia* larvae on neuronal function remains to be elucidated. We have hypothesised that the host's immune response in the brain may increase neuronal excitability and predispose the brain towards seizures. In turn, we hypothesised that the ability of *T. crassiceps* larvae to block the inflammatory response could also serve to impede possible inflammation-induced changes in neuronal excitability and thereby have seizure suppressing effects. Based on these two hypotheses, I was interested in firstly exploring what effect acute innate immune activation has on cell-type-specific transcription and on the intrinsic electrical properties of neurons. This was with the goal of gaining deeper insight into whether an inflammatory challenge by itself affects network excitability. Secondly, I wanted to investigate how the *Taenia* homogenate by itself affects cell-

type-specific transcription and the electrical properties of neurons. Finally, building from the experimental design of previous members in the lab, I set out to explore how the addition of the *Taenia* homogenate to a pro-inflammatory stimulus such as LPS would affect gene expression at single-cell resolution and on neuronal electrical properties.

A relatively recent advance in transcriptomic profiling is single-cell RNA sequencing (scRNAseq) or single-nucleus RNA sequencing (snRNAseq) which allows for a readout of mRNA levels within individual cells or nuclei[202]. We chose to use single-cell profiling for the purposes of this study as it offers two main advantages over other methods of measuring molecular changes in cells. Firstly, unlike other methods of measuring levels of molecules such as enzyme-linked immunosorbent assays (ELISAs), immunohistochemistry, Luminex, or microarrays which rely on a pre-selection of sets of genes to assay, RNA sequencing allows for a relatively unbiased, exploration of gene expression levels for almost all genes expressed in a tissue without requiring a decision on which molecules might be important to measure in advance[203]. Secondly, in contrast to the earlier RNA sequencing method known as bulk RNA sequencing which measures average RNA expression levels across tissue, single-cell or single-nucleus RNA sequencing approaches allow for transcriptomic changes to be traced to individual cells or nuclei[204]. Computational methods can then be used to group together cells or nuclei with similar gene expression profiles and label them according to the likely cell type they represent, thereby enabling an exploration of how specific cell types drive gene expression changes in response to the stimulus[204]. For this project, snRNAseq was chosen over scRNAseq for several reason. Firstly, we wanted to be able to freeze the brain tissue to have flexibility in planning the experiments and therefore snRNAseq is necessary as nuclei remain intact during freezing and thawing whilst cell membranes become ruptured during the freezing process and therefore result in low viability of whole cells[205]. Additionally, snRNAseq offers some advantages over scRNAseq when working with brain tissue. Firstly, scRNAseq often introduces a bias in terms of which brain cells are represented due to certain cells dying more easily or being captured at different rates in droplet-based methods because of large variability in morphology and size of brain cells[205]. In contrast, nuclei are relatively uniform across different cell types and thus their capture in droplets is not affected by the cell type they come from[205]. Nuclei are also less susceptible to spurious activation of gene expression during tissue dissection and isolation than whole cells[205]. However, a potential disadvantage of snRNAseq for brain tissue is that it is not able to detect changes in levels of transcripts that may occur in the cytoplasm after being exported out of the nucleus[205]. Nonetheless, all cytoplasmic and synaptic transcripts are first synthesised in the nucleus, and thus nuclear levels of these transcripts can arguably still serve as a proxy for how their expression is being modulated in response to conditions of interest[205]. There are also some general considerations

and limitations of single-cell and single-nucleus RNA sequencing methods. For one, standard scRNAseq and snRNAseq only provides an indication of the *levels* of transcripts and it is more expensive and resource-intensive to use technologies such as Smart-seq2 that allow for the detection of alternatively spliced transcripts[206]. Moreover, as RNA-seq is a transcriptomic method, it means it does not detect changes at the protein level such as breakdown of proteins and post-translational modifications which can drastically alter function. This is an important consideration when it comes to exploring the molecular changes underlying neuronal excitability, as post-translational changes that modify the structure or abundance of synaptic proteins are known to play a role in modulating neurotransmission[207–210].

Despite these limitations, using snRNAseq is of value when it comes to understanding how an immunomodulatory stimulus such as LPS affects signalling pathways in the brain, as there is evidence for cell-type-specific responses including distinct roles of glial cells and neurons[210–212]. To my knowledge, this has not been investigated in mouse hippocampal OBSCs using snRNAseq which is another gap I would like to address in this project. Understanding which cell types are responsible for different pathophysiological or neuroprotective pathways following exposure to either LPS or *Taenia* larvae may have important implications down the line when it comes to developing new therapeutics for neurocysticercosis and other neuroinfections. Furthermore, carrying out this research in mouse hippocampal OBSCs can lend further insight into the utility and limitations of this model system.

In addition to measuring transcriptomic changes in response to the different treatment conditions, I wanted to investigate how these same treatments affect changes in the intrinsic electrical properties of neurons as this could provide one way in which network excitability is mediated. I chose to use whole-cell patch-clamping as this is the gold-standard method for measuring electrophysiological changes of cells[213]. There are various electrophysiological properties that can be studied in neurons using whole-cell patch-clamp including synaptic properties such as excitatory and inhibitory post-synaptic potentials and currents, action potentials, and the intrinsic properties of neurons. I was specifically interested in building off previous work of the Raimondo lab to test whether innate immune activation and *Taenia* larval material affects the intrinsic properties of neurons as this can improve our understanding of the effect these stimuli have on the fundamental functioning of neurons. I then wanted to contextualise these findings with regards to possible seizure likelihood in the brain slices. To my knowledge, there are currently no published studies that have investigated this.

Due to its complex immunomodulatory activity, NCC represents a powerful model system to investigate the relationship between inflammation and seizures. Insights into seizure mechanisms in models of NCC may have relevance to other seizure conditions. The next

section outlines the aims formulated for this master's project to address the abovementioned gaps in knowledge regarding neuroimmune and cestode modulation of brain function.

1.4 Aims

Aim 1: Characterise the effects of acute innate immune activation and *Taenia crassiceps* exposure on cell-type-specific gene expression in mouse hippocampal organotypic brain slice cultures.

Aim 2: Explore the effects of acute innate immune activation and *Taenia crassiceps* exposure on the intrinsic electrical properties of neurons in mouse hippocampal organotypic brain slice cultures.

1.5 Objectives

1.5.1 Aim 1: Characterise the effects of acute innate immune activation and *Taenia crassiceps* exposure on cell-type-specific gene expression in mouse hippocampal organotypic brain slice cultures.

Objective 1: Generate snRNAseq datasets from mouse hippocampal OBSCs treated with LPS; T. crassiceps; LPS + T. crassiceps; or regular growth media (control).

Objective 2: Carry out computational pre-processing of the snRNAseq datasets.

Objective 3: Perform a differential expression analysis and other custom analyses to explore cell-type-specific gene expression changes between the LPS and control group.

Objective 4: Use Hybridisation Chain Reaction (HCR) RNA-Fluorescence In Situ Hybridisation (RNA-FISH) to validate some results from the differential expression analyses between the control and LPS group.

Objective 5: Run a differential expression analysis and other custom analyses to explore cell-type-specific gene expression changes between the *T. crassiceps* and control group.

Objective 6: Run a differential expression analysis and other custom analyses to explore cell-type-specific gene expression changes between the LPS + *T. crassiceps* and LPS group.

1.5.2 Aim 2: Explore the effects of acute innate immune activation and *Taenia crassiceps* exposure on the intrinsic electrical properties of pyramidal neurons.

Objective 1: Carry out whole-cell patch-clamping to measure the intrinsic electrical properties of pyramidal neurons from mouse hippocampal OBSCs treated with LPS, *T. crassiceps,* LPS + *T. crassiceps,* or regular growth media (control).

Objective 2: Run multiple comparisons statistical tests and pair-wise comparisons to look for differences in the intrinsic electrical properties of neurons between the different treatment groups.

CHAPTER 2

Materials and Methods

2.1 Establishing *ex vivo* models of innate immune activation and cestode infection in the brain.

2.1.1 Preparation of mouse hippocampal organotypic brain slices.

Mouse hippocampal organotypic brain slices were prepared by euthanising postnatal day 6-8 C57BL/6 mice pups via cervical dislocation and decapitation. The brain was removed from the skull and placed in iced (4 °C) dissection media. The dissection media consisted of EBSS with 6.1 g/l HEPES, 6.6 g/l glucose, and 5% 1M NaOH (all reagents from Sigma Aldrich). Both hippocampi were dissected in the dissection media on ice. Hippocampi were cut into 350 µm slices using a chopper. The hippocampal organotypic brain slices were then plated on semi-permeable cell culture Millicell-CM membrane inserts (pore size = 0.4 µm) in a 6-well plate (Sigma-Aldrich). The slices were cultured with standard growth media consisting of (volume/volume): 25% heat-inactivated horse serum (Biochrom), 2% B27, 23% EBSS, 50% MEM, and 6.5 g/l glucose (from Sigma Aldrich unless otherwise specified). Slices were cultured in a humidified incubator at 35 – 37 °C with 5% carbon dioxide (CO_2). Three slices were plated per well with 1.2 ml of growth media. All preparation steps were carried out with attention to sterility, and both the dissection media and growth media were sterilised upon preparation.

2.1.2 Treatments of hippocampal brain slice cultures

Tissue was cultured for 6 days with regular growth media to recover from the disruption of the dissection. Treatments were then carried out on day 6. To model innate immune activation, slices were exposed to 10 ng/ml LPS diluted in growth media. To model the cestode infection, slices were treated with 200 ug/ml of a *T. crassiceps* homogenate diluted in growth media. To model both an inflammatory challenge together with the cestode larvae, slices were treated with both 10 ng/ml LPS as well as 200 µg/ml *T. crassiceps* homogenate. Regular growth media served as the negative control condition for all treatment groups. The *T. crassiceps* homogenate was prepared from *T. crassiceps* whole larval cysts that were frozen at -80 °C. Frozen cysts were placed in a glass tissue grinder and ground until no pieces of membrane were visible. 1X Phosphate Buffer Saline (PBS) and protease inhibitor were added to the *T.*

crassiceps pulp, and the solution was ground again until it appeared homogenous. The solution was centrifuged at 3100 G for 20 min at 4 °C. After centrifugation three layers are apparent: a floating fatty layer, a middle liquid layer, and a solid bottom pellet. The supernatant was removed leaving behind the fatty layer and the solid pellet. The remaining solution was filter sterilised using a 0.2 µm sterile syringe filter. Aliquots of the *T. crassiceps* homogenate were prepared and stored at -80 °C.

To validate the effectiveness of the treatments, growth media was collected from the wells and frozen at -80 °C for later analysis. ELISAs were run on the growth media to measure concentrations of pro-inflammatory cytokines, including TNF-α and IL-6 (Detailed protocol previously described by de Lange et al.[214]). This allowed for verification that the treatments were effective by looking for the expected inflammatory activity of LPS and immunosuppressive effect of the *T. crassiceps* homogenate. The Kruskal-Wallis one-way ANOVA was used to test for statistical significance between multiple groups with post hoc Dunn's Multiple Comparison test for pairwise comparisons. For comparisons between just two groups, the Mann-Whitney U test was carried out.

2.2 Single-nucleus RNA sequencing

2.2.1 Single-nucleus RNA sequencing dataset generation.

Single-nucleus RNA sequencing datasets were generated via the 10X Genomics platform[215]. To obtain sufficient tissue for each condition, hippocampal brain slices were pooled together with slices that received the same treatment (control, LPS, Hom, and LPS+Hom) and stored at -80 °C. A single sample for one treatment group had approximately thirty-six hippocampal brain slices pooled together from multiple different animals and a total of four samples for each treatment group were generated. As much as possible, we tried to mix and match the combination of samples in each snRNAseq run to minimise batch effects (For summary of the batches, see Supplementary 1). The nuclear isolation protocol was carried out as follows: the pooled frozen slices were homogenised in lysis buffer and cells were lysed in the lysis buffer using a micro tissue grinder. After cell lysis, the sample was incubated on ice, centrifuged, the supernatant removed, and the pellet resuspended in lysis buffer. The sample was then centrifuged again and resuspended in nuclear suspension buffer. To estimate nuclear viability, 20 µL of a 1:1 nuclear suspension and trypan blue solution were loaded onto a haemocytometer and the nuclei counted under a microscope. We aimed for a nuclear viability of >5%. Additional nuclear suspension buffer was added to the sample to make up to 1 ml, and the nuclear suspension was then filtered through a 40 µm cell strainer. Nuclear viability was once again measured on the haemocytometer with either trypan blue or a DAPI stain.

Samples were kept on ice throughout. After confirming a high enough concentration of nuclei in the sample stock, we proceeded with the snRNAseq run.

For the first few samples, we targeted 10000 nuclei per sample. To improve sequencing depth, we adapted this for later samples to target 6000 nuclei per sample (See Supplementary 1 for summary of sample metadata). The snRNAseq runs were then carried out according to the Chromium Next GEM 3' Single Cell 3 Reagent Kits v3.1 user guide. The required concentration of the nuclear suspension stock was determined according to the number of nuclei we were targeting (as outlined in the 10X protocol). Sample dilutions were carried out with nuclease-water and the nuclear suspension was then combined with the required volume of the Master Mix prepared on ice according to the protocol (59.1% RT Reagent B, 7.5% Template Switch Oligo, 6.3% Reducing Agent B, and 27.4% RT Enzyme C). The samples consisting of the nuclear suspension in Master Mix were loaded into the row labelled 1 on the 10X Genomics Single cell 3'chip G. Gel Beads were loaded into the used wells corresponding to samples in the row labelled 2. Partitioning Oil was loaded into the corresponding sample wells in the row labelled 3. A solution of 50% Glycerol was prepared and pipetted into the unused wells of the chip. The 10x Gasket was attached to the chip before placing the chip in the 10X Genomic chromium controller which uses a microfluidics system to capture individual nuclei in oil droplets along with a barcoded bead. Reverse transcription is carried out within the droplets which converts the RNA to cDNA. During this step, the cDNA barcodes are added onto the cDNA transcripts. Following GEM generation and barcoding, the preparation of cDNA libraries was carried out, including cDNA PCR amplification, size selection of transcripts, adaptor ligation for sequencing, and the addition of sample-specific indices for demultiplexing with Illumina. After the post-library construction quality control checks, samples were sent for sequencing via Illumina[216]. Sequencing library samples were multiplexed and sequenced on a Novaseq machine using the recommended read length from 10X Genomics. Raw base calls were demultiplexed to obtained FastQ files for each sample.

2.2.2 Single-nucleus RNA sequencing bioinformatics analysis.

All snRNAseq analyses were performed on facilities provided by the University of Cape Town's ICTS High Performance Computing team.

Cell Ranger version 7.1.0 was used to map paired end sequencing reads to the mouse reference transcriptome (refdata-gex-mm10-2020-A) from the 10X Genomics downloads site, as well as filter the data to exclude any empty barcodes[217]. Default arguments were used including the inclusion of introns. The estimated number

Quality control

After running the Cell Ranger pipeline, the filtered feature-barcode matrix of each sample was converted into a Seurat object. Samples were then processed according to the standard Seurat pipeline[218] in R version 4.0.5 or 4.2.0[219]. The data was filtered to remove poor quality nuclei or droplets that had not captured nuclei. This involved filtering the data to only include barcodes with greater than 500 unique molecular identifiers (UMIs), greater than 250 genes expressed, and log10GenesPerUMI greater than 0.8, as well as a mitochondrial ratio less than 0.2. Additionally, all mitochondrial genes were excluded from the dataset because we were capturing nuclei and were therefore not expecting mitochondrial transcripts in the data. Thus, mitochondrial genes were assumed to potentially drive artefactual sources of variation in the data and removed to limit their effect on downstream analyses[220].

Several doublet identification tools were employed including DoubletFinder[221], Scrublet[222], and DoubletDecon[223]. These tools vary in their sensitivity and specificity for accurately identifying barcodes that represent doublets. One benchmarking paper found DoubletFinder to be the leading doublet-detection tool in terms of its accuracy, while Scrublet tends to have good specificity but poorer sensitivity for detecting doublets, and DoubletDecon tends to overestimate doublets[224]. The most common tools for identifying doublets (including DoubletFinder and Scrublet) simulate artificial doublets by randomly combining gene expression profiles of two droplets in the dataset and then comparing each droplet to the artificial doublets to determine their similarity. Both DoubletFinder and Scrublet use a K-nearest neighbors (KNN) approach to compare each droplet to the artificial doublets and give each droplet a doublet score based on its similarity to the artificial doublets. A user-defined threshold score can be set to decide which droplets end up being classified as doublets. For this analysis the threshold doublet score for DoubletFinder was set according to the proportion of expected doublets in the dataset based on an estimated homotypic doublet rate of 10%. The threshold doublet score for Scrublet was set at 0.3 which approximates the point at which the two peaks of a bimodal simulated doublet score histogram are separated from each other. DoubletDecon, on the other hand, uses a deconvolution algorithm to determine if a droplet resembles a doublet, and does not have a doublet score. I chose to employ all three of these doublet-detection tools to diversify the methods used to identify doublets and maximise the chances of correctly calling true doublets. I decided to take all the doublets called by DoubletFinder together with the intersection of doublets called by Scrublet and DoubletDecon for each sample. The latter choice to only include the intersection of doublets identified by Scrublet and DoubletDecon was with the goal of modifying DoubletDecon's high false positive rate. Effectively, this is the equivalent of taking all doublets called by DoubletFinder along with

the doublets that have agreement between any of the three tools. The set of identified doublets for each sample was then filtered out of the merged data containing all 16 samples.

Integration and clustering

Following the quality control steps, normalisation was performed using the SCTransform() function to correct the data for differences in the sequencing depth across cells. SCTransform also performs variance stabilisation to ensure that it is not only highly expressed genes driving the greatest sources of variation in the data as highly expressed genes tend to exhibit the highest amounts of variation. This is necessary as the top 2000 most variable genes are used in downstream analyses to perform integration and so we would like to avoid only highly expressed genes being included in the set of top highly variable genes. In addition, I included an argument to regress out the mitochondrial ratio of each barcode as this is an "uninteresting" source of variation in the data. I also assessed whether cell cycle phase contributed substantially to the variation in the data by performing a Principal Component Analysis (PCA) and finding that cell cycle phase did not substantially contribute to variation between nuclei (Supplementary 6). Integration of the different samples was performed by first running Seurat's FindIntegrationAnchors() function which identifies a set of anchors between the samples. Integration anchors were obtained using the top 2000 most variable features and 30 dimensions. The IntegrateData() function then performs a canonical correlational analysis on the SCT normalised data to integrate/align similar cells across the 16 different samples. Integration is important for downstream annotation and analysis of the data to ensure that cells belonging to the same cell type/populations across samples can be identified and annotated as such. PCA was then run on the integrated data followed by clustering using the FindNeighbors() and FindClusters() functions to group cells according to the largest sources of variation in the data. These functions use a graph-based clustering approach, which embeds cells in a graph structure, using a KNN graph with edges drawn between cells with similar gene expression patterns. The graph is then partitioned into interconnected 'quasi-cliques' or 'neighbourhoods' which form the discrete clusters that each nucleus belongs to.

Marker identification and annotation

To annotate clusters, several methods were used to gain consensus from various approaches. The FindAllMarkers() function was used to identify differentially expressed genes (DEGs) between the clusters (Supplementary 2.1). A resolution of 0.4 was set as the active identity and consisted of 30 clusters to be annotated. An automated annotation tool known as SCSA[225] was then used to compare the list of DEGs per cluster obtained from FindAllMarkers() to sets of known cell-type-specific markers. Several reference databases were used including SCSA's built-in reference databases obtained from CellMarker[226] and CancerSEA[227], as well

as creating my own user-defined databases with brain cell type markers curated from mousebrain.org[228] (See Supplementary 2.2). SCSA then provides an output file with predicted cell type annotations for each cluster along with a score for the predictions as well as other score-based indications of the confidence of the predicted cell type relative to the next best predicted cell type (Supplementary 2.3).

To supplement this automated annotation method, I used more bias/manual inspection methods including visualising the expression of a small set of known cell-type-specific markers across the different clusters in featureplots and bubbleplots as well as searching for these known cell-type-specific markers in the list of all DEGs across clusters from the FindAllMarkers() output. Overall, there was relatively good consensus between the automated annotation method and manual inspection methods with a few exceptions. Cluster 0 was predicted as endothelial cells by SCSA whilst visual inspection methods showed higher expression of astrocyte markers in cluster 0 (Figure 3.2 F). I also found that at least 4 of the astrocyte markers (*Gfap*, *Aqp4*, *Lhx4*, and *Ndrg2*) were in the list of DEGs for cluster 0, whereas none of the endothelial markers (*Apold1*, *Cldn5*, *Ly6a*, *Car4*, *Pecam1*, *Eng*, *Mcam*, and *Tek*) were in this set of DEGs (Supplementary 2.1). On the other hand, cluster 24 which had also been called endothelial cells by SCSA had both *Cldn5* and *Pecam1* in its list of cluster-specific DEGs, thereby serving as a good positive control. Based on this, as well as cluster's 0's proximity to the neighbouring high-confidence astrocyte clusters, I chose to consider cluster 0 as an astrocyte cluster rather than an endothelial cell cluster (Supplementary 2.1). In addition, cluster 21 has increased expression for both the DG-specific marker (Prox1) as well as microglia-specific markers relative to other clusters, while cluster 29 showed increased expression of cell-type-specific markers for both Microglia and OPCs relative to the other clusters (Figure 3.2 F). These ambiguous clusters were labelled as Prox1-microglia and Microglia/OPCs, respectively, and were mostly excluded from downstream analyses. The 30 clusters (resolution 0.4) were then labelled with my user-defined putative annotations. These were relatively broad annotations and did not include sub-populations of excitatory and inhibitory neurons.

In addition to these manual and automated annotation methods, a label transfer was carried out using the Allen Mouse Brain atlas as the reference. Briefly, the Whole Cortex & Hippocampus - 10x Genomics (2020) with 10x-Smart-Seq Taxonomy (2021) was downloaded from the Allen Brain database[229]. The data was filtered by region to only include the hippocampus. As the dataset was very large and would not be efficient for computational analysis, the reference dataset was filtered to only include nuclei that were expressing at least 500 genes and less than 7500 genes. This ceiling threshold was used to reduce the size of

the dataset to make for more efficient computational processing. The same pre-processing steps that were carried out on our query dataset were applied to the Allen reference dataset including SCTransform to perform the normalisation and scaling. The Seurat FindTransferAnchors() function was used to find anchors between the reference and query datasets with “SCT” specified as the normalisation method. FindTransferAnchors() first performs dimensional reduction (using the top 30 dimensions in this case) to project the query dataset onto the reference dataset in the same PCA structure. A set of anchor nuclei are then identified between the reference and query dataset (i.e., inter-dataset pairs of nuclei that are contained within each other's neighbourhoods). The anchors are filtered to ensure only high confidence anchors remain. Next, the nearest k.score anchors for each anchor nucleus is obtained to find its nearest neighbours within its own dataset and within its pair’s dataset. A neighbor graph is constructed based on these neighbourhoods and the shared neighbor overlap between the query and reference dataset is calculated and stored as an AnchorSet object. Using the TransferAnchors() function, nuclei in the query dataset then get the label/annotation of the nuclei they are anchored to in the Allen reference dataset.

Once the user-defined annotations and Allen brain annotations were obtained, I chose to use a filtering method to exclude nuclei that did not have agreement between the two annotation methods. This was done by adding two new cluster annotation columns to the metadata of the Seurat object in which both my own annotations and the Allen’s subclass annotations were converted into a broad cell type annotation (Astrocytes, Microglia, Oligos, Endothelial cells, Pericytes/VLMCs, Excitatory neurons, Inhibitory neurons, Dentate gyrus cells, and Cajal-Retzius cells). These two lists were then compared and any nuclei that did not have consensus between the converted user-defined annotation and the converted Allen annotation were excluded. I noticed, however, that the Allen did not have equivalent cell types to match my user-defined annotations of the Ependymal cells, OPCs, Prox1-microglia, and Microglia/OPCs. To get around this, all nuclei that had been labelled as Ependymal cells in the user-defined annotations were kept in the dataset. All nuclei labelled as OPCs in the user-defined annotations were retained provided their Allen subclass annotation was Oligos. All nuclei labelled as Prox1-microglia in the user-defined annotations were retained provided their Allen subclass annotation was either Microglia or Dentate gyrus cells (as these are Prox1 positive cells). All nuclei labelled as Microglia/OPCs in the user-defined annotations were retained provided their Allen subclass annotation was either Microglia or Oligos.

While this was a considerably stringent filtering step, I decided to go forward with this as I wanted to be as certain as possible of the cell type annotations for each cluster to increase confidence in downstream analyses. After all filtering steps were performed there were 33271 nuclei in the control group, 30291 nuclei in the Hom group, 31286 nuclei in the LPS group,

and 25923 nuclei in the LPS+Hom group (Supplementary 5.1). The differences in the number of nuclei per group were mainly a result of differences in the number of nuclei targeted per sample (which was adapted for later snRNAseq runs) as well as randomness in capture rate of droplets per sample.

With the remaining nuclei, I created four "levels" of cluster annotations including user-defined nuanced annotations; user-defined coarse annotations; Allen mouse brain cluster annotations; and Allen mouse brain subclass annotations. Due to the Allen brain dataset having higher resolution annotations for the neuronal populations, I made use of the Allen's annotations for my nuanced annotations to identify 3 excitatory neuron sub-populations (CA1, CA2/CA3, and Subiculum/Entorhinal) along with the Dentate gyrus cells and Cajal-Retzius cells. Similarly, I used the Allen's inhibitory neuron annotations to identify 5 inhibitory neuron sub-populations (Lamp5, Vip, Sncg, Pvalb, and Sst).

Differential expression analysis

After annotation of the clusters, a differential expression (DE) analysis was run using a pseudobulk approach via the DESeq2 package[230] and associated packages including ashr[231]. Pairwise DE analyses were run between the following groups: 1) control and LPS group for the coarse clusters, 2) control and Hom group for the nuanced and coarse clusters, 3) LPS and LPS+Hom group for the coarse clusters, and 4) control and LPS+Hom group for the coarse clusters. As recommended in the DESeq2 pipeline for single-cell data, the DE test was applied to each cell type individually. Counts of each gene are aggregated per sample and the median of ratios method used to estimate size factors for each sample which accounts for sequencing depth and differences in the total number of nuclei per sample. DESeq2 then estimates the gene-wise dispersions and shrinks these estimates to generate more accurate estimates of dispersion for modelling the counts. It then fits a negative binomial generalised linear model for each gene and makes use of the Wald Test for pairwise statistical testing. Before running DESeq2, variation in the dataset was explored by plotting PCA plots and colouring them according to group_id (treatment condition), sample_id (samples), and batch (based on the snRNAseq run that the sample was processed in). These plots revealed batch to be a significant contributor to the variation in the dataset. As a result, the design formula of the DESeqDataSetFromMatrix() function was used to adjust for batch. This was done by specifying batch as a known source of variation to be treated as a covariate in the regression model whilst specifying treatment group as the conditions of interest design(~ batch + group_id). P-values were corrected using the Benjamini and Hochberg method. The significance threshold was set at p.adj < 0.05. A foldchange threshold was also set at the absolute Log2FoldChange >= 0.58.

EnrichR[232] was used to carry out an enrichment analyses on various sets of upregulated and downregulated genes separately for each cell type to identify biological pathways associated with the DEGs for each cell type. EnrichR uses the Fisher's exact test to assess the significance of overlap between the input list and the gene sets and rank a functional term's relevance to the input list[233]. An adjusted p-value is calculated using the Benjamini-Hochberg method to correct for multiple comparisons[233]. The threshold for the gene list to be considered significantly enriched for a particular pathway was set at p.adj < 0.05. The GO Biological Processes 2021 database was chosen as the reference database against which to compare our sets of DEGs. Customised analyses were run to further explore cell-type-specific differences between the treatment groups of interest.

2.3 Hybridisation chain reaction RNA-Fluorescence in situ hybridisation.

To validate some of the snRNAseq results between the control and LPS condition, a hybridisation chain reaction HCR RNA-FISH protocol was optimised for three different combinations of genes in mouse hippocampal OBSCs. The protocol was adapted from the Molecular Instruments HCR v3.0 protocol[234] for a sample on a slide as well as a protocol published by the Allen Institute for FISH in 350 µm paraformaldehyde-fixed mouse cortex tissue slices[235].

2.3.1 RNA-FISH sample preparation

Mouse hippocampal OBSCs were cut out of the inserts. Slices were fixed in 4% paraformaldehyde (PFA) for 30 minutes. Slices then underwent three wash steps in 1X PBS for 10 minutes each and then maintained in 70% ethanol (EtOH) at 4 °C for a maximum of 33 days. Slices were kept on their membranes for the entire tissue preparation and in situ HCR protocol.

2.3.2 HCR RNA-FISH

Slices were permeabilised in 8% SDS for 10 minutes at room temperature followed by a 1-minute wash step in 70% EtOH. After permeabilisation, slices were prehybridised in probe hybridsation buffer for 10 minutes at room temperature. Probe solutions were prepared with one of three probes (Timp1, Ccl5, or Lcn2) at a concentration of 8 nM in probe hybridisation buffer. Slices were incubated overnight in their respective probe solution at 37 °C. The negative probe control slices were incubated in probe hybridisation buffer instead of a probe solution. A series of four 15-minute wash steps were carried out in four different concentrations of probe wash buffer (25%, 50%, 75%, and 100%) diluted in 5X SSCT where applicable. The wash solutions were pre-warmed at 37 °C. Slices were pre-amplified with amplification buffer for 30 minutes. The paired fluorescent hairpins (h1 and h2) corresponding to the probes were

heated to 95 °C for 90 seconds then cooled to room temperature for 30 mins. A hairpin solution with fluorescent hairpins was prepared at a concentration of 20 nM in amplification buffer. The Timp1, Ccl5, and Lcn2 probes received hairpins with amplifier fluorophores that are excited by the 647 nm laser. Slices were incubated with the hairpin solution at room temperature overnight. Negative probe and negative hairpin slices were incubated in amplification buffer instead of the hairpin solution (Supplementary 3 for representative images of negative probe slice). Slices were washed twice in 5X SSCT for 30 minutes per wash step. This was followed by another 5X SSCT wash step for 5 minutes and a 1-minute 1X PBS wash. A Hoescht solution (0.6 uM) was prepared in 1X PBS. Slices were incubated in the 0.6 uM Hoescht for 20 minutes to stain the nuclei blue. Slices were then removed from the membranes and mounted on slides with mowial mounting medium. Cover slips were added on top.

2.3.3 Image processing and quantification

Slides were imaged on the LSM 880 airyscan confocal microscope (Carl Zeiss, ZEN SP 2 software). The C-Apochromat 40x objective was used. Gain was set at 600 for the Hoescht channel, and at 700 for the other 3 channels (488, 546, and 647). Images were obtained across different spatial points in each slice and at several different levels within one position starting at the sheath and moving lower towards the bottom of the slice. The average fluorescent signal for each probe was obtained for each image taken within the mid-slice regions. These data points were pooled across slices and experiments to create biological replicates for quantification. A Mann-Whitney test was run to compare the mean fluorescent intensity of each of the probes between the control and LPS group.

2.4. Whole-cell patch-clamp recordings

After 24 hours of exposure to their respective condition, brain slices belonging to either the control (N=17), Hom (N=22), LPS (N=20), or LPS+Hom (N=18) group were transferred one at a time onto a patch-clamp rig. Each slice was bathed in a continuous flow of artificial cerebral spinal fluid (aCSF) bubbled with carbogen (95 % O_2: 5 % CO_2) and maintained between 28 - 32°C using a temperature regulator. The 10X artificial cerebral spinal fluid stock solution was made from NaCl (120 mM), KCl (3 mM), Sodium phosphate Monobasic dihydrate (1.2 mM), Sodium Bicarbonate (23 mM), and D-Glucose (11 mM) (Sigma-Aldrich). A 1X aCSF dilution was prepared on the day of patching from the 10X stock. Micropipettes were pulled from boroscilicate glass capillaries and had a tip resistance between 2 MOhm and 7 MOhm. Pipettes were loaded with a K-Gluconate low chloride internal solution with osmolarity 282 mOsm and pH 7.29. The internal solution was made from K-gluconate (120 mM), KCl (10 mM), HEPES (10 mM), Na2ATP (4 mM), NaGTP (0.3 mM), Na2-phosphocreatine (10 mM). Neurons in either the CA1 or CA3 areas of the hippocampus were selected by visual

inspection under a Zeiss Axioskop or Olympus BX51W upright microscope. Cells that were on the surface and had a typical pyramidal cell body morphology were targeted. Micropipettes were lowered towards the neurons and a gigaseal formed by firstly releasing the positive pressure and then using small negative suctions. The seal was broken to create a whole-cell patch. Any cells with an access resistance greater than 30 MOhm or a resting membrane potential greater than -40 mV were excluded. Cells were either held in voltage clamp or current clamp and various recordings taken using WinWCP Strathclyde Electrophysiology Software version 5.2.7[236]. Recordings were analysed on Matlab version 9.9.0.1524771 (R2020b)[237] to extract various properties of the cells. Statistical tests were run on Graphpad Prism version 8.0.1[238] to look for significant differences between the intrinsic electrical properties of the different treatment groups. The Shapiro-Wilk test was used to determine if the data for each intrinsic electrical property was normally distributed. If data was normally distributed, one-way analysis of variance (ANOVA) tests were used to look for significant differences between the four treatment groups. If the data did not meet the criteria for normal distribution, it was taken as non-parametric and the Kruskal-Wallis test was used to run a multiple comparisons test between the four groups. For the statistical analysis of the relationship between the firing rate and current density, a two-way ANOVA test was performed to look for differences in the average firing rate at different binned current densities between the four treatment groups.

CHAPTER 3

Results

3.1 Modelling acute immune activation and *Taenia* infection in mouse hippocampal organotypic brain slice cultures.

The Raimondo lab has demonstrated an immunosuppressive effect of the *T. crassiceps* larval homogenate in mouse hippocampal OBSCs. As discussed previously, it is a well-established hypothesis in the NCC field that the capacity of viable *Taenia* larval cysts to suppress inflammation may have seizure-suppressing effects while any upregulation of the host immune response to *Taenia* larvae may trigger seizures. I wanted to explore this hypothesis experimentally by testing the effects of both a pro-inflammatory stimulant as well as the immunosuppressive homogenate on cell-type-specific gene expression and on neuronal excitability in mouse hippocampal OBSCs. To this end, mouse hippocampal OBSCs were prepared from postnatal day 6-8 mice and cultured for 6 days before being exposed to one of four different treatment conditions for 24 hours: 1) regular growth media that served as a

control; 2) 10 ng/ml LPS to simulate immune activation; 3) 200 ug/ml of the *T. crassiceps* homogenate to test what effect the homogenate is having by itself; and 4) both 10 ng/ml LPS and 200 ug/ml *T. crassiceps* homogenate to better understand the effect of the homogenate in the presence of a pro-inflammatory stimulus (Figure 3.1 A). This preparation with the different treatment conditions was used for several different experiments, including the snRNAseq experiments, HCR RNA-FISH experiments, and the whole-cell patch-clamp experiments (Figure 3.1 A). ELISAs were run on the growth media from the different wells to measure the concentration of well-known pro-inflammatory cytokines, IL-6 and TNF-α (Figure 3.1 A). Exposure to LPS significantly increased the release of IL-6 and TNF-α relative to control conditions (Figures 3.1 B-D), while the addition of the *T. crassiceps* homogenate to LPS abolished this effect (Figures 3.1 B, D) ($p < 0.05$, Kruskal-Wallis test or Mann-Whitney test, Supplementary 4). The concentrations of IL-6 and TNF-α were not significantly different between the *T. crassiceps* alone condition and the control condition (Figures 3.1 B, D; $p > 0.05$, Kruskal-Wallis test, Supplementary 4). ELISAs run on the control, Hom, and LPS+Hom groups for the HCR RNA-FISH and whole-cell patch-clamp experiments had a concentration of TNF-α that was below the assay detection limit (7.8 pg/ml) (Figures 3.1 C, D).

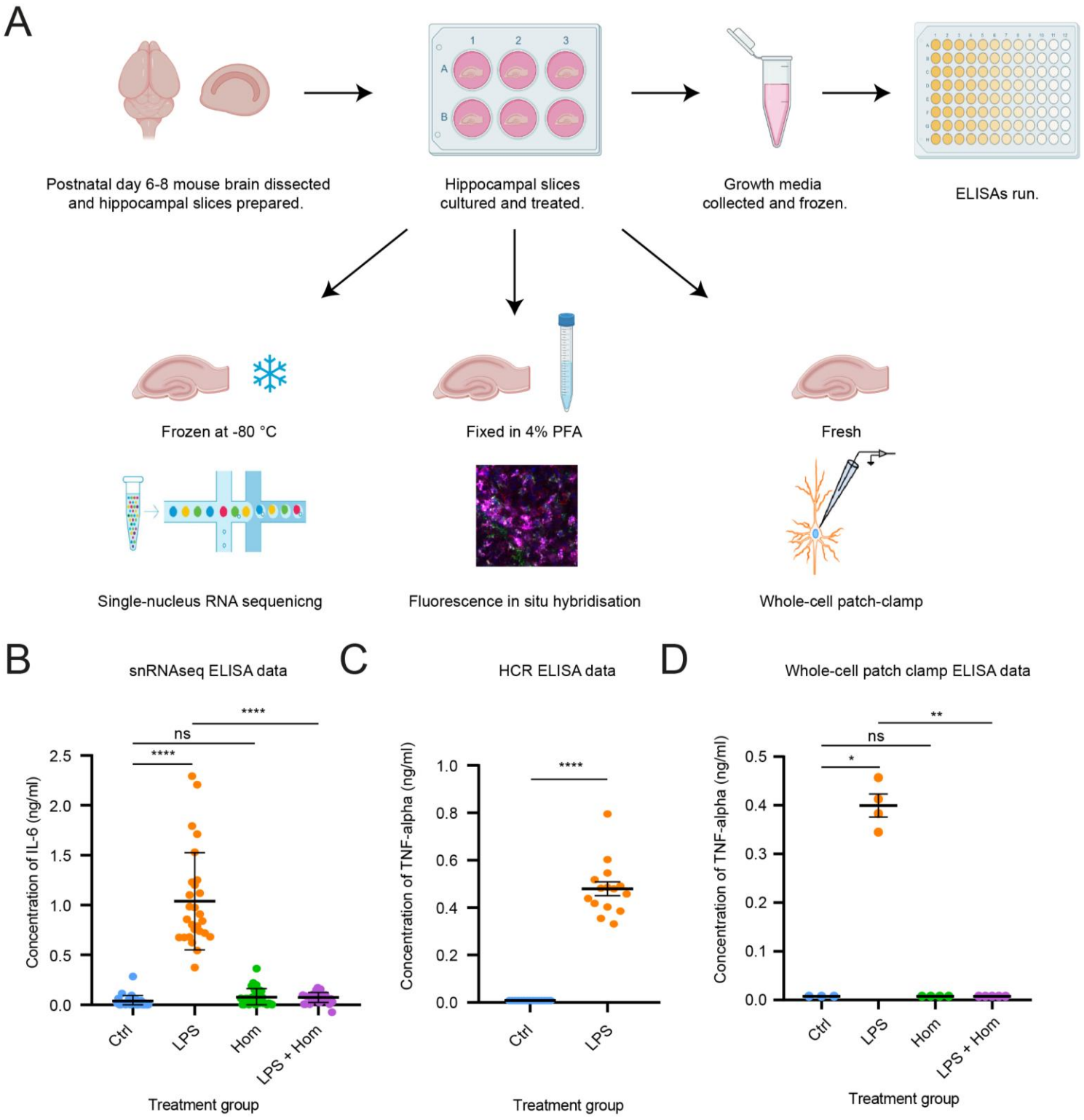

Figure 3.1 Modelling acute immune activation and *Taenia* infection in mouse hippocampal organotypic brain slice cultures.

A) Hippocampal organotypic brain slices prepared from post-natal day 6-8 mice and cultured for 6 days. Slices were treated for 24 hours with either regular growth media (Ctrl), 10 ng/ml LPS (LPS), 200 ug/ml *T. crassiceps* homogenate (Hom); or both 10 ng/ml LPS and 200 ug/ml *T. crassiceps* homogenate (LPS+Hom). Slices were either frozen at -80 °C for the snRNAseq experiments, fixed in 4% PFA for the HCR RNA-FISH experiments, or

used fresh for the whole-cell patch-clamp experiments. Enzyme-linked immunosorbent assays (ELISAs) were carried out on the growth media to measure the concentrations of interleukin-6 (IL-6) and tumor-necrosis factor alpha (TNF-α) to confirm whether the expected inflammatory/immunosuppressive response was present. **B)** ELISA data for the snRNAseq experiments show a significant increase in the concentration of IL-6 in response to LPS (N=28) relative to Ctrl (N=30), Hom (N=30), and LPS+Hom (N=28). There was no significant difference in the concentration of IL-6 between the Ctrl and Hom conditions. **C)** ELISA data for the HCR RNA-FISH experiments show a significant increase in the concentration of TNF-α in the LPS condition (N=15) compared to the Ctrl condition (N=15). **D)** ELISA data for the whole-cell patch-clamp experiments show a significant increase in the concentration of TNF-α in response to LPS (N=4) relative to Ctrl (N=3), Hom (N=4), and LPS+Hom (N=5). There was no significant difference in the concentration of TNF-α between the Ctrl and Hom conditions. Values with means ± SEM; ns = not significant; *p ≤ 0.05; **p ≤ 0.01; ****p ≤ 0.0001; Kruskal-Wallis test with Dunn's multiple comparison post-hoc test.

3.2 Single-nucleus RNA sequencing reveals all major brain cell types present in integrated mouse hippocampal organotypic brain slice culture datasets.

Single-nucleus RNA sequencing libraries were generated from the treated tissue using the 10X Genomics platform and sequenced via Illumina (Figure 3.2 A). Standard quality control, doublet removal, and normalisation steps using Seurat's SCT normalisation method were performed (See Supplementary 5.1 for summary of filtering steps). Interestingly, most nuclei already met the quality control criteria, and thus very few nuclei were filtered out at this processing step (Supplementary 5.2). Using the combination of doublet tools described in the methods, a total of 18981 (11.8%) droplets were called as doublets across the 16 samples and removed from the merged data that included all samples (Supplementary 5.3). Integration was performed on the datasets to be able to identify the same cell type populations across different samples when annotating the clusters. After integration, all four treatment groups were well-aligned and showed relatively uniform representation across the UMAP space (Figure 3.2 B). PCA plots of the integrated samples using the top 2000 most variable features revealed that the treatment group of the samples as well as the snRNAseq run (i.e., batch) that the sample belonged to are major contributors to variation in the data (Figure 3.2 C, Supplementary 6). After integration, clustering was performed with the top 40 PCs. A total of 30 clusters were identified at a resolution of 0.4 (Supplementary 7). Using the annotation methods outlined in the methods, I filtered out 40055 nuclei from the dataset that did not show agreement between my user-defined annotations and the Allen label transfer annotations (Supplementary 5.1). This left a total of 120771 nuclei (75.1% of original total) across all 16 sample (Supplementary 5.1). Following this filtering step, a total of 22 distinct sub-classes were identified by the label transfer method using the Allen reference dataset (Figure 3.2 D), 12 distinct cell types were labelled for the coarse cluster annotation level (Figure 3.2 E), and 19 nuanced clusters were identified using the Allen Mouse Brain annotations to identify the CA1, CA2/CA3, and Subiculum/Entorhinal cells within the excitatory neuron clusters, as well

as the Pvalb, Vip, Sst, Sncg, and Lamp5 neurons within the inhibitory neuron clusters (Figure 3.2 E). The nuanced cluster annotations were validated by visualising the average expression levels of a set of known cell-type-specific markers (Figure 3.2 F). Interestingly, there were two ambiguous clusters, one which showed increased expression of cell-type-specific markers for both Microglia and OPCs relative to the other clusters, and another cluster which differentially expressed the DG-specific marker (Prox1) as well as microglia-specific markers (Figures 3.2 E, F). These ambiguous clusters were labelled as Microglia/OPCs and Prox1 microglia, respectively, and were mostly excluded from downstream analyses. The proportions of the different cell types across the four treatment groups were comparable (Supplementary 8). Astrocytes made up the largest proportion of cells followed by Dentate gyrus (DG) cells and CA1 neurons (Supplementary 8).

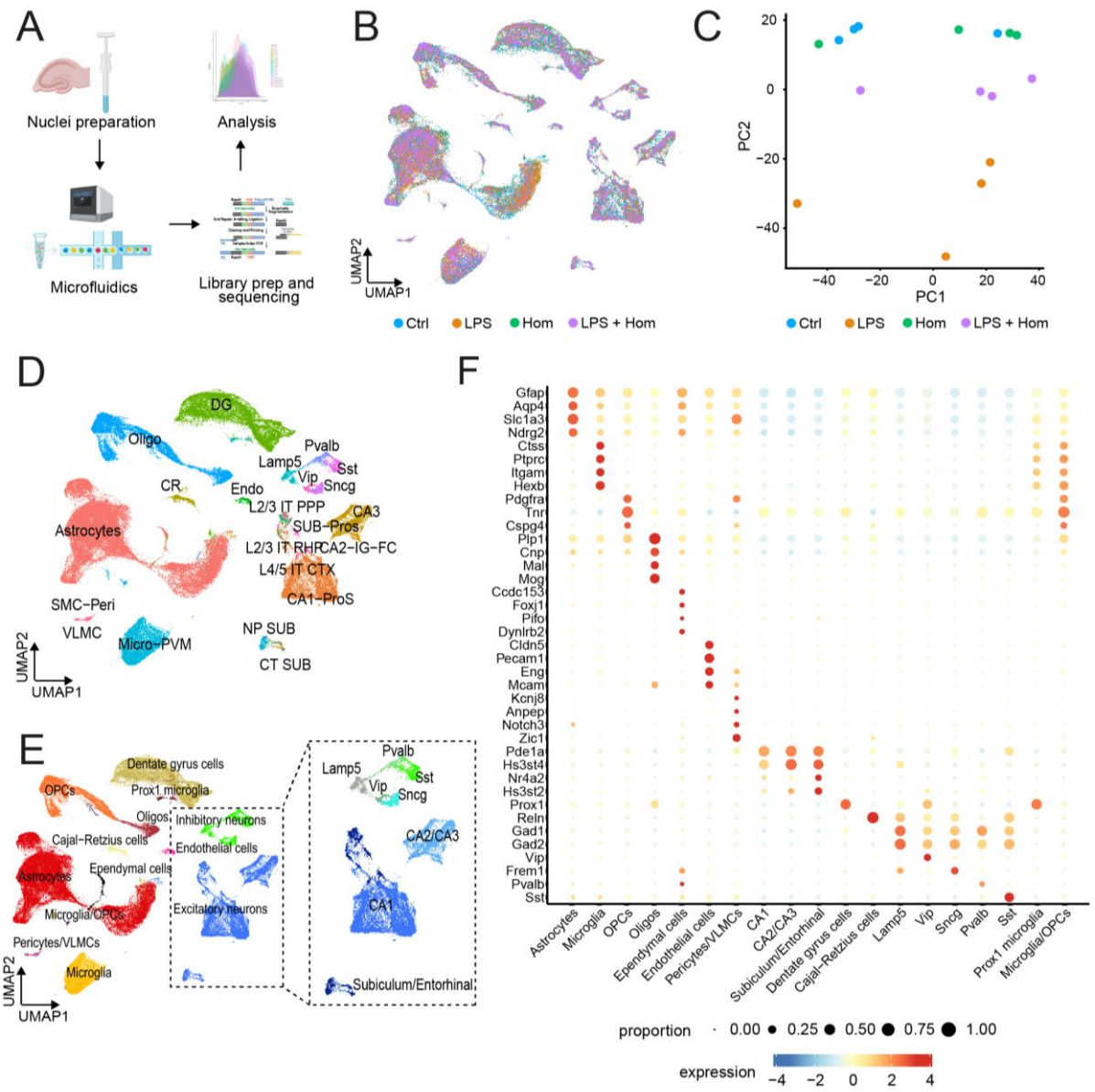

Figure 3.2 Single-nucleus RNA sequencing reveals all major brain cell types present in integrated mouse hippocampal organotypic brain slice culture datasets.

A) Nuclei from the 24-hour treated mouse hippocampal organotypic brain slice cultures were dissociated in lysis buffer. A single-nucleus RNA sequencing pipeline was carried out using the 10X Genomics platform which included gel bead in emulsion (GEM) generation and barcoding as well as library preparation. Samples were sent for sequencing via Illumina. Computational processing and analyses were performed on the datasets. **B)** Uniform Manifold Approximation and Projection (UMAP) plot of integrated samples coloured by treatment group. **C)** Principal Component Analysis (PCA) plot of sample average coloured by treatment group to visualise variation in the data in a reduced dimensional space **D)** UMAP plot of 22 sub-clusters annotated using the label transfer method with the Allen Mouse Brain hippocampal database as reference. **E)** UMAP plot of 12 user-defined coarse clusters using automated and manual methods; zoom-in on nuanced neuronal sub-populations annotated using the Allen Mouse Brain annotations **F)** Bubble plot showing the expression of cell-type-specific markers across the 19 user-defined nuanced clusters.

3.3 Lipopolysaccharide triggers generalised inflammatory gene expression changes across different cell types in mouse hippocampal organotypic brain slice cultures.

A DE analysis using DESeq2 was run between the control and LPS samples to look for changes in gene expression across the different cell types in response to acute innate immune activation in the brain (See Supplementary 9 for the control versus LPS DE results per cluster). The most prominent response to LPS was seen in astrocytes and microglia which had the largest number of significant DEGs (Figure 3.3 A). However, relatively generalised changes in gene expression were seen across the clusters with the majority of gene expression changes being upregulated in response to LPS (Figure 3.3 A). There were 161 DEGs that were shared between any two cell types or more (Figure 3.3 B), including genes such as *Timp1*, *Ccl5*, *Lcn2*, *Saa3*, *Mmp3*, *Ifitm3*, *C3* (Supplementary 9). The expression of the top 50 DEGs across all clusters ranked according to their absolute Log2FoldChange was visualised and highlighted the trend for an upregulation of the majority of these DEGs in response to LPS (Figure 3.3 C). An enrichment analysis was carried out on the list of all significant DEGs across all clusters to identify GO biological terms associated with the sets of genes (Supplementary 10). The enrichment analysis confirmed an upregulation of inflammatory pathways, including cytokine-mediated signalling, cellular response to cytokine stimulus, and cellular response to interferon gamma (IFN-γ) (Figure 3.3 D, Supplementary 10). Additionally, both the MyD88-dependent and MyD88-independent toll-like receptor signalling pathways that are known to be activated by LPS binding to TLR4 were found to be upregulated (Supplementary 10). The downregulated control versus LPS DEGs were not significantly enriched for any of the pathways in the GO Biological Processes 2021 database (Supplementary 10). Three “general” LPS-response genes (*Timp1*, *Ccl5*, and *Lcn2*) were selected for validation via HCR RNA-FISH (For representative images see Figures 3.4 A-F). Population analysis across images of the control and LPS-treated tissue confirmed significantly higher mRNA levels of these three genes in the LPS-treated tissue compared to the control tissue ($p < 0.0001$; Mann-Whitney test; Figures 3.4 G-I).

Additionally, I looked at the expression of genes known to encode receptors and binding proteins for LPS. Notably, *Tlr4* was found to be expressed in all cell types although often in a low percentage of nuclei (Supplementary 11). Non-neuronal cells, including endothelial cells, pericytes/VLMCs, microglia, and astrocytes had a greater percentage of nuclei expressing *Tlr4* compared to neuronal cells (Supplementary 11). On the other hand, *Trpm3* which encodes another receptor for LPS was found to be expressed in a larger percentage of neuronal cells compared to non-neuronal cells (Supplementary 11). Curiously, this gene was downregulated in astrocytes and OPCs in response to LPS, while *Tlr4* was not found to be

differentially expressed in any cell types in response to LPS (Supplementary 9). In addition to this, *Cd14* which encodes a protein that helps bind LPS to TLR4 was upregulated in astrocytes and microglia, whilst *Lbp* which performs a similar function was upregulated in astrocytes (Supplementary 9). However, both *Cd14* and *Lbp* were expressed in a relatively low percentage of nuclei (Supplementary 11). Several other receptors for LPS including *Trpm8*, *Trpa1*, *Trpv1*, *Trpv4* were expressed in only very low percentages of nuclei and were not differentially expressed in response to LPS (Supplementary 9, 11).

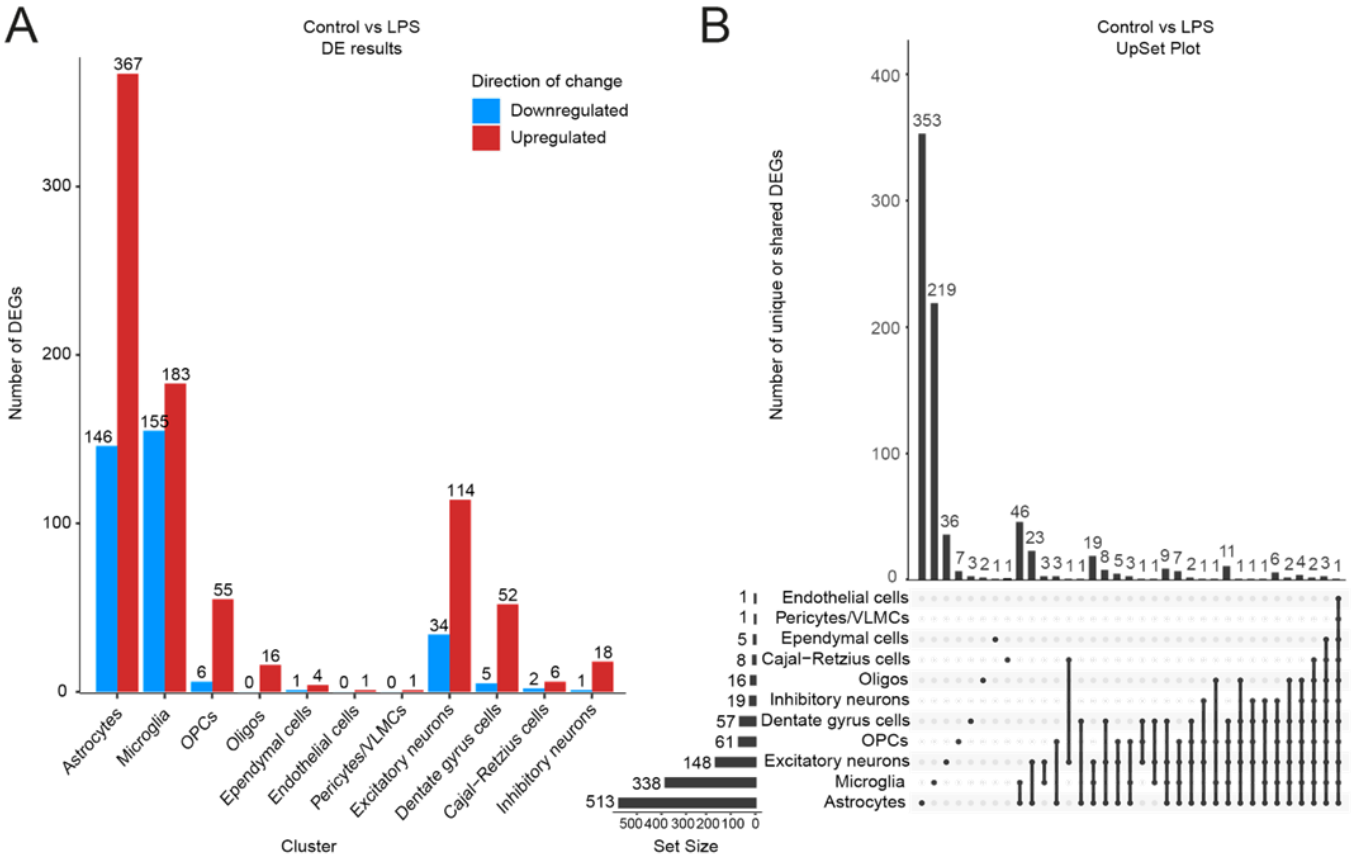
A
Control vs LPS
DE results
Direction of change
Downregulated
Upregulated
Number of DEGs
Astrocytes
Microglia
OPCs
Oligos
Ependymal cells
Endothelial cells
Pericytes/VLMCs
Excitatory neurons
Dentate gyrus cells
Cajal−Retzius cells
Inhibitory neurons
Cluster
B
Control vs LPS
UpSet Plot
Number of unique or shared DEGs
Endothelial cells
Pericytes/VLMCs
Ependymal cells
Cajal−Retzius cells
Oligos
Inhibitory neurons
Dentate gyrus cells
OPCs
Excitatory neurons
Microglia
Astrocytes
Set Size

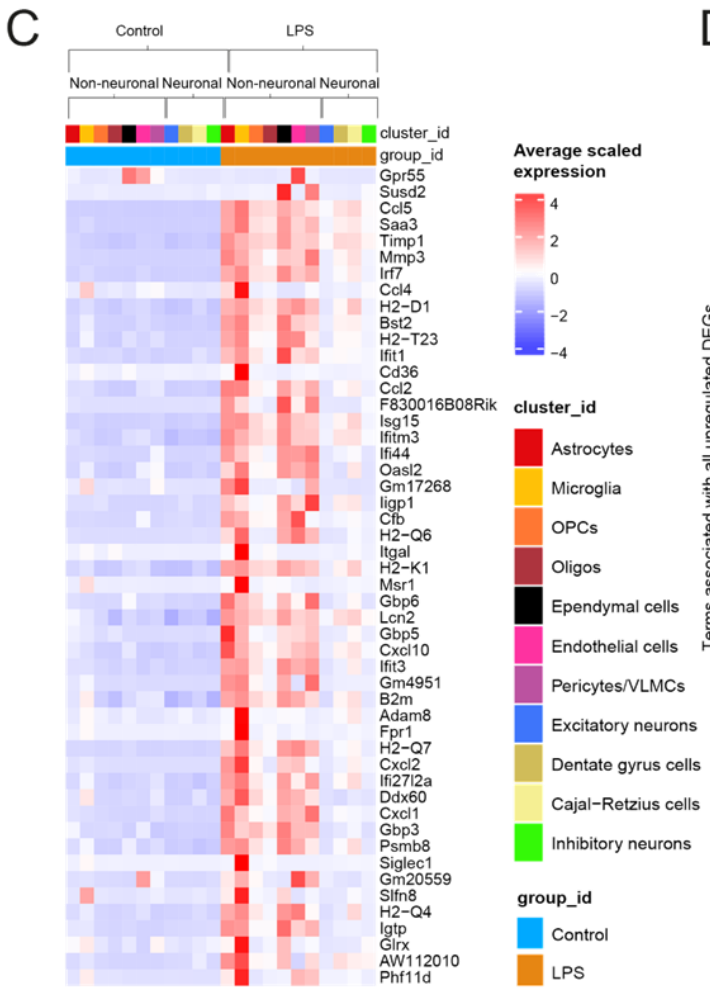
C
Control
LPS
Non-neuronal
Neuronal
Non-neuronal
Neuronal
cluster_id
group_id
Average scaled expression
cluster_id
Astrocytes
Microglia
OPCs
Oligos
Ependymal cells
Endothelial cells
Pericytes/VLMCs
Excitatory neurons
Dentate gyrus cells
Cajal−Retzius cells
Inhibitory neurons
group_id
Control
LPS

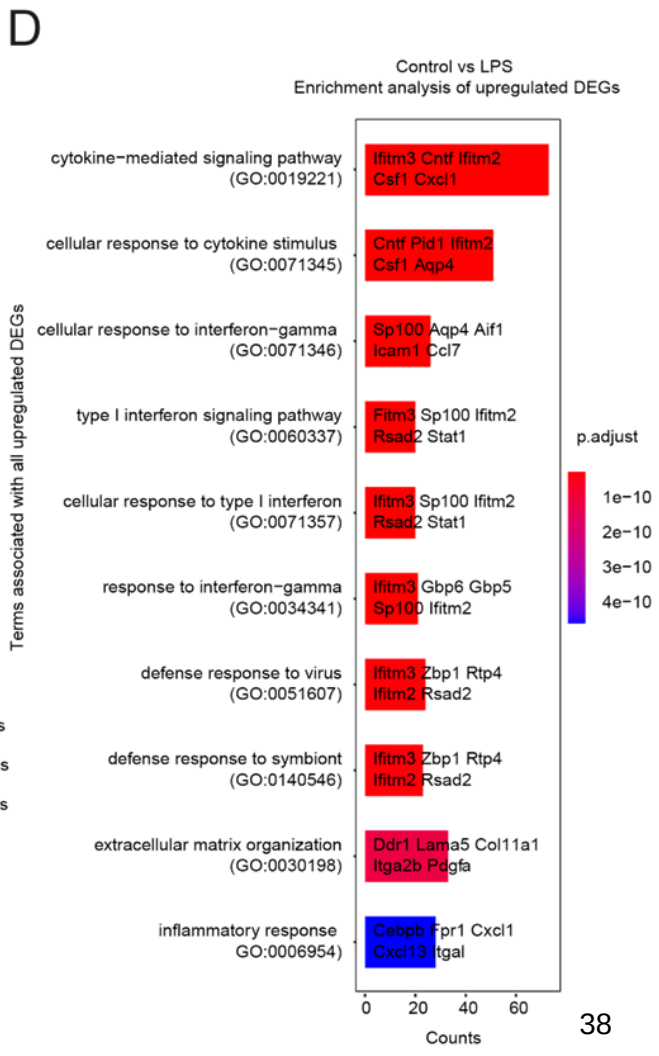
D
Control vs LPS
Enrichment analysis of upregulated DEGs
Terms associated with all upregulated DEGs
cytokine−mediated signaling pathway (GO:0019221)
cellular response to cytokine stimulus (GO:0071345)
cellular response to interferon−gamma (GO:0071346)
type I interferon signaling pathway (GO:0060337)
cellular response to type I interferon (GO:0071357)
response to interferon−gamma (GO:0034341)
defense response to virus (GO:0051607)
defense response to symbiont (GO:0140546)
extracellular matrix organization (GO:0030198)
inflammatory response GO:0006954)
p.adjust
Counts

Figure 3.3 Lipopolysaccharide triggers generalised inflammatory gene expression changes across different cell types in mouse hippocampal organotypic brain slice cultures.

A) Number of upregulated and downregulated differentially expressed genes (DEGs) across the coarse clusters for the control versus LPS differential expression analysis. **B)** UpSet plot showing the unique and shared DEGs across the coarse clusters for the control versus LPS differential expression analysis. Single dots indicate uniquely differentially expressed genes for a cluster, while dots joined by lines indicated shared DEGs between clusters. **C)** Heatmap showing the average expression of the top 50 DEGs for the control versus LPS differential expression analysis. Normalised and scaled average expression levels are shown for the set of genes across the coarse clusters in the control and LPS group. Genes are ranked according to their absolute Log2FoldChange with upregulated genes at the top. **D)** Enrichment analysis showing the top GO Biological Processes 2021 terms associated with all upregulated genes across all coarse clusters for the control versus LPS differential expression analysis. Bars are coloured according to the adjusted p-value for the corresponding term (p.adjust). The length of each bar reflects the number of genes associated with the corresponding term (counts).

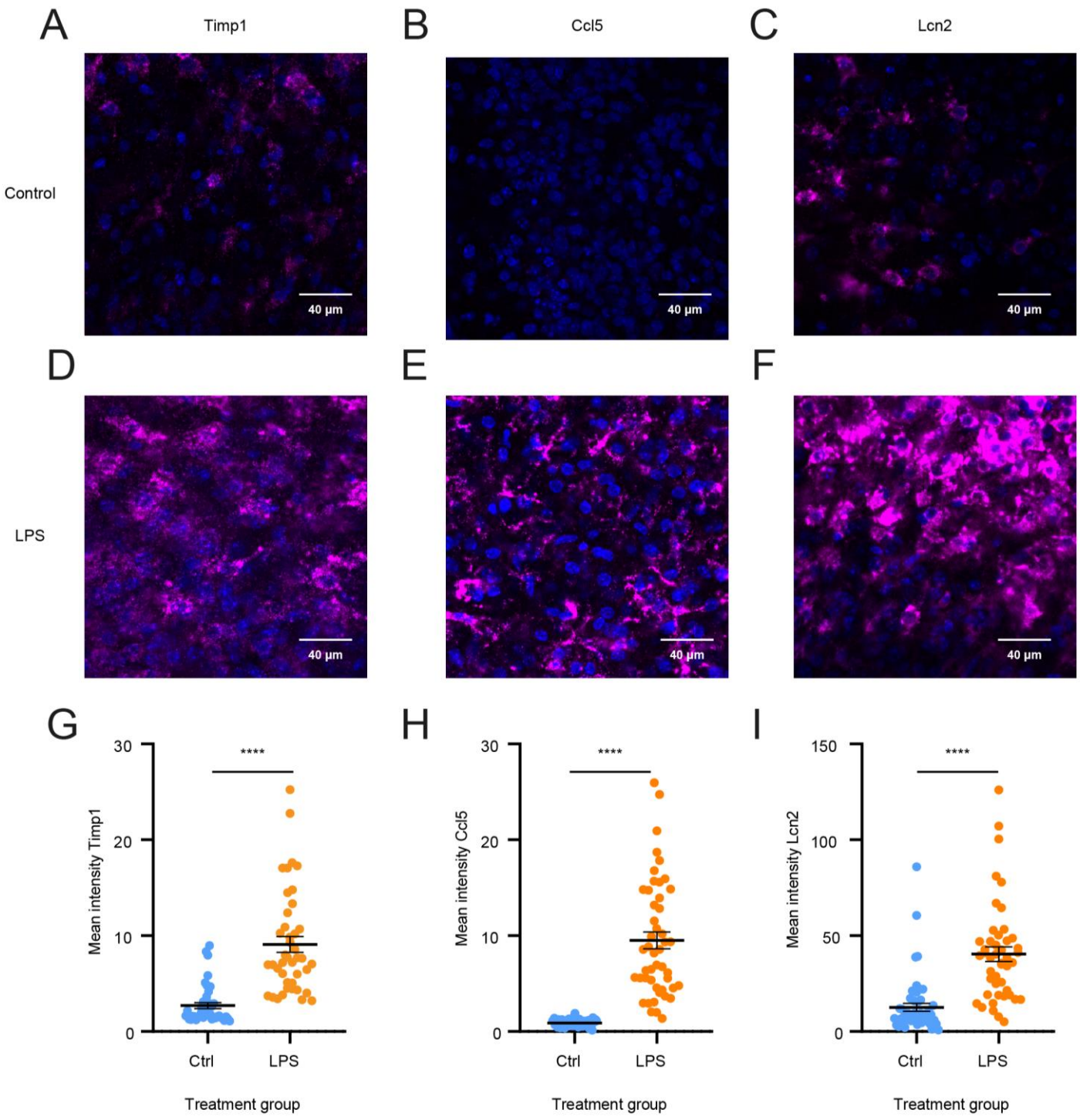

Figure 3.4 HCR RNA-FISH confirm differential expression of general inflammatory genes between control and LPS condition.

A-B) Representative HCR RNA-FISH confocal images of A) Timp1, B) Ccl5, C) Lcn2 in control mouse hippocampal brain slices. Nuclei stained blue with Hoescht. **D-F)** Representative HCR RNA-FISH confocal images of A) Timp1, B) Ccl5, C) Lcn2 in LPS mouse hippocampal brain slices. Nuclei stained blue with Hoescht. **G-H**) The mean fluorescent intensity was greater in the LPS group compared to the control group for G) Timp1, H) Ccl5, and I) Lcn2 across their mid-slice images. Values with means ± SEM; ****p ≤ 0.0001; Mann-Whitney test.

3.4 Lipopolysaccharide evokes cell-type-specific transcriptomic changes from astrocytes and microglia in mouse hippocampal organotypic brain slice cultures.

In addition to its more generalised inflammatory effects, LPS elicited cell-type-specific gene expression changes. To probe into cell-type-specific effects, I chose to examine the genes that were uniquely differentially expressed in either astrocytes or microglia between the control and LPS condition. Out of a total of 513 astrocyte DEGs, 353 (68.8%) were uniquely differentially expressed in the astrocyte cluster and no other cluster (Figure 3.3B). Similarly, out of 338 microglial DEGs, 219 (64.8%) were uniquely differentially expressed in microglia. The average expression of the top 20 astrocyte DEGs and top 20 microglial DEGs was plotted across all clusters for the control and LPS group (Figures 3.5 A, B). The heatmaps indicate that the astrocyte DEGs are more broadly differentially expressed across other clusters, whereas the microglial DEGs appear to show slightly more cell-type-specific differential expression (Figures 3.5 A, B). Volcano plots of the DE results for the astrocytes and microglia indicated some overlapping and unique DEGs for these two clusters (Figures 3.5 C, D). Additionally, the volcano plots demonstrate generally higher Log2FoldChanges and more significant adjusted p-values for the astrocyte DEGs than the microglial DEGs (Figures 3.5 C, D). In addition to the upregulation of various pro-inflammatory genes in the microglial clusters such as *Tnf*, *Il1b*, and *Cll2*, I also observed a downregulation of several homeostatic genes, including *Siglech*, *Gpr34*, *P2ry12*, and *Mef2c*[239]. On the other hand, transforming growth factor-β (TGF-β) has been implicated in homeostatic microglial signalling[240], and the gene encoding its receptor, *Tgfbr1*, was found to be upregulated in microglia in my dataset (Supplementary 9). An enrichment analysis was performed on all upregulated control vs LPS DEGs for astrocytes and microglia, respectively, and showed the same or very similar enriched pathways between the two cell types, including cytokine-mediated signalling, type I interferon signalling, and cellular responses to cytokines which were linked to genes such as *Ifitm3*, *Iftim2*, *Cxcl1*, *Stat1*, *Gbp6*, and *Sp100* (Figures 3.5 E, F, Supplementary 12). There were no significantly enriched pathways for the astrocyte downregulated DEGs (Supplementary 12), and only very few pathways enriched for the downregulated microglial DEGs, including cell differentiation and lipoxin metabolic process (Supplementary 12).

To home in on genes that show the largest differences in expression between astrocytes and microglia in response to LPS, I decided to look at the set of DEGs in the astrocyte and microglia clusters and compare the Log2FoldChanges, the percentage of nuclei expressing a gene in the LPS condition, as well as the average expression levels in the LPS condition for the astrocytes and microglia, respectively. To carry out this comparison, the following scatterplots were generated for the set of all DEGs in both the astrocyte and microglia clusters:

1) the Log2FoldChanges of the genes in the astrocytes plotted against the Log2FoldChanges of the genes in microglia (Figure 3.5 G); 2) the percentage of nuclei expressing the genes in the LPS astrocytes versus LPS microglia (Figure 3.5 H); 3) the average expression levels of the genes across the LPS samples in the astrocytes versus microglia (Figure 3.5 I). Using these scatterplots, several DEGs were identified as showing distinct differential expression between astrocytes and microglia including *Pid1* and *Pik3ap* that were Microglia-specific LPS response genes, as well as *Chl1* which was an Astrocyte-specific LPS response gene (Figures 3.5 G-I). Moreover, there were a few genes that showed the opposite direction of change in microglia and astrocytes, such as *Pde7b, Cd38*, and *Otog* which were upregulated in microglia but downregulated in astrocytes (Figure 3.5 G).

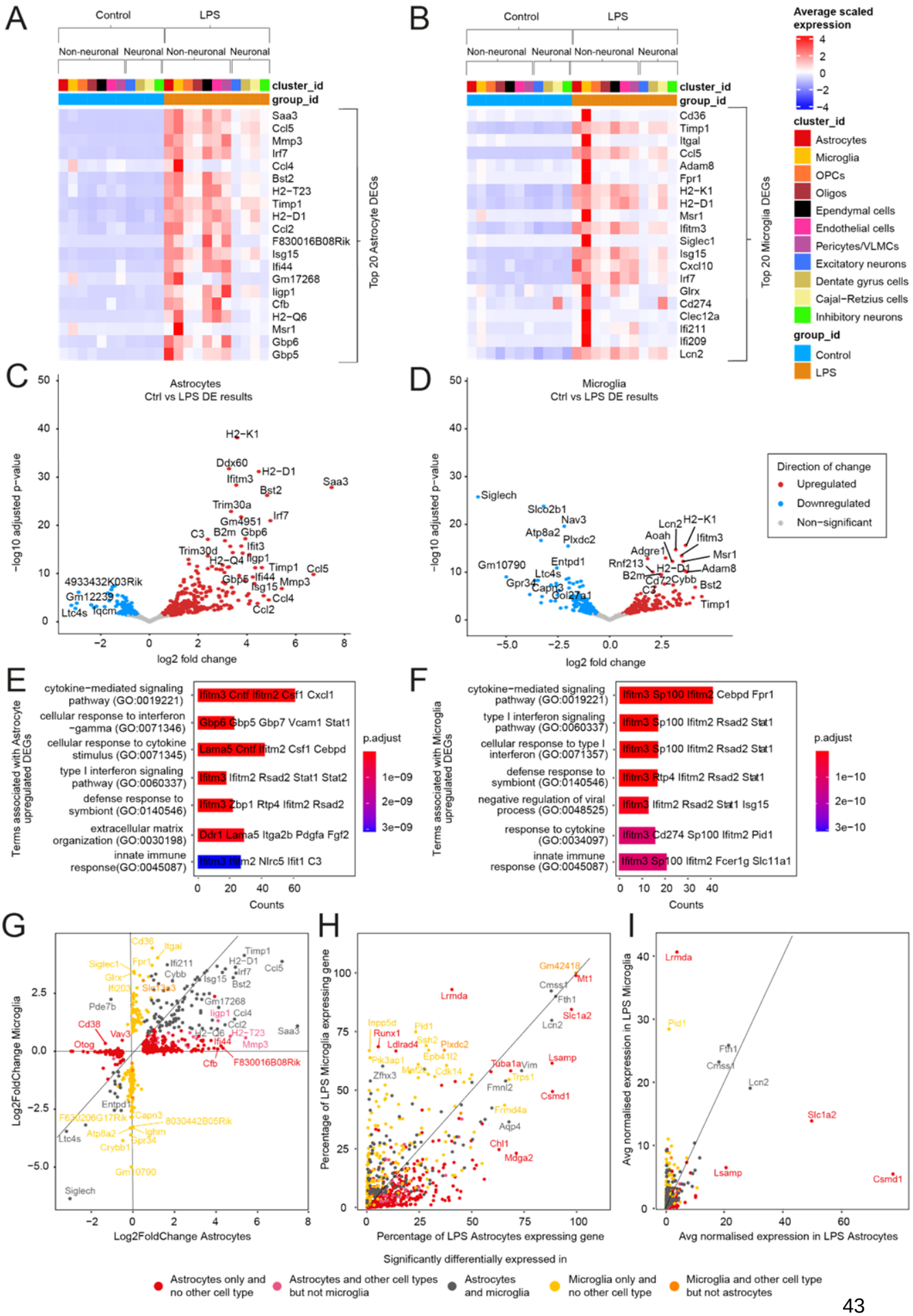
A
Control
LPS
Non-neuronal
Neuronal
Non-neuronal
Neuronal
cluster_id
group_id
Saa3
Ccl5
Mmp3
Irf7
Ccl4
Bst2
H2−T23
Timp1
H2−D1
Ccl2
F830016B08Rik
Isg15
Ifi44
Gm17268
Iigp1
Cfb
H2−Q6
Msr1
Gbp6
Gbp5
Top 20 Astrocyte DEGs
B
Control
LPS
Non-neuronal
Neuronal
Non-neuronal
Neuronal
cluster_id
group_id
Cd36
Timp1
Itgal
Ccl5
Adam8
Fpr1
H2−K1
H2−D1
Msr1
Ifitm3
Siglec1
Isg15
Cxcl10
Irf7
Glrx
Cd274
Clec12a
Ifi211
Ifi209
Lcn2
Top 20 Microglia DEGs
Average scaled expression
4
2
0
−2
−4
cluster_id
Astrocytes
Microglia
OPCs
Oligos
Ependymal cells
Endothelial cells
Pericytes/VLMCs
Excitatory neurons
Dentate gyrus cells
Cajal−Retzius cells
Inhibitory neurons
group_id
Control
LPS
C
Astrocytes
Ctrl vs LPS DE results
−log10 adjusted p−value
log2 fold change
H2−K1
Ddx60
H2−D1
Ifitm3
Saa3
Bst2
Trim30a
Irf7
Gm4951
C3
B2m
Gbp6
Ifit3
Trim30d
H2−Q4
Iigp1
Timp1
Ccl5
Gbp5
Ifi44
Mmp3
Isg15
Ccl4
Ccl2
4933432K03Rik
Gm12239
Ltc4s
Iqcm
D
Microglia
Ctrl vs LPS DE results
−log10 adjusted p−value
log2 fold change
Siglech
Slco2b1
Nav3
Atp8a2
Plxdc2
Gm10790
Entpd1
Ltc4s
Gpr34
Capn3
Gol27a1
Lcn2
H2−K1
Aoah
Ifitm3
Adgre1
Msr1
Rnf213
H2−D1
Adam8
B2m
Cd72
Cybb
Bst2
C3
Timp1
Direction of change
Upregulated
Downregulated
Non−significant
E
Terms associated with Astrocyte upregulated DEGs
cytokine−mediated signaling pathway (GO:0019221)
cellular response to interferon −gamma (GO:0071346)
cellular response to cytokine stimulus (GO:0071345)
type I interferon signaling pathway (GO:0060337)
defense response to symbiont (GO:0140546)
extracellular matrix organization (GO:0030198)
innate immune response(GO:0045087)
Ifitm3 Cntf Ifitm2 Csf1 Cxcl1
Gbp6 Gbp5 Gbp7 Vcam1 Stat1
Lama5 Cntf Ifitm2 Csf1 Cebpd
Ifitm3 Ifitm2 Rsad2 Stat1 Stat2
Ifitm3 Zbp1 Rtp4 Ifitm2 Rsad2
Ddr1 Lama5 Itga2b Pdgfa Fgf2
Ifitm3 Ifitm2 Nlrc5 Ifit1 C3
p.adjust
1e−09
2e−09
3e−09
Counts
F
Terms associated with Microglia upregulated DEGs
cytokine−mediated signaling pathway (GO:0019221)
type I interferon signaling pathway (GO:0060337)
cellular response to type I interferon (GO:0071357)
defense response to symbiont (GO:0140546)
negative regulation of viral process (GO:0048525)
response to cytokine (GO:0034097)
innate immune response (GO:0045087)
Ifitm3 Sp100 Ifitm2 Cebpd Fpr1
Ifitm3 Sp100 Ifitm2 Rsad2 Stat1
Ifitm3 Sp100 Ifitm2 Rsad2 Stat1
Ifitm3 Rtp4 Ifitm2 Rsad2 Stat1
Ifitm3 Ifitm2 Rsad2 Stat1 Isg15
Ifitm3 Cd274 Sp100 Ifitm2 Pid1
Ifitm3 Sp100 Ifitm2 Fcer1g Slc11a1
p.adjust
1e−10
2e−10
3e−10
Counts
G
Log2FoldChange Microglia
Log2FoldChange Astrocytes
Cd36
Itgal
Timp1
Siglec1
Fpr1
Ifi211
H2−D1
Ccl5
Glrx
Cybb
Isg15
Irf7
Ifi203
Slc1a3
Bst2
Pde7b
Gm17268
Iigp1
Ccl4
Cd38
Vav3
Ccl2
Saa3
Otog
H2−Q6
H2−T23
Mmp3
Ifi44
Cfb
F830016B08Rik
Entpd1
F630206G17Rik
Capn3
8030442B05Rik
Ltc4s
Atp8a2
Ighm
Spr34
Crybb1
Gm10790
Siglech
H
Percentage of LPS Microglia expressing gene
Percentage of LPS Astrocytes expressing gene
Gm42418
Mt1
Cmss1
Fth1
Lrmda
Slc1a2
Lcn2
Inpp5d
Pid1
Runx1
Ldlrad4
Ssh2
Plxdc2
Epb41l2
Lsamp
Pik3ap1
Tuba1a
Vim
Mef2c
Cdk14
Trps1
Zfhx3
Fmnl2
Csmd1
Frmd4a
Aqp4
Chl1
Mdga2
I
Avg normalised expression in LPS Microglia
Avg normalised expression in LPS Astrocytes
Lrmda
Pid1
Fth1
Cmss1
Lcn2
Slc1a2
Lsamp
Csmd1
Significantly differentially expressed in
Astrocytes only and no other cell type
Astrocytes and other cell types but not microglia
Astrocytes and microglia
Microglia only and no other cell type
Microglia and other cell type but not astrocytes

Figure 3.5 Lipopolysaccharide evokes cell-type-specific transcriptomic changes from astrocytes and microglia in mouse hippocampal organotypic brain slice cultures.

A-B) Heatmap showing the average expression of the top 20 A) Astrocyte and B) Microglia differentially expressed genes (DEGs) for the control versus LPS differential expression analysis. Normalised and scaled average expression levels are shown for the set of genes across the coarse clusters in the control and LPS group. Genes are ranked according to their absolute Log2FoldChange with upregulated genes at the top. **C-D)** Volcano plots of the differential expression results between control and LPS for the C) Astrocyte and D) Microglia clusters. Upregulated genes are coloured red; downregulated genes are coloured blue; genes that were not significantly differentially expressed are coloured grey. **E, F)** Enrichment analysis showing the top GO Biological Processes 2021 terms associated with the E) Astrocyte and F) Microglia upregulated genes for the control versus LPS differential expression analysis. Bars are coloured according to the adjusted p-value for the corresponding term (p.adjust). The length of each bar reflects the number of genes associated with the corresponding term (counts). **G)** Scatterplot showing the Log2FoldChanges for each of the Astrocyte and Microglia DEGs in Astrocytes versus Microglia. **H)** Scatterplot showing the percentage of LPS Astrocytes versus the percentage of LPS Microglia expressing each of the Astrocyte and Microglia DEGs. **I)** Scatterplot showing the average expression levels of each of the Astrocyte and Microglia DEGs in LPS Astrocytes versus LPS Microglia.

3.5 Lipopolysaccharide has little effect on the expression of neuronal excitability genes in mouse hippocampal organotypic brain slice cultures.

Based on previous literature that has suggested a role for neuroinflammation in contributing to seizure activity, I was interested to explore how LPS affects the expression of genes that may mediate changes in excitability in neurons. To begin, I looked at the results of the DE analysis between the control and LPS group in the coarse neuronal clusters including the excitatory neurons, Cajal-Retzius cells, dentate gyrus cells, and inhibitory neurons. The excitatory neurons had the largest number of DEGs with 114 upregulated genes and 34 downregulated genes, whilst the inhibitory neurons had only 18 upregulated genes and 1 downregulated gene (Figure 3.6 A). A heatmap showing the average expression of all the neuronal DEGs across the nuanced neuronal clusters demonstrates a widespread upregulation of genes in response to LPS (Figure 3.6 B). This general upregulation can also be seen in the volcano plots showing the results of the DE analysis for the excitatory neurons, dentate gyrus cells, and inhibitory neurons (Figures 7 D-F). The main pathways associated with the upregulated genes for the excitatory neurons, dentate gyrus cells, and inhibitory neuron clusters in response to LPS were inflammatory pathways, including cytokine mediated signalling pathways, type I interferon signalling, and the innate immune response (Figures 7 G-I, Supplementary 12). There were no significantly enriched terms for the downregulated excitatory neuron DEGs, and only one downregulated gene for the inhibitory neuron population and thus no enrichment analysis was performed for this. On the other hand, the downregulated DEGs of the dentate gyrus cells were associated with terms including phosphorylation and kinase activity as well as phagocytosis, implying a downregulation of these processes (Supplementary 12). These pathways could potentially mediate changes in

excitability as phosphorylation of receptors and ion channels is one way in which synaptic transmission is mediated. There was only one other enriched term that appeared to potentially be linked to neurotransmission which was the purinergic nucleotide signalling pathways that was associated with the upregulated *C3* gene in inhibitory neurons (Supplementary 12). Other than these pathways, no other terms relating to neurotransmission, synaptic changes, or excitability were found to be associated with the neuronal DEGs (Supplementary 12).

Additionally, a more biased analysis was carried out by curating a list of 608 “excitability genes” which could potentially be implicated in modulating network excitability (To see list of genes see Supplementary 13). The list was constructed by using the Ensembldb[241] package to obtain the Ensembl database gene descriptions for all genes in the dataset. These Ensembl gene descriptions were then searched to select any genes that included at least one of the following key words in its description: ("voltage", "cation", "gated", "sodium", "potassium", "calcium", "chloride", "glutamate", "NMDA", "AMPA", "Kainate", "GABA", "purinergic", "succinate", "serotonin", "dopamine", "cholinergic", "glycine", "neuropeptide", "metabotropic", "ionotropic"). It is acknowledged that the list of genes derived from this method is neither exhaustive of all genes that may mediate neuronal excitability, nor does it necessarily include only genes that may mediate excitability as some of the search terms are relatively broad. As this was an exploratory analysis, I justified using this relatively lenient approach as I wanted to get a general sense whether genes that may mediate neuronal excitability (i.e., “excitability genes”) are differentially expressed between the control and LPS group. To validate the excitability genes, I performed an enrichment analysis on the list of genes and was able to confirm that they are predominantly associated with neurotransmission and other related pathways (Supplementary 13). The heatmap displaying the average expression of a subset of the excitability genes shows few obvious changes in gene expression between the control and LPS condition across the different neuronal clusters (Figure 3.6 C). This contrasts the heatmap depicting the average expression of the neuronal DEGs across the neuronal clusters (Figure 3.6 B). Out of the 608 excitability genes, only 5 were found to be differentially expressed in one or more of the neuronal clusters in response to LPS (See bolded genes in Figure 3.6 C). The 5 differentially expressed excitability genes were all upregulated in response to LPS and included *Slc13a3*, *S100a6*, *S100a11*, *Npy2r*, and *S100a13* (See Supplementary 14 for the clusters they were differentially expressed in). An enrichment analysis was carried out on the 5 putative excitability genes to see if they were in fact related to neurotransmission. The enriched terms were found to mostly be linked to inflammatory and metabolic pathways such as regulation of interleukin-1 alpha production, succinate transport, and mast cell activation (Supplementary 14). Aside from *Slc13a3’s* involvement in anion transmembrane transport and

S100a6 association with axon development, there were no distinct enriched pathways relating to neuronal excitability for the set of 5 excitability DEGs (Supplementary 14).

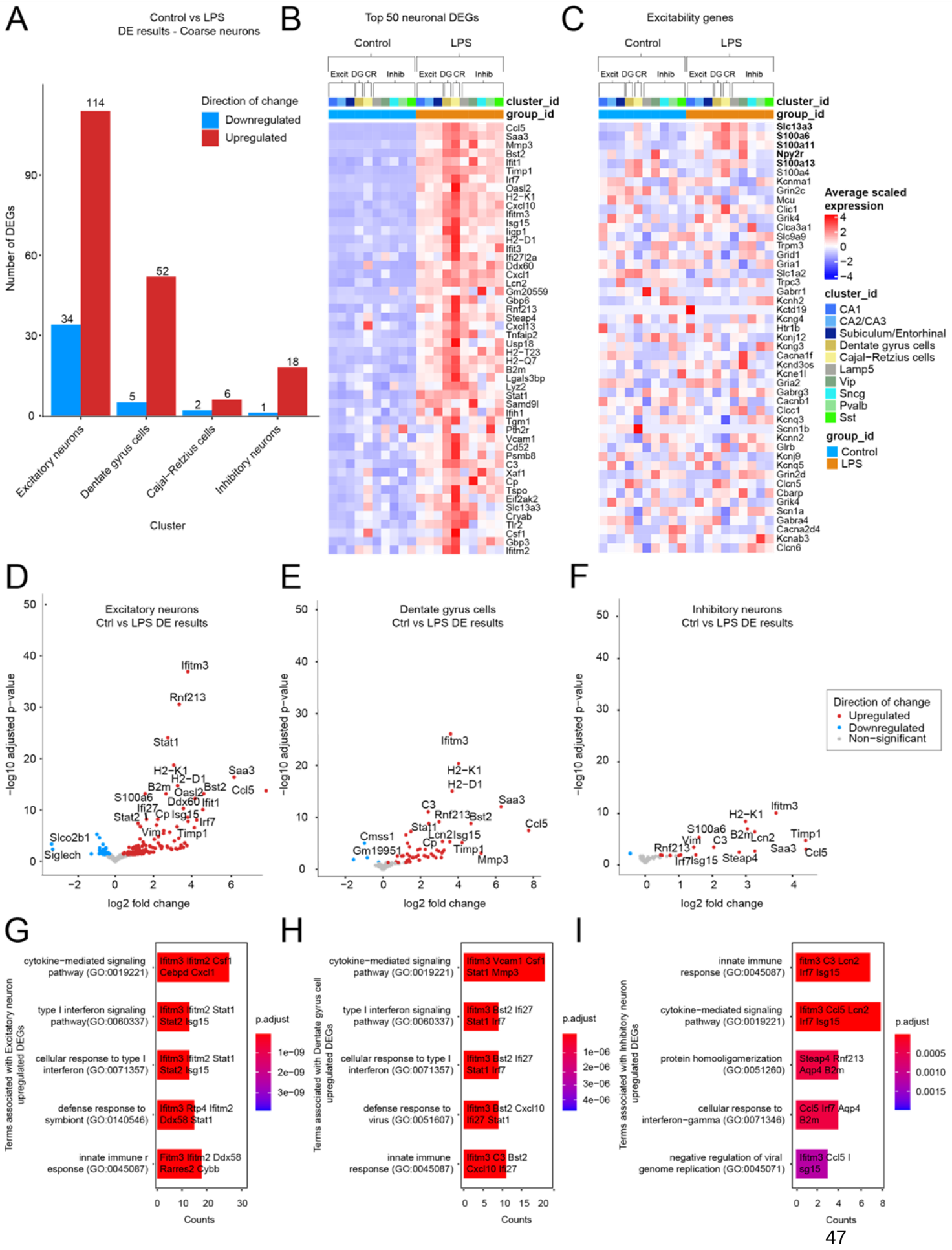
A
Control vs LPS
DE results - Coarse neurons
Direction of change
Downregulated
Upregulated
Number of DEGs
Cluster
Excitatory neurons
Dentate gyrus cells
Cajal−Retzius cells
Inhibitory neurons
114
34
52
5
6
2
18
1
B
Top 50 neuronal DEGs
Control
LPS
Excit DG CR Inhib
cluster_id
group_id
C
Excitability genes
Average scaled expression
cluster_id
CA1
CA2/CA3
Subiculum/Entorhinal
Dentate gyrus cells
Cajal−Retzius cells
Lamp5
Vip
Sncg
Pvalb
Sst
group_id
Control
LPS
D
Excitatory neurons
Ctrl vs LPS DE results
−log10 adjusted p−value
log2 fold change
E
Dentate gyrus cells
Ctrl vs LPS DE results
F
Inhibitory neurons
Ctrl vs LPS DE results
Direction of change
Upregulated
Downregulated
Non−significant
G
Terms associated with Excitatory neuron upregulated DEGs
cytokine−mediated signaling pathway (GO:0019221)
type I interferon signaling pathway(GO:0060337)
cellular response to type I interferon (GO:0071357)
defense response to symbiont (GO:0140546)
innate immune response (GO:0045087)
p.adjust
Counts
H
Terms associated with Dentate gyrus cell upregulated DEGs
I
Terms associated with Inhibitory neuron upregulated DEGs
protein homooligomerization (GO:0051260)
cellular response to interferon−gamma (GO:0071346)
negative regulation of viral genome replication (GO:0045071)

Figure 3.6 Lipopolysaccharide has little effect on the expression of neuronal excitability genes in mouse hippocampal organotypic brain slice cultures.

A) Number of upregulated and downregulated differentially expressed genes (DEGs) across the coarse neuronal clusters for the control versus LPS differential expression analysis. **B)** Heatmap showing the average expression across of the top 50 coarse neuron DEGs for the control versus LPS differential expression analysis. Normalised and scaled average expression levels are shown for the set of genes across the nuanced neuronal clusters in the control and LPS group. Genes are ranked according to their absolute Log2FoldChange with upregulated genes at the top. **C)** Heatmap showing the average expression of a subset of excitability genes. Normalised and scaled average expression levels are shown for the set of genes across the nuanced neuronal clusters in the control and LPS group. Differentially expressed excitability genes are bolded and at the top. **D-F)** Volcano plots of the differential expression results between control and LPS for the D) Excitatory neuron, E) Dentate gyrus cell, and F) Inhibitory neuron clusters. Upregulated genes are coloured red; downregulated genes are coloured blue; genes that were not significantly differentially expressed are coloured grey. **G-I)** Enrichment analysis showing the top GO Biological Processes 2021 terms associated with the G) Excitatory neuron, H) Dentate gyrus cell, and I) Inhibitory neuron upregulated genes for the control versus LPS differential expression analysis. Bars are coloured according to the adjusted p-value for the corresponding term (p.adjust). The length of each bar reflects the number of genes associated with the corresponding term (counts).

3.6 The *Taenia crassiceps* homogenate has little effect on gene expression compared to control conditions.

Having explored the effect of LPS on cell-type-specific transcription, I next wanted to carry out a similar analysis but this time looking at how the *T. crassiceps* homogenate affects gene expression relative to control conditions at single-cell resolution (See Supplementary 15 for the control versus Hom significant DEGs per cluster). The same integrated snRNAseq dataset from the previous analysis was used (Figure 3.2 A-C) but this time the control samples were compared to the Hom samples. A pairwise DE analysis was run between the control and Hom condition for each nuanced cluster and revealed only 48 DEGs in total across the clusters (Figure 3.7 A). A heatmap to visualise these gene expression changes also indicated no obvious effect of the *T. crassiceps* homogenate relative to the control condition, suggesting only small changes in gene expression between these two conditions (Figure 3.7 C). Interestingly, all of the DEGs were uniquely differentially expressed in their respective clusters as seen in the UpSet plot in which the set size for each cluster's set of DEGs is equal to the number of DEGs uniquely differentially expressed in that cluster (Figure 3.7 B). An enrichment analysis of all upregulated DEGs in response to the homogenate revealed an association with terms including negative regulation of cGMP and cAMP signalling associated with *Pde11a* which was upregulated in CA1 neurons; cellular polysaccharide catabolic process, carbohydrate derivative, and lipid catabolic process associated with *Aoah* which was upregulated in Sst neurons; as well as peptidyl-threonine and peptidyl-tyrosine dephosphorylation associated with *Dusp5* which was upregulated in Sncg neurons (Figure 3.7 D, Supplementary 16). There were no GO Biological Processes terms significantly enriched

for the set of downregulated control vs Hom DEGs for the nuanced clusters (Supplementary 16). Furthermore, none of the excitability DEGs were found to be differentially expressed between the control vs Hom coarse neuronal clusters (Supplementary 17) It was notable, nonetheless, that the gene encoding the receptor for Substance P, *Tacr1,* was downregulated in microglia in response to the homogenate (Supplementary 15). Interestingly, however, it was the Lamp5 interneurons that had the greatest percentage of nuclei expressing the *Tacr1* gene (Supplementary 11). On the other hand, *Tac1* which is the gene that encodes the precursor protein for Substance P was not differentially expressed in any cell type between the control and Hom condition (Supplementary 15). It was noteworthy, nonetheless, that the Parvalbumin (Pvalb) interneurons had the greatest percentage of nuclei expressing the *Tac1* gene (Supplementary 11).

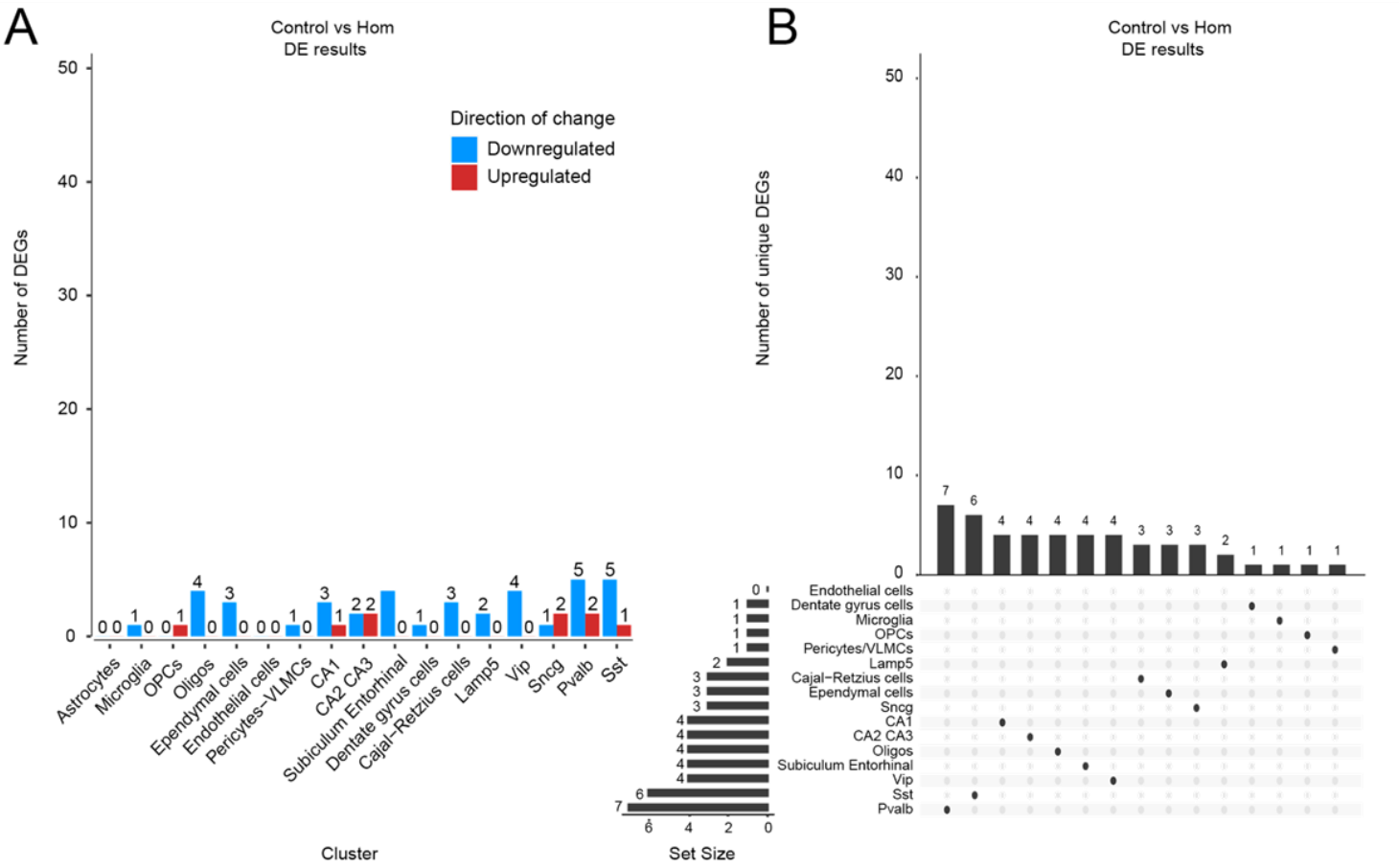
A
Control vs Hom
DE results
Direction of change
Downregulated
Upregulated
Number of DEGs
Astrocytes
Microglia
OPCs
Oligos
Ependymal cells
Endothelial cells
Pericytes−VLMCs
CA1
CA2 CA3
Subiculum Entorhinal
Dentate gyrus cells
Cajal−Retzius cells
Lamp5
Vip
Sncg
Pvalb
Sst
Cluster
Set Size
B
Control vs Hom
DE results
Number of unique DEGs

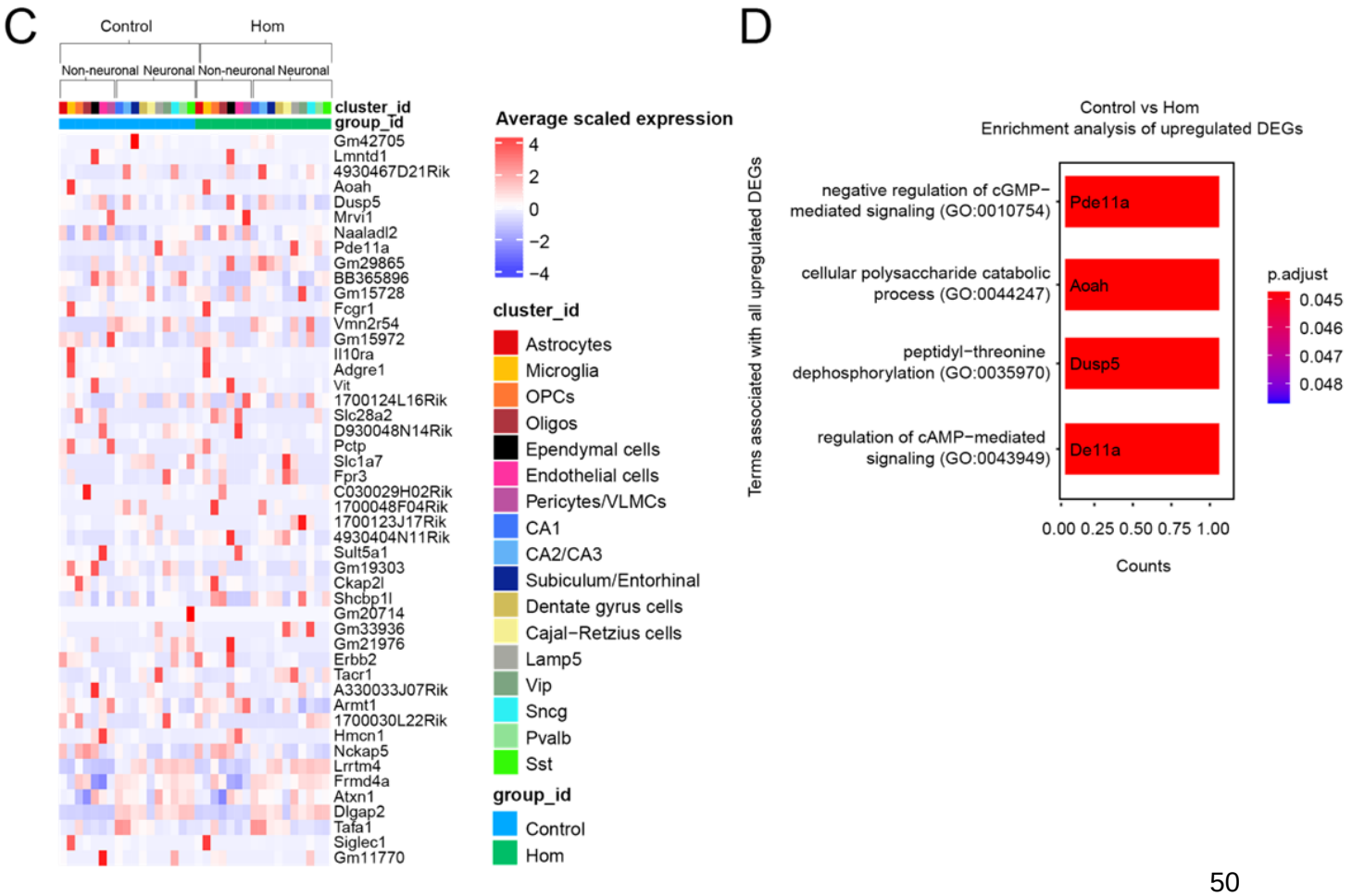
C
Control
Hom
Non-neuronal
Neuronal
Non-neuronal
Neuronal
cluster_id
group_id
Gm42705
Lmntd1
4930467D21Rik
Aoah
Dusp5
Mrvi1
Naaladl2
Pde11a
Gm29865
BB365896
Gm15728
Fcgr1
Vmn2r54
Gm15972
Il10ra
Adgre1
Vit
1700124L16Rik
Slc28a2
D930048N14Rik
Pctp
Slc1a7
Fpr3
C030029H02Rik
1700048F04Rik
1700123J17Rik
4930404N11Rik
Sult5a1
Gm19303
Ckap2l
Shcbp1l
Gm20714
Gm33936
Gm21976
Erbb2
Tacr1
A330033J07Rik
Armt1
1700030L22Rik
Hmcn1
Nckap5
Lrrtm4
Frmd4a
Atxn1
Dlgap2
Tafa1
Siglec1
Gm11770
Average scaled expression
cluster_id
Astrocytes
Microglia
OPCs
Oligos
Ependymal cells
Endothelial cells
Pericytes/VLMCs
CA1
CA2/CA3
Subiculum/Entorhinal
Dentate gyrus cells
Cajal−Retzius cells
Lamp5
Vip
Sncg
Pvalb
Sst
group_id
Control
Hom
D
Control vs Hom
Enrichment analysis of upregulated DEGs
Terms associated with all upregulated DEGs
negative regulation of cGMP−mediated signaling (GO:0010754)
cellular polysaccharide catabolic process (GO:0044247)
peptidyl−threonine dephosphorylation (GO:0035970)
regulation of cAMP−mediated signaling (GO:0043949)
Pde11a
Aoah
Dusp5
De11a
p.adjust
Counts

Figure 3.7 The *Taenia crassiceps* homogenate has little effect on gene expression compared to control conditions.

A) Number of upregulated and downregulated differentially expressed genes (DEGs) across the nuanced clusters for the control versus Hom differential expression analysis. **B)** UpSet plot showing all 48 DEGs across the nuanced clusters for the control versus Hom differential expression analysis. Single dots indicate uniquely differentially expressed genes for a cluster. All DEGs were unique to their respective cluster. **C)** Heatmap showing the average expression levels of all 48 DEGs for the control versus Hom differential expression analysis. Normalised and scaled average expression levels are shown for the set of genes across the nuanced clusters in the control and Hom group. Genes are ranked according to their absolute Log2FoldChange with upregulated genes at the top. **D**) Enrichment analysis showing the top GO Biological Processes 2021 terms associated with all upregulated genes across all coarse clusters for the control versus Hom differential expression analysis. Bars are coloured according to the adjusted p-value for the corresponding term (p.adjust). The length of each bar reflects the number of genes associated with the corresponding term (counts).

3.7 The *Taenia crassiceps* homogenate elicits prominent immunosuppressive transcriptomic changes across different cell types when added to LPS.

Based on previous work in the Raimondo lab, I was aware that the immunosuppressive effects of the *T. crassiceps* homogenate can only be fully appreciated if there is an existing inflammatory reaction against which to compare the homogenate's effects. I therefore ran a DE analysis to compare how the addition of the homogenate to LPS (LPS+Hom) affects cell-type-specific gene expression relative to LPS by itself. DESeq2 was used to run a pairwise DE analysis between the LPS group and the LPS+Hom group for each of the coarse clusters (Supplementary 18). This analysis yielded a considerable set of DEGs across the clusters with the most obvious effects seen in astrocytes and microglia which had the largest number of significantly differentially expressed genes (Figure 3.8 A). The majority of DEGs were downregulated (Figure 3.8 A) and relatively generalised transcriptional changes were seen across the cell types with 149 DEGs overlapping across two or more clusters (Figure 3.8 B). The average expression levels of the top 20 DEGs for the LPS versus LPS+Hom DE analysis ranked according to absolute Log2FoldChange was visualised for each sample (Figure 3.8 C). This plot illustrates a tendency for the control and Hom samples to have very similar gene expression levels, the LPS samples to deviate noticeably from these, and the average gene expression levels of the LPS+Hom samples tending to fall somewhere in between (Figure 3.8 C). A similar trend can be observed in the heatmap showing the average expression levels of these same top 20 DEGs across the coarse clusters for each treatment group (Figure 3.8 D). The heatmap suggests that the same DEGs that are upregulated in response to LPS relative to control, are being downregulated by the addition of the homogenate to LPS (Figure 3.8 D). An enrichment analysis was run on the downregulated DEGs between the LPS and LPS+Hom conditions. The enrichment analysis revealed that the addition of the *T. crassiceps* to LPS is

primarily associated with a downregulation of inflammatory functions including cytokine-mediated signalling, responses to cytokines, and type I interferon signalling pathways (Figure 3.9 E, Supplementary 19). In addition, the MyD88-independent toll-like receptor signalling pathways, including the TRIF-dependent toll-like receptor signalling and its downstream pathways, including the MAPK cascade and NF-kappaB signalling were downregulated (Supplementary 19). The MyD88-dependent toll-like receptor signalling pathway was also associated with the downregulated DEGs, but this was not statistically significant when looking at the adjusted p-value (Supplementary 19). There were only three significantly enriched terms for the upregulated LPS versus LPS+Hom genes, and these were related to nervous system development and extracellular structure organisation (Supplementary 19). To further explore the effect of the homogenate on the toll-like receptor signalling pathways, I also performed a DE analysis between the control and LPS+Hom groups (Supplementary 20) and ran an enrichment analysis on the DEGs (Supplementary 21). I found that none of the toll-like receptor signalling pathways were significantly enriched for the upregulated genes except for the downstream I-kappaB kinase/NF-kappaB signalling (Supplementary 21). This confirms that most toll-like receptor signalling pathways were suppressed by the homogenate.

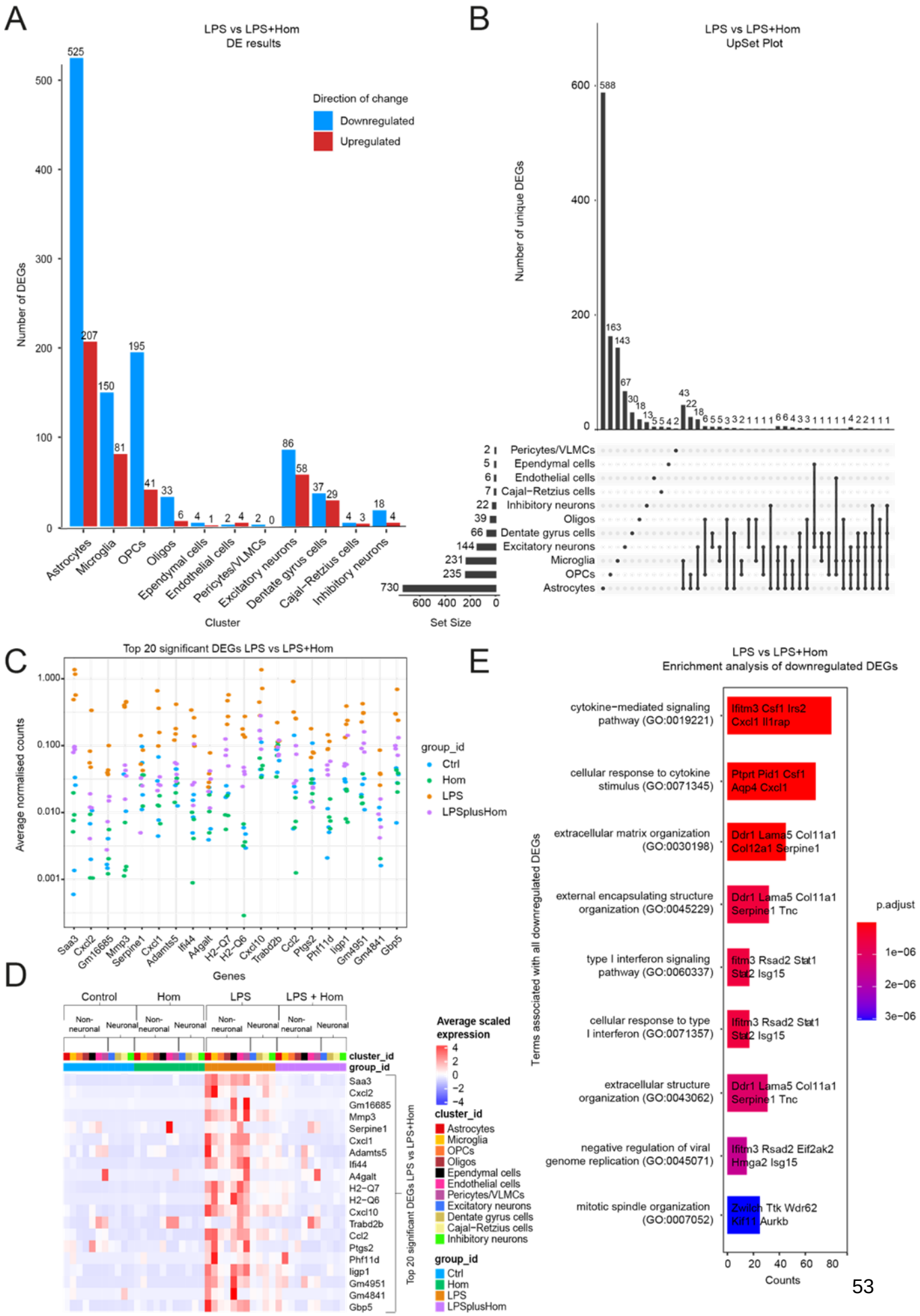
A
LPS vs LPS+Hom
DE results
Direction of change
Downregulated
Upregulated
Number of DEGs
Cluster
Astrocytes
Microglia
OPCs
Oligos
Ependymal cells
Endothelial cells
Pericytes/VLMCs
Excitatory neurons
Dentate gyrus cells
Cajal−Retzius cells
Inhibitory neurons
B
LPS vs LPS+Hom
UpSet Plot
Number of unique DEGs
Set Size
Pericytes/VLMCs
Ependymal cells
Endothelial cells
Cajal−Retzius cells
Inhibitory neurons
Oligos
Dentate gyrus cells
Excitatory neurons
Microglia
OPCs
Astrocytes
C
Top 20 significant DEGs LPS vs LPS+Hom
Average normalised counts
Genes
group_id
Ctrl
Hom
LPS
LPSplusHom
D
Control
Hom
LPS
LPS + Hom
Non-neuronal
Neuronal
cluster_id
group_id
Top 20 significant DEGs LPS vs LPS+Hom
Average scaled expression
cluster_id
Astrocytes
Microglia
OPCs
Oligos
Ependymal cells
Endothelial cells
Pericytes/VLMCs
Excitatory neurons
Dentate gyrus cells
Cajal−Retzius cells
Inhibitory neurons
group_id
Ctrl
Hom
LPS
LPSplusHom
E
LPS vs LPS+Hom
Enrichment analysis of downregulated DEGs
Terms associated with all downregulated DEGs
cytokine−mediated signaling pathway (GO:0019221)
Ifitm3 Csf1 Irs2 Cxcl1 Il1rap
cellular response to cytokine stimulus (GO:0071345)
Ptprt Pid1 Csf1 Aqp4 Cxcl1
extracellular matrix organization (GO:0030198)
Ddr1 Lama5 Col11a1 Col12a1 Serpine1
external encapsulating structure organization (GO:0045229)
Ddr1 Lama5 Col11a1 Serpine1 Tnc
type I interferon signaling pathway (GO:0060337)
Ifitm3 Rsad2 Stat1 Stat2 Isg15
cellular response to type I interferon (GO:0071357)
Ifitm3 Rsad2 Stat1 Stat2 Isg15
extracellular structure organization (GO:0043062)
Ddr1 Lama5 Col11a1 Serpine1 Tnc
negative regulation of viral genome replication (GO:0045071)
Ifitm3 Rsad2 Eif2ak2 Hmga2 Isg15
mitotic spindle organization (GO:0007052)
Zwilch Ttk Wdr62 Kif11 Aurkb
p.adjust
Counts

Figure 3.8 The *Taenia crassiceps* homogenate elicits prominent immunosuppressive transcriptomic changes across different cell types in the presence of LPS.

A) Number of upregulated and downregulated differentially expressed genes (DEGs) across the coarse clusters for the LPS versus LPS+Hom differential expression analysis. **B)** UpSet plot showing the unique and shared DEGs across the coarse clusters for the LPS versus LPS+Hom differential expression analysis. Single dots indicate uniquely differentially expressed genes for a cluster, while dots joined by lines indicated shared DEGs between clusters. **C)** Average expression per sample of the top 20 DEGs for the LPS versus LPS+Hom differential expression analysis. Each data point represents the average expression of a sample coloured by the treatment group it belongs to (control, Hom, LPS, LPS+Hom). **D)** Heatmap showing the average expression of the top 20 DEGs for the LPS versus LPS+Hom differential expression analysis. Normalised and scaled average expression levels are shown for the set of genes across the coarse clusters in all four groups (control, Hom, LPS, and LPS+Hom). Genes are ranked according to their absolute Log2FoldChange with downregulated genes at the top. **E)** Enrichment analysis showing the top GO Biological Processes 2021 terms associated with all downregulated genes across all coarse clusters for the LPS versus LPS+Hom differential expression analysis. Bars are coloured according to the adjusted p-value for the corresponding term (p.adjust). The length of each bar reflects the number of genes associated with the corresponding term (counts).

3.8 The *Taenia crassiceps* homogenate elicits cell-type-specific gene expression changes in astrocytes and microglia when added to LPS.

In addition to its more generalised inflammatory effects, the *T. crassiceps* homogenate elicited cell-type-specific transcriptional changes. The most prominent cell-type-specific responses were observed in the astrocytes and microglia which had 588 and 163 uniquely differentially expressed genes, respectively (Figure 3.9 B). The average expression of the top 20 astrocyte DEGs and top 20 microglial DEGs was plotted across all clusters for the LPS and LPS+Hom group ranked by absolute Log2FoldChange (Figures 3.9 A, B). These heatmaps show similar patterns for the astrocyte and microglia DEGs, with the top DEGs being downregulated by the homogenate when added to LPS (Figures 3.9 A, B). However, the microglia had some genes in this list of top 20 DEGs that were upregulated in the LPS+Hom condition relative to the LPS condition, and this upregulation appears to be relatively specific to the microglia (Figure 3.9 B). Volcano plots of the DE results for the astrocytes and microglia indicated some of the overlapping and unique DEGs for these two clusters (Figures 3.9 C, D). The volcano plots also demonstrate generally higher absolute Log2FoldChanges and more significant adjusted p-values for the astrocyte DEGs than the microglial DEGs (Figures 3.9 C, D). An enrichment analysis was performed on all astrocyte and microglia downregulated DEGs, respectively (Supplementary 22). The enrichment analysis found some of the top enriched pathways of the downregulated genes to be similar between the two cell-types, including cytokine-mediated signalling, type I interferon signalling, and cellular responses to cytokines (Figures 3.9 E, F; Supplementary 22). This suggests that the homogenate elicits immunosuppressive activity in both astrocytes and microglia.

In addition, an exploration was carried out of the uniquely differentially expressed genes of the astrocytes and microglia for the LPS vs LPS+Hom DE analysis. Markedly, 588 out of 732 astrocyte DEGs (80.3%) were uniquely differentially expressed in the astrocyte cluster, while 163 out of 231 microglia DEGs (70.6%) were specifically differentially expressed in the microglia cluster.

The effect of the homogenate on the expression of receptors and binding proteins for LPS was also examined. *Cd14* was found to be downregulated in astrocytes and microglia between the LPS and LPS+Hom groups (Supplementary 18). Similarly, *Lbp* was downregulated in microglia between the LPS and LPS+Hom conditions (Supplementary 18).

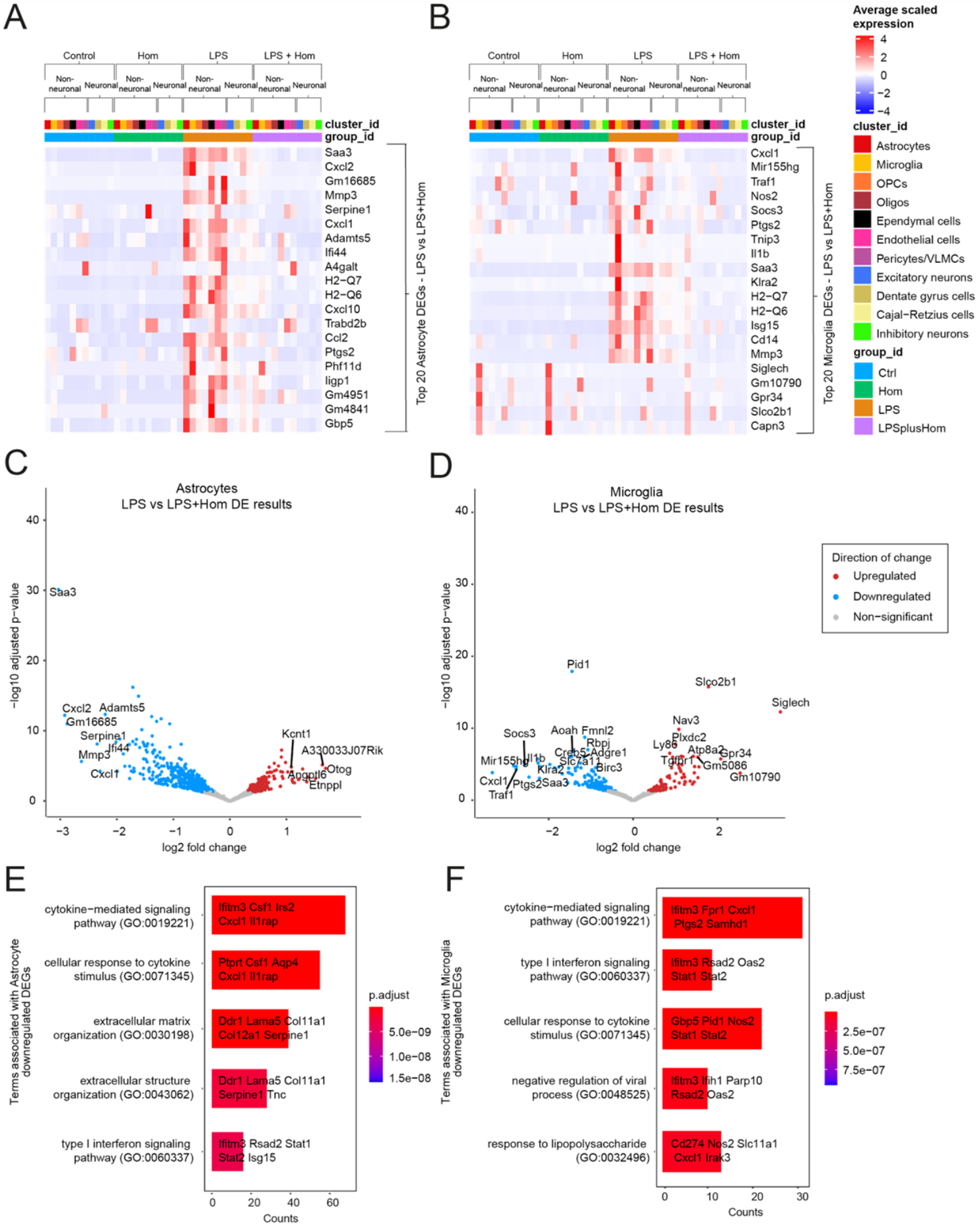
A
Control
Hom
LPS
LPS + Hom
Non-neuronal
Neuronal
cluster_id
group_id
Saa3
Cxcl2
Gm16685
Mmp3
Serpine1
Cxcl1
Adamts5
Ifi44
A4galt
H2−Q7
H2−Q6
Cxcl10
Trabd2b
Ccl2
Ptgs2
Phf11d
Iigp1
Gm4951
Gm4841
Gbp5
Top 20 Astrocyte DEGs - LPS vs LPS+Hom
B
Cxcl1
Mir155hg
Traf1
Nos2
Socs3
Ptgs2
Tnip3
Il1b
Saa3
Klra2
H2−Q7
H2−Q6
Isg15
Cd14
Mmp3
Siglech
Gm10790
Gpr34
Slco2b1
Capn3
Top 20 Microglia DEGs - LPS vs LPS+Hom
Average scaled expression
4
2
0
−2
−4
cluster_id
Astrocytes
Microglia
OPCs
Oligos
Ependymal cells
Endothelial cells
Pericytes/VLMCs
Excitatory neurons
Dentate gyrus cells
Cajal−Retzius cells
Inhibitory neurons
group_id
Ctrl
Hom
LPS
LPSplusHom
C
Astrocytes
LPS vs LPS+Hom DE results
−log10 adjusted p−value
log2 fold change
Saa3
Cxcl2
Adamts5
Gm16685
Serpine1
Ifi44
Mmp3
Cxcl1
Kcnt1
A330033J07Rik
Angptl6
Otog
Etnppl
D
Microglia
LPS vs LPS+Hom DE results
Direction of change
Upregulated
Downregulated
Non−significant
Pid1
Slco2b1
Siglech
Nav3
Plxdc2
Ly86
Atp8a2
Gpr34
Tgfbr1
Gm5086
Gm10790
Socs3
Aoah
Fmnl2
Rbpj
Creb5
Adgre1
Slc7a11
Birc3
Mir155hg
Il1b
Klra2
Cxcl1
Ptgs2
Saa3
Traf1
E
Terms associated with Astrocyte downregulated DEGs
cytokine−mediated signaling pathway (GO:0019221)
Ifitm3 Csf1 Irs2 Cxcl1 Il1rap
cellular response to cytokine stimulus (GO:0071345)
Ptprt Csf1 Aqp4 Cxcl1 Il1rap
extracellular matrix organization (GO:0030198)
Ddr1 Lama5 Col11a1 Col12a1 Serpine1
extracellular structure organization (GO:0043062)
Ddr1 Lama5 Col11a1 Serpine1 Tnc
type I interferon signaling pathway (GO:0060337)
Ifitm3 Rsad2 Stat1 Stat2 Isg15
p.adjust
5.0e−09
1.0e−08
1.5e−08
Counts
F
Terms associated with Microglia downregulated DEGs
cytokine−mediated signaling pathway (GO:0019221)
Ifitm3 Fpr1 Cxcl1 Ptgs2 Samhd1
type I interferon signaling pathway (GO:0060337)
Ifitm3 Rsad2 Oas2 Stat1 Stat2
cellular response to cytokine stimulus (GO:0071345)
Gbp5 Pid1 Nos2 Stat1 Stat2
negative regulation of viral process (GO:0048525)
Ifitm3 Ifih1 Parp10 Rsad2 Oas2
response to lipopolysaccharide (GO:0032496)
Cd274 Nos2 Slc11a1 Cxcl1 Irak3
p.adjust
2.5e−07
5.0e−07
7.5e−07
Counts

Figure 3.9 The *Taenia crassiceps* homogenate elicits cell-type-specific gene expression changes in astrocytes and microglia when added to LPS.

A-B) Heatmap showing the average expression of the top 20 A) Astrocyte and B) Microglia differentially expressed genes (DEGs) for the LPS versus LPS+Hom differential expression analysis. Normalised and scaled average expression levels are shown for the set of genes across the coarse clusters across all four groups (control, Hom, LPS, LPS+Hom). Genes are ranked according to their absolute Log2FoldChange with downregulated genes at the top. **C-D)** Volcano plots of the differential expression results between LPS and LPS+Hom for the C) Astrocyte and D) Microglia clusters. Upregulated genes are coloured red; downregulated genes are coloured blue; genes that were not significantly differentially expressed are coloured grey. **E, F)** Enrichment analysis showing the top GO Biological Processes 2021 terms associated with the E) Astrocyte and F) Microglia downregulated genes for the LPS versus LPS+Hom differential expression analysis. Bars are coloured according to the adjusted p-value for the corresponding term (p.adjust). The length of each bar reflects the number of genes associated with the corresponding term (counts).

3.9 The *Taenia crassiceps* homogenate has minimal effects on the expression of neuronal excitability genes when added to LPS.

Based on previous literature that has suggested a relationship between the immunomodulatory properties of *Taenia* larvae and seizure activity, I was interested to explore how the *T. crassiceps* homogenate affects the expression of genes that may mediate changes in network excitability in the brain. I first chose to explore the results of the DE analysis between the LPS and LPS+Hom conditions in the coarse neuronal clusters, including the excitatory neurons, Cajal-Retzius cells, dentate gyrus cells, and inhibitory neurons. The excitatory neurons had the largest number of DEGs including 86 downregulated genes and 58 upregulated genes, whilst the inhibitory neurons had only 18 downregulated genes and 4 upregulated genes (Figure 3.10 A). Heatmaps were generated to visualise the average expression of the top 20 excitatory neuron, dentate gyrus cell, and inhibitory neuron DEGs across the nuanced neuronal clusters (Figure 3.10 C-E). These figures highlight a set of DEGs for each of the three clusters that are downregulated by the homogenate in response to LPS (Figure 3.9 C-E). Furthermore, it is apparent that when the homogenate is added to LPS, it often brings expression levels of genes that were upregulated in response to LPS back down to similar levels seen in the control and Hom conditions (Figure 3.10 C-E). This relatively generalised downregulation of gene expression in the neuronal clusters can also be appreciated in the volcano plots showing the results of the DE analysis for the excitatory neuron, dentate gyrus cells, and inhibitory neurons (Figures 3.10 F-H). The main pathways associated with the downregulated genes for the excitatory neurons, dentate gyrus cells, and inhibitory neuron clusters in response to the *T. crassiceps* homogenate being added to LPS included cytokine mediated signalling pathways, type I interferon signalling, and interleukin-mediate signalling (Figures 3.10 G-I). There were no significantly enriched terms for the upregulated genes of the excitatory neurons or the dentate gyrus cells (Supplementary 22).

Two of the upregulated DEGs in inhibitory neurons (*Areg* and *Aldoc*) were associated with fructose metabolic process, glucose catabolic process to pyruvate, and glycolytic processes (Supplementary 22). There were a few pathways associated with the downregulated genes that may be linked to neurotransmission including regulation of calcium ion transmembrane transport, regulation of pre-synapse organization, and synaptic membrane adhesion in excitatory neurons; as well as adenylate cyclase-modulating G protein-coupled receptor signalling pathway in dentate gyrus cells (Supplementary 22).

In addition to this, I looked at my curated list of excitability genes and compared this to the DE results between the LPS and LPS+Hom group to see if any of the neuronal DEGs are genes that may mediate excitability. Out of the 608 excitability genes, only 9 were found to be differentially expressed in one or more neuronal clusters (See bolded genes in Figure 3.10 B). The differentially expressed excitability genes between the LPS and LPS+Hom group included *Kcnk13*, *Slc9b2*, *Scn9a*, *Gabrg3*, *Camk1d*, *Catspere2*, *Gria2*, *Hcn1*, and *Cacnb2* (See Supplementary 23 for the clusters they were differentially expressed in). These excitability DEGs were related to various neurotransmission terms, including sodium ion transport, neuronal action potential, GABAergic synaptic transmission, and chloride ion transport for the upregulated excitability genes as well as potassium ion transport, glutamatergic synaptic transmission, and voltage-gated calcium channel activity for the downregulated excitability genes (Supplementary 23). The gene mediating the GABAergic signalling *(Gabrg3*) was upregulated in dentate gyrus cells, whereas the gene mediating glutamatergic activity (*Gria2*) was downregulated in the excitatory neuron cluster (Supplementary 18). On the other hand, looking at overall expression of the other excitability genes across the different neuronal clusters indicated few distinct changes in gene expression between the four treatment groups (Figure 3.10 B). This is contrasted by the heatmaps depicting the average expression of the genes that were differentially expressed in neurons which show quite clear differences across the treatment conditions (Figure 3.10 C-E). To verify whether the set of 9 excitability DEGs between the LPS versus LPS+Hom condition were an effect seen specifically when LPS and Hom act together, I also examined whether any of the excitability genes were differentially expressed between the control and LPS+Hom condition (Supplementary 20). I found that none of the 9 LPS versus LPS+Hom excitability DEGs were differentially expressed between control and LPS+Hom, indicating that they are not genes which are specifically differentially expressed when the brain is exposed to both LPS and the *T. crassiceps* homogenate in combination. However, there were four other excitability genes found to be differentially expressed in one or more of the neuronal clusters between control and LPS+Hom including *Kcnab1*, *S100a6*, *Npsr1*, and *Trpc4* (See Supplementary 24 for the clusters they were differentially expressed in).

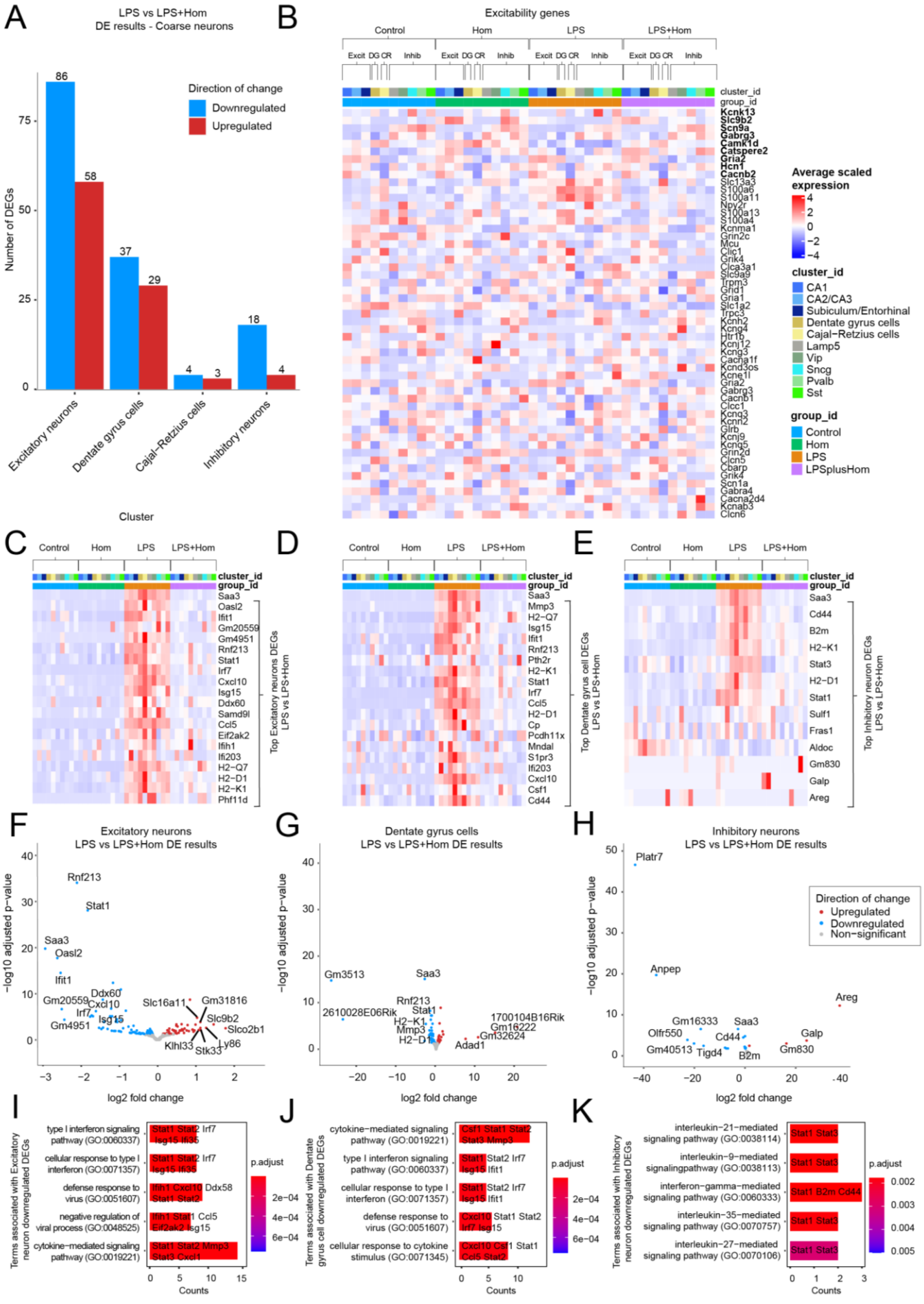
A
LPS vs LPS+Hom
DE results - Coarse neurons
Direction of change
Downregulated
Upregulated
Number of DEGs
86
58
37
29
4
3
18
4
Excitatory neurons
Dentate gyrus cells
Cajal−Retzius cells
Inhibitory neurons
B
Excitability genes
Control
Hom
LPS
LPS+Hom
Excit DG CR Inhib
cluster_id
group_id
Average scaled expression
cluster_id
CA1
CA2/CA3
Subiculum/Entorhinal
Dentate gyrus cells
Cajal−Retzius cells
Lamp5
Vip
Sncg
Pvalb
Sst
group_id
Control
Hom
LPS
LPSplusHom
Cluster
C
Top Excitatory neurons DEGs
LPS vs LPS+Hom
D
Top Dentate gyrus cell DEGs
LPS vs LPS+Hom
E
Top Inhibitory neuron DEGs
LPS vs LPS+Hom
F
Excitatory neurons
LPS vs LPS+Hom DE results
−log10 adjusted p−value
log2 fold change
G
Dentate gyrus cells
LPS vs LPS+Hom DE results
H
Inhibitory neurons
LPS vs LPS+Hom DE results
Direction of change
Upregulated
Downregulated
Non−significant
I
Terms associated with Excitatory neuron downregulated DEGs
J
Terms associated with Dentate gyrus cell downregulated DEGs
K
Terms associated with Inhibitory neuron downregulated DEGs
p.adjust
Counts

Figure 3.10 The *Taenia crassiceps* homogenate has minimal effects on the expression of neuronal excitability genes when added to LPS.

A) Number of upregulated and downregulated differentially expressed genes (DEGs) across the coarse neuronal clusters for the LPS versus LPS+Hom differential expression analysis. **B)** Heatmap showing the average expression of a subset of excitability genes. Normalised and scaled average expression levels are shown for the set of genes across the nuanced neuronal clusters for all four treatment groups (control, Hom, LPS, LPS+Hom). Differentially expressed excitability genes between the LPS and LPS+Hom group are bolded and at the top. **C-E)** Heatmap showing the average expression of the top 20 C) Excitatory neuron, D) Dentate gyrus cell, and E) Inhibitory neuron DEGs for the LPS versus LPS+Hom differential expression analysis. Normalised and scaled average expression levels are shown for the set of genes across the nuanced clusters in all four groups (control, Hom, LPS, LPS+Hom). Genes are ranked according to their absolute Log2FoldChange with downregulated genes at the top and only genes that had average expression levels > 0 in the LPS+Hom condition represented. **F-H)** Volcano plots of the differential expression results between LPS and LPS+Hom for the D) Excitatory neuron, E) Dentate gyrus cell, and F) Inhibitory neuron clusters. Upregulated genes are coloured red; downregulated genes are coloured blue; genes that were not significantly differentially expressed are coloured grey. **I-K)** Enrichment analysis showing the top GO Biological Processes 2021 terms associated with the I) Excitatory neuron, J) Dentate gyrus cell, and K) Inhibitory neuron upregulated genes for the LPS versus LPS+Hom differential expression analysis. Bars are coloured according to the adjusted p-value for the corresponding term (p.adjust). The length of each bar reflects the number of genes associated with the corresponding term (counts).

3.10 Exposure to LPS and *Taenia crassiceps* larval products for 24 hours has no effect on the intrinsic electrical properties of pyramidal neurons in mouse hippocampal organotypic brain slice cultures.

In the first part of the results, I explored changes in gene expression in response to the pro-inflammatory stimulant, LPS, as well as to *Taenia* larval products in mouse hippocampal organotypic brain slice cultures. I next wanted to explore how these same treatments affect neuronal function using whole-cell patch clamp electrophysiology. I was particularly interested in testing the effects of these treatments on the intrinsic electrical properties of neurons as this can give a sense as to whether exposure to these stimuli affects fundamental neuronal function and excitability. Changes in the neuronal firing properties or ion currents of neurons in response to either LPS or the *Taenia* homogenate could indicate a change in the excitability of the cells and represent a mechanism by which the likelihood or severity of seizures is moderated. However, aside from a few putative genes and pathways that could be mediating neurotransmission, the snRNAseq data mostly showed very few changes in the expression of neuronal genes that may mediate excitability across the different treatment conditions. I therefore hypothesised that these treatments may have limited effects on the intrinsic electrical properties of neurons. As outlined in section 3.1, the same mouse hippocampal OBSC model system used for the snRNAseq and HCR RNA-FISH experiments was used for the whole-cell patch-clamp experiments (Figure 3.1 A). After 24 hours of exposure to the respective

treatments, brain slices were moved to a patch rig and pyramidal neurons from either the CA1 or CA3 areas of the hippocampus were patched (Figure 3.14 A). Both voltage-clamp and current-clamp recordings were taken to obtain various properties of the cells which will be described below.

3.10.1 LPS and the *Taenia crassiceps* homogenate have no effect on the basic membrane properties of pyramidal neurons.

The access resistance from a patch-clamp recording can serve as an indication of the quality of the patch as it represents how effective the electrical access (conductance) is to the neuron. The mean access resistance for the control, Hom, LPS, and LPS+Hom groups was 18.20 MOhm (SEM 1.536 MOhm, N=17), 17.51 MOhm (SEM 1.339 MOhm, N =22), 16.10 MOhm (SEM 1.010 MOhm, N=20), and 17.23 MOhm (SEM 0.8117 MOhm, N=18), respectively, and were not significantly different to each other ($p > 0.05$, one-way ANOVA test; Figure 3.11 B; Supplementary 25). This provided confirmation that the quality patches were comparable across the different treatment groups.

I next proceeded to examine various basic membrane properties of neurons across the treatment groups, including the membrane resistance, membrane capacitance, and resting membrane potential which all reflect fundamental signalling processes of neurons. The membrane resistance provides an indication of how easily ions can flow across the cell membrane. If the membrane has a high resistance, it implies it is not very leaky and it is difficult for ions to move across the membrane. On the other hand, a low membrane resistance suggests that more current can leak out of the cell due to there being more ion channels, transporters, and in particular K^+ leak channels in the membrane. Thus, the fewer channels there are for ions to flow through, the higher the resistance of the cell will be. The mean membrane resistance for the control, Hom, LPS, and LPS+Hom groups was 163.2 MOhm (SEM 12.14 MOhm, N=17), 152.8 MOhm (SEM 14.77 MOhm, N =22), 129.2 MOhm (SEM 10.06 MOhm, N=20), and 121.3 MOhm (SEM = 9.443 MOhm, N=18), respectively, and there were no significant differences between the groups ($p > 0.05$, one-way ANOVA test; Figure 3.11 C; Supplementary 25).

The membrane capacitance refers to the ability of the membrane to store charge at a given potential. The membrane capacitance is proportional to the cell surface area and, together with the membrane resistance, determines the membrane time constant which dictates how fast the cell membrane potential responds to the flow of ion channel currents. The mean membrane capacitance for the control, Hom, LPS, and LPS+Hom groups was 170.0 pF (SEM 11.59 pF, N=17), 173.6 pF (SEM 11.88 pF, N=22), 170.6 pF (SEM 8.409 pF, N= 20), and

163.0 pF (SEM 9.835 pF, N=18) respectively, and they did not differ significantly to one another ($p > 0.05$, one-way ANOVA test; Figure 3.11 D; Supplementary 25).

The resting membrane potential of a neuron is the difference in voltage between the inside and outside of the cell at baseline conditions when the cell is not firing. Changes to the resting membrane potential may affect how excitable a neuron is. The mean resting membrane potential control, Hom, LPS, and LPS+Hom treatment groups was -62.55 mV (1.480 mV, N=17), -59.34 mV (SEM 1.681 mV, N =22), -59.92 mV (SEM 1.772 mV, N=20), and -60.17 mV (SEM = 1.524 mV, N=18), respectively, and no significant differences were found between the groups ($p > 0.05$, one-way ANOVA test; Figure 3.11 E; Supplementary 25).

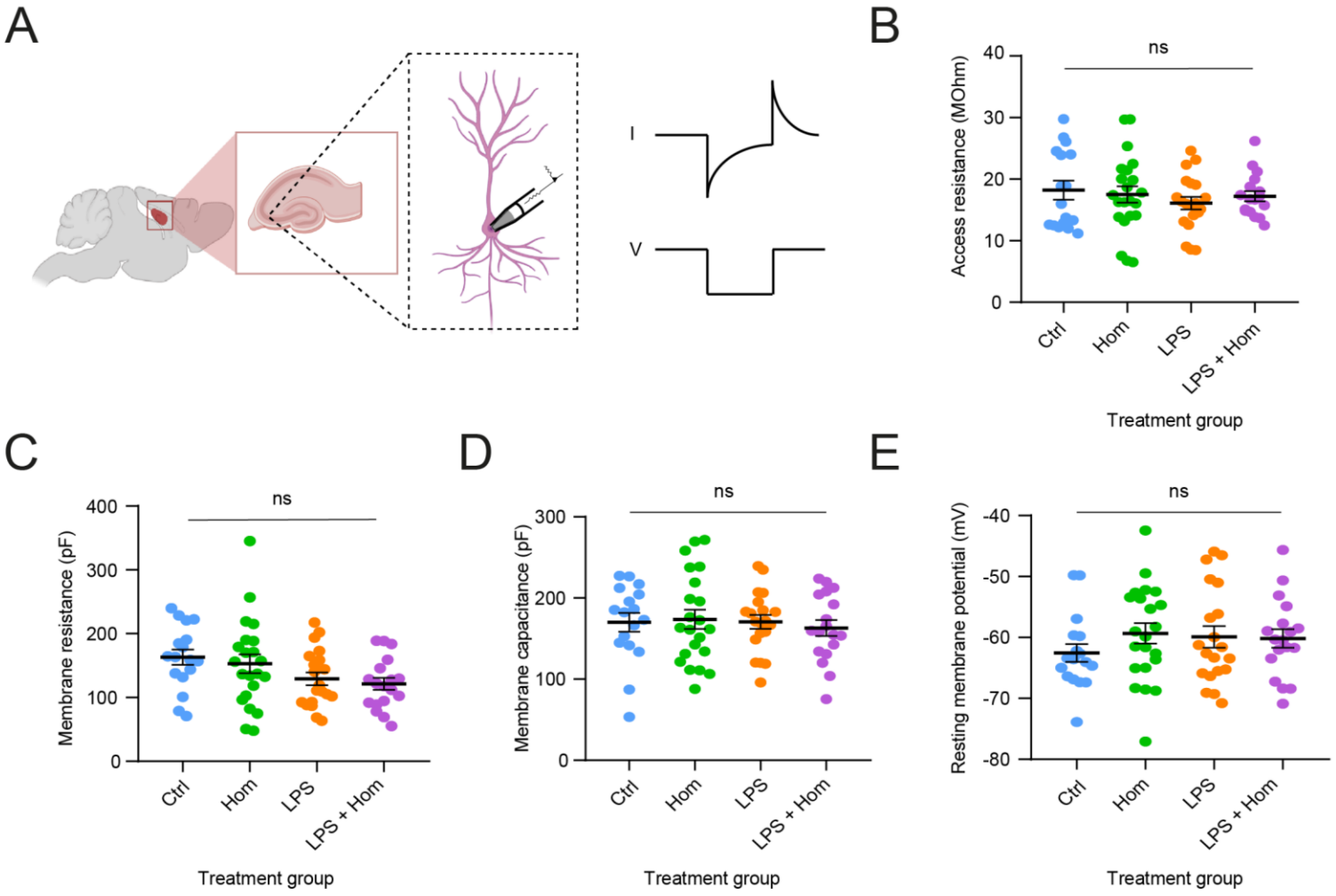

Figure 3.11 LPS and the *Taenia crassiceps* homogenate have no effect on the basic membrane properties of pyramidal neurons.

A) Whole-cell patch clamp recording from pyramidal neurons in either the CA1 or CA3 areas were taken from mouse hippocampal organotypic brain slices exposed to one of the four treatment conditions (control, LPS, Hom, or LPS+Hom) for 24 hours. Voltage-clamp and current-clamp recordings were obtained to measure the basic membrane properties of the neurons. **B)** There was no significant difference in the access resistance of the four treatment groups. **C)** There was no significant difference in the membrane resistance between the four treatment groups. **D)** There was no significant difference in the membrane capacitance of the four treatment groups. **E)** There

was no significant difference in the resting membrane potential between the four treatment groups. Values with means ± SEM; ns = not significant; each data point represents a recording from a single neuron.

3.10.2 LPS and the *Taenia crassiceps* homogenate have no effect on the active firing properties of pyramidal neurons.

A neuron's excitability is largely determined by its active firing properties. For example, the membrane voltage at which an action potential fires, the current required to evoke an action potential, the rate at which the cell can fire action potentials, as well as the relationship between the amount of current injected and the firing rate all contribute to how easily a neuron fires. In turn, the intrinsic excitability of neurons can play a role in how predisposed the tissue is towards seizures[242]. I therefore wanted to investigate the effect of the four different treatment groups on various active firing properties of pyramidal neurons.

The first property I looked at was the action potential threshold which is the minimum membrane potential at which an action potential fires. This can be obtained by carrying out a series of current steps that systematically increases the membrane potential of the cell until an action potential is evoked (Figure 3.12 A). The corresponding membrane potential at which the first action potential is evoked is then recorded (Figure 3.12 A). A more negative spike threshold indicates that less depolarising synaptic input is required for the cell to spike, while a more positive action potential threshold shows that a larger depolarising input is needed for the neuron to fire. In this way, the higher the action potential threshold (i.e., the more depolarised the spike threshold) the less excitable the cell. The mean action potential threshold for the control, Hom, LPS, and LPS+Hom groups was -36.83 mV (SEM 0.99 mV, N=17), -35.79 mV (SEM 0.88 mV, N=22), -34.77 mV (SEM 1.58 mV, N=20), and -38.03 mV (SEM 1.66 mV, N=18), respectively, and there was no significant difference between the four groups ($p > 0.05$, one-way ANOVA test; Figure 3.12 B; Supplementary 25).

The rheobase or current threshold is the minimum amount of current required to trigger an action potential. Intuitively, a larger amount of current required to trigger an action potential implies that the neuron is less excitable. The median rheobase for the control, Hom, LPS, and LPS+Hom treatment groups was 139.1 pA (IQR 82.7 – 211.0, N=17), 100.2 pA (IQR 88.6 – 195.7, N=22), 128.5 pA (IQR 107.1 – 144.8, N=20), and 147.5 pA (IQR 84.7 – 222.5, N=18), respectively, and no significant differences were found between the four groups ($p > 0.05$, Kruskal-Wallis test; Figure 3.12 C; Supplementary 25). Notably, the size of the cell can influence the current threshold as larger cells require more current to initially overcome the change in stored charge. To account for this, we can divide the current threshold by the capacitance of the cell which effectively adjusts for the cell size. This adjusted rheobase measure is called the current threshold density. The median current threshold density of the control, Hom, LPS, and LPS+Hom conditions was 0.8996 pA/pF (IQR 0.5976 – 1.186, N=17),

0.6903 pA/pF (IQR 0.5020 – 0.9847, N=22), 0.7631 pA/pF (IQR 0.6442 – 0.8000, N=20), and 0.9790 pA/pF (IQR 0.5641 – 1.271, N=18), respectively, and there were no significant differences between the groups ($p > 0.05$, Kruskal-Wallis test; Figure 3.12 D; Supplementary 25).

The maximum firing rate of a neuron can also provide an indication of its excitability as it measures the fastest rate at which the cell can send signals. This metric is obtained by performing a series of increasing current steps each of which evokes a train of spikes. Generally, the firing rate of each train of spikes increases as the current used to generate them increases until eventually a maximum firing rate is achieved. The maximum firing rate for each neuron can therefore be measured by taking the fastest firing frequency in the first 500 ms across the trains of spikes. The median maximum firing rate in 500 ms for the control, Hom, LPS, and LPS+Hom group was 10.0Hz (IQR 4.0 – 20.0, N=17), 15.0 Hz (IQR 7.5 – 28.5, N=22), 13.0 Hz (IQR 10.0 – 33.5, N=20), 20.0 Hz (IQR 6.0 – 30.0, N=18), respectively, and there was no significant difference between the four treatment groups ($p > 0.05$, Kruskal-Wallis test; Figure 3.13 B; Supplementary 25).

In addition to the maximum firing rate in the first 500 ms, another way of measuring the firing capacity of a cell is to look at the shortest time between two action potentials (i.e., the fastest firing rate between two time points). This measurement represents the fastest a cell can possibly fire, although it remains a theoretical estimate of the maximum firing rate as a neuron is unlikely to be able to maintain this frequency of firing between most action potentials. The median maximum firing rates between two points for the control, Hom, LPS, and LPS+Hom condition were 10.06 Hz (IQR 5.5 – 31.6, N=17), 24.29 Hz (IQR 10.81 – 56.9, N=22), 21.21 Hz (IQR 13.3 – 66.8, N=20), and 28.29 Hz (IQR 10.6 – 58.9, N=18), respectively, and no significant differences were observed between the groups ($p > 0.05$, Kruskal-Wallis test; Figure 3.13 C; Supplementary 25).

Alongside looking at the maximum firing rates, we can also explore the input-output function of neurons, that is the sub-maximum relationship between current input and firing rate. By plotting the average firing rate corresponding to given current inputs, we can see whether a particular treatment condition results in a change in the input-output function of the neurons. I found that the relationship between the firing rate and the current density (current input adjusted for cell size) did not differ significantly between the treatment groups ($p > 0.05$, Two-way ANOVA test; Figure 3.13 D; Supplementary 25).

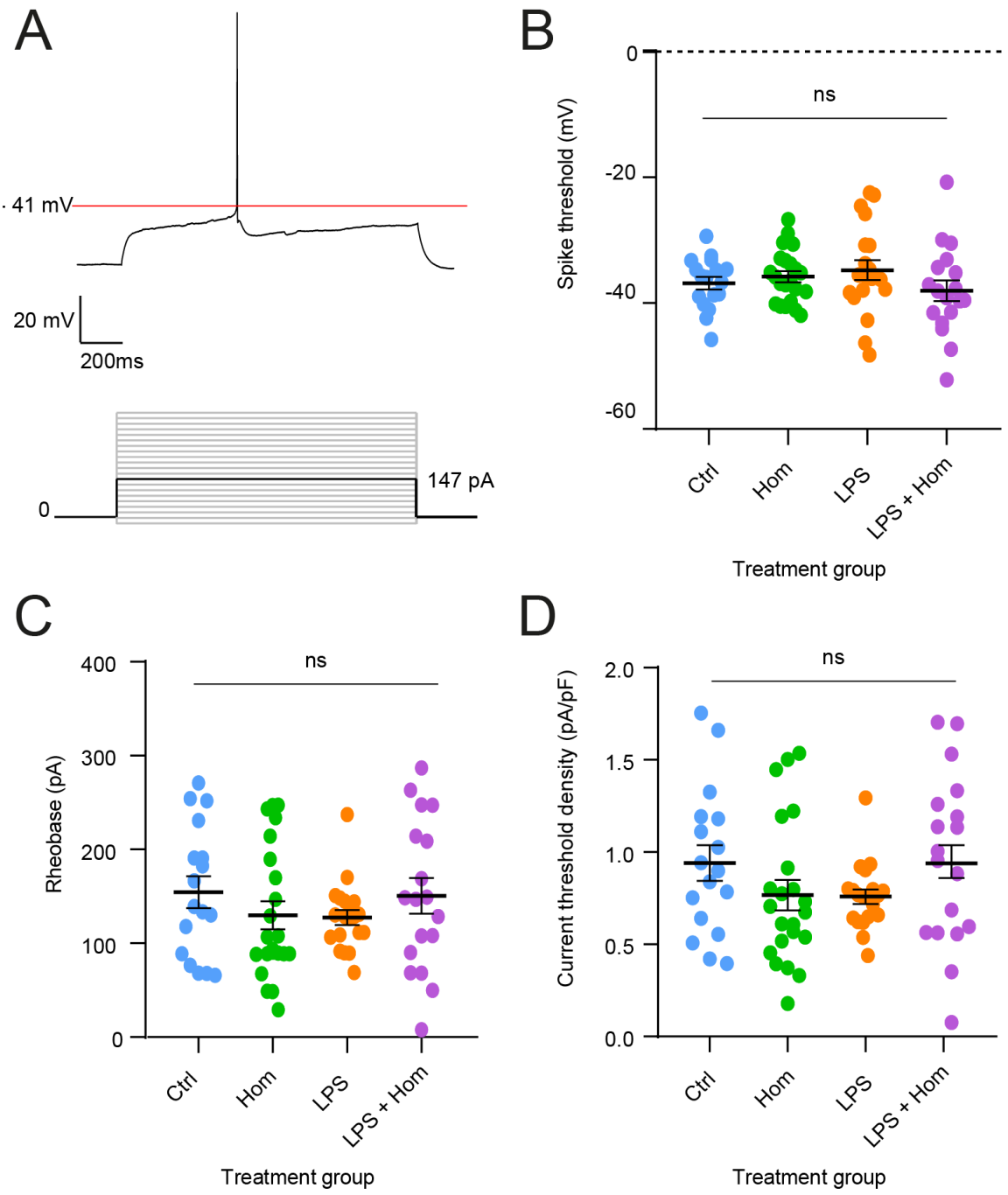

Figure 3.12 LPS and the *Taenia crassiceps* homogenate have no effect on the active firing properties of pyramidal neurons, including the action potential threshold, rheobase, and current threshold density.
A) Representative current-clamp recording showing the membrane potential at which an action potential is generated as well as the accompanying required amount of current required to trigger the first action potential. **B)** There were no significant differences in the action potential threshold of neurons between the four treatment groups. **C)** There were no significant differences in the rheobase of neurons between the four treatment groups. **D)** No significant differences existed in the current threshold density of neurons between the four treatment groups. Values with means ± SEM; ns = not significant; each data point represents a recording from a single neuron.

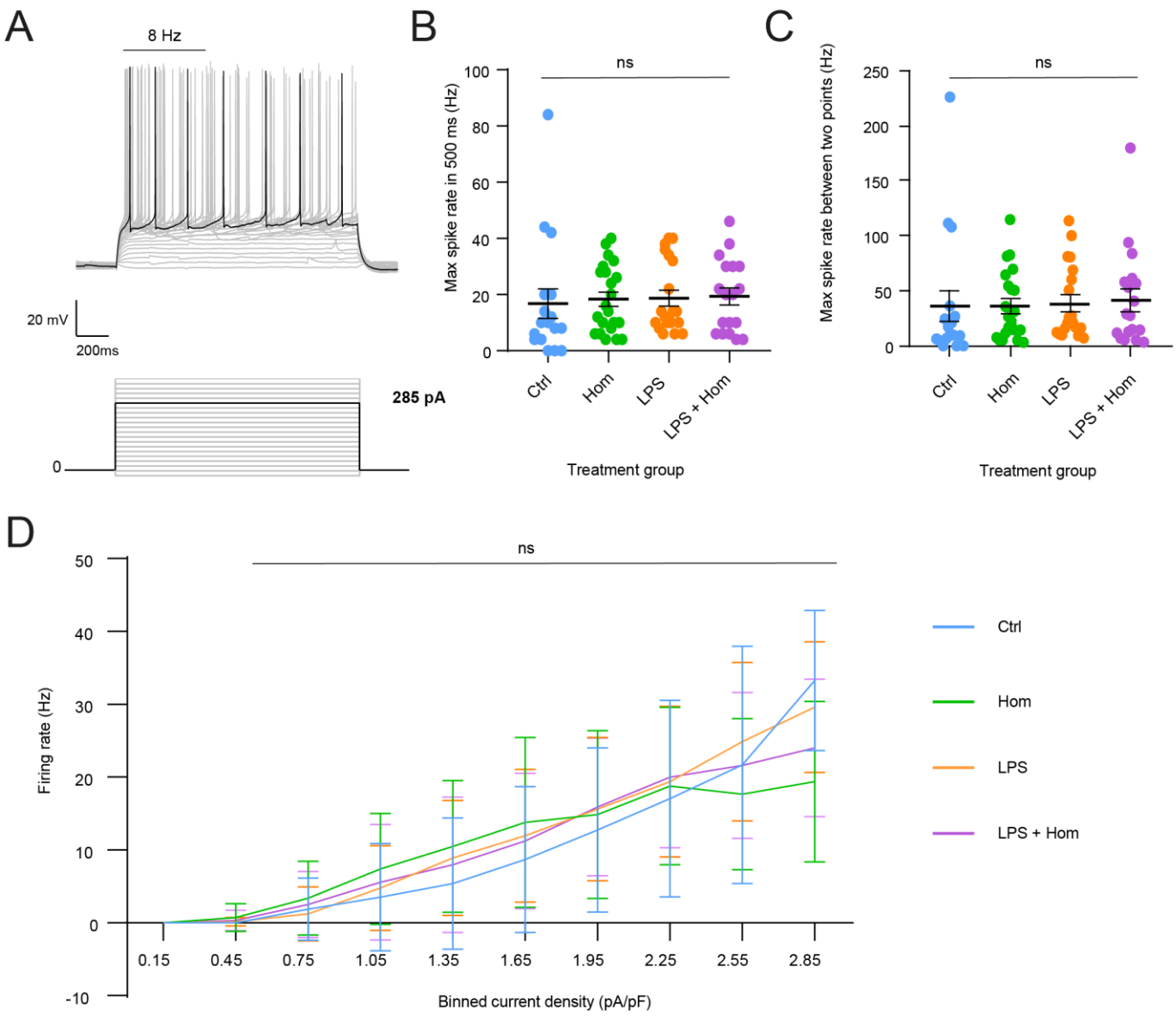

Figure 3.13 LPS and the *Taenia crassiceps* homogenate have no effect on the active firing properties of pyramidal neurons, including the maximum firing rate and its relation to the current density.

A) Representative current-clamp recording showing a train of consecutive spikes evoked by a series of current steps. **B)** There were no significant differences in the maximum firing rate in the first 500 ms of neurons between the four treatment conditions. **C)** There were no significant differences in the maximum spike rate of neurons between two points across the four treatment conditions. **D)** The relationship between the firing rate and the current threshold density did not differ significantly between the four treatment groups. Values with means ± SEM; ns = not significant; each data point represents a recording from a single neuron.

3.10.3 LPS and the *Taenia crassiceps* homogenate do not affect the size of voltage-gated sodium and potassium currents in neurons.

The movement of ions across the neuronal membrane is another parameter that controls neuronal signalling by modulating changes in the membrane potential. Two of the main ions that drive changes in the membrane voltage are sodium (Na^+) and potassium (K^+). Voltage-

gated sodium channels are the primary ion channels that mediate membrane depolarisation by allowing Na^+ ions to flow into the cell and play a pivotal role in the generation and propagation of action potentials[243]. A representative voltage-clamp recording illustrates the Na^+ current that is evoked when voltage-gated channels open secondary to a depolarising voltage step (Figure 3.14 A). By measuring the maximum sodium currents generated in response to voltage-steps in neurons across the different treatment conditions, we can examine whether the sodium ion flux across the neuronal membranes is altered by the treatments. The mean maximum Na^+ current of the control, Hom, LPS, and LPS+Hom group was -6235 pA (SEM 435.7, N=17), -6251 pA (SEM 492.3, N=22), -6254 pA (SEM 379.5, N=20), and -6494 pA (SEM 340.2, N=18), respectively. There were no significant differences in the maximum sodium current between the four treatment groups ($p > 0.05$, one-way ANOVA test; Figure 3.14 B; Supplementary 25).

Additionally, the flux of K^+ ions out of the cell is required for maintaing the neuronal membrane at negative voltages. An example voltage-clamp trace shows the currents produced in response to the opening of the K^+ ion channels when the membrane is maximally depolarised in our protocol (Figure 3.14 C). The median maximum K^+ current of the control, Hom, LPS, and LPS+Hom group was 2064 pA (IQR 1378 – 2585, N=17), 1692 pA (IQR 1332 – 2417, N=22), 1638 pA (IQR 1384 – 2382, N=20), and 1962 pA (IQR 1712 – 2295, N=18), respectively. There were no significant differences in the maximum potassium current between the four conditions ($p > 0.05$, Kruskal-Wallis test; Figure 3.14 D; Supplementary 25).

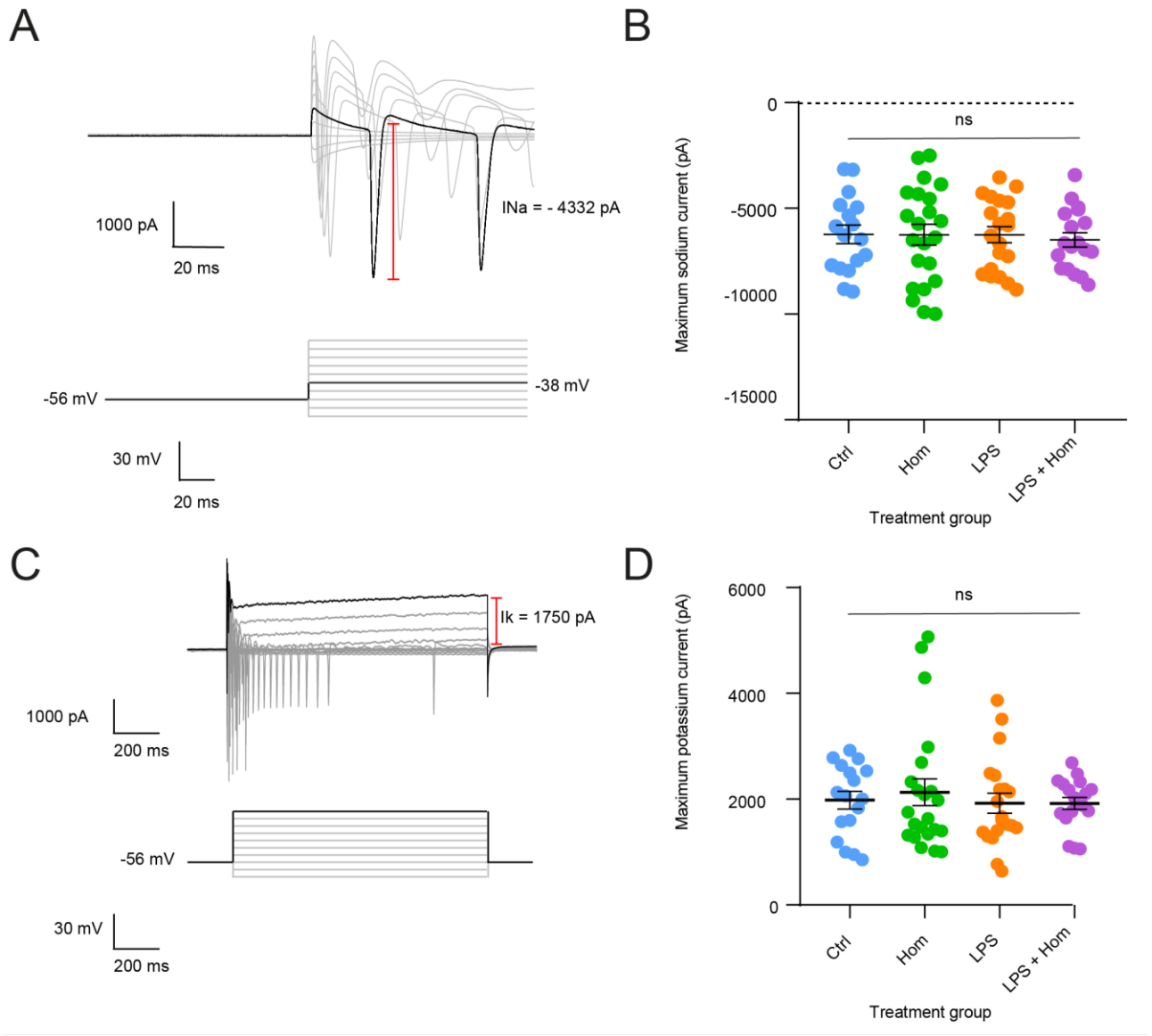

Figure 3.14 LPS and the *Taenia crassiceps* homogenate do not affect the size of voltage-gated sodium and potassium currents in neurons.

A) Representative voltage-clamp recording showing the measurement of the absolute maximum voltage-gated sodium current elicited following positive voltage steps. **B)** There were no significant differences in the mean maximum sodium current between the four treatment groups. **C)** Representative voltage-clamp recording showing the measurement of the absolute maximum potassium current elicited following positive voltage steps. **D)** There were no significant differences in the mean maximum potassium current between the four treatment groups. Values with means ± SEM; ns = not significant; each data point represents a recording from a single neuron.

CHAPTER 4

Discussion and Conclusion

4.1 Summary of project background and aims

There is a large body of literature supporting a relationship between immunomodulation and seizure activity in neurocysticercosis as well as other epilepsy conditions [4,8,31,91,244]. However, exact mechanisms by which neuroinflammation and/or cestode larvae can cause seizures are yet to be fully understood. Towards this end, I used an *ex vivo* mouse hippocampal OBSC model system to firstly explore how an innate immune activation as well as *Taenia* larvae affect gene expression within different cell types in the brain and whether any transcriptional changes occur that are associated with possible changes in neuronal excitability. Secondly, the project examined whether innate immune activation in the brain by itself modulates intrinsic neuronal function as well as whether *Taenia* larvae affect basic neuronal function. This work has the potential to shed light on how innate immune activation as well as infection by *Taenia* larvae affect cell type function and excitability in the brain at a transcriptomic and electrophysiological level.

4.2 LPS elicited neuroinflammatory transcriptional changes across all cell types in mouse hippocampal OBSCs with the most prominent effects in astrocytes and microglia.

The first part of the project used snRNAseq to explore how brain cells exposed to LPS in culture for 24-hours compared in their transcriptional profiles to brain cells exposed to regular growth media. As expected, a global upregulation of inflammatory genes was found to occur across all cell types in response to LPS. This agrees with numerous studies demonstrating an initial upregulation of various pro-inflammatory mediators in the brain following systemic LPS exposure including pro-inflammatory cytokines, chemokines, components of the complement system, and prostaglandins[245–250]. Astrocytes and microglia were found to have the largest number of DEGs in response to LPS, confirming the common understanding that they are the main immune responders in the brain[246–248,251,252]. The astrocyte and microglial DEGs were associated with the same or similar immune-related pathways, suggesting crosstalk between these cell types to orchestrate functions such as cytokine-mediated signalling and type 1 interferon signalling. Interestingly, many of the DEGs were uniquely differentially expressed in either astrocytes or microglia but were still associated with similar pathways, implying that cell-type-specific DEGs can converge on related functional pathways. On the other hand, there were some genes that were differentially expressed in both astrocytes and microglia but had

considerably higher Log2FoldChanges, higher average expression levels, or were expressed in a larger percentage of nuclei in one cell type compared to another. There was also a small set of genes that were found to have the opposite direction of change in astrocytes and microglia, further supporting the idea of cell-type-specific changes in response to immune activation.

When it comes to interpreting my findings, it can be valuable to compare the results to other single-cell transcriptomic papers that have delineated the roles of reactive astrocyte and microglial sub-populations in response to LPS. At the time of writing, there is one snRNAseq paper on the effects of LPS in microglia[239] and one on astrocytes[253]. The snRNAseq study on microglia characterised transcriptomic changes of immune-activated microglia from whole brain tissue of mice 24 hours after a systemic LPS injection[239]. In accordance with my findings, they observed an upregulation of various pro-inflammatory genes in the microglial clusters and a downregulation of several homeostatic genes[239]. However, a few genes that Sousa et al.[239] reported as being downregulated in microglia in response to LPS such as *Olfml3*, *Fcrls*, *Tmem119* were not differentially expressed in my dataset. As with the Sousa et al.[239] paper, the snRNAseq astrocyte paper by Hasel et al.[253] explored how systemic LPS administration affects various sub-populations of reactive astrocytes as well as astrocytic gene expression after 3, 24, and 72 hours. They found that 24 hours of LPS exposure resulted in an upregulation of common reactivity genes such as *Serpina3n, Saa3, C3, and Ccl5;* an upregulation of genes involved in angiogenesis and blood pressure, such as *Adamts1*, *Ecm1*, and *Stat1*; as well as an upregulation of genes involved in extracellular matrix remodelling, including *Timp1*, *Icam1*, and *Col6a1*. My results corresponded to these findings. Interestingly, Hasel et al.[253] found that there were quite substantial differences in astrocytic gene expression and the associated enriched pathways depending on the time after LPS exposure. It is worth acknowledging this as an inherent limitation of my project which only examined a single time-point (24 hours after exposure to LPS). It is possible that different gene expression profiles in response to LPS would also be seen in the mouse hippocampal OBSCs if shorter or longer treatment periods were used.

Sousa et al.[239] also identified two sub-populations of microglia, while Hasel et al.[253] identified 10 reactive astrocyte clusters in response to 24-hour LPS exposure. I did not characterise the clusters in my dataset to this resolution as this was beyond the scope of the project. However, future work could align the mouse hippocampal OBSC dataset generated in this project with the snRNAseq datasets of these two publications to see if the same sub-populations of astrocytes and microglia can be characterised in mouse hippocampal OBSCs following innate immune activation.

Notably, there are few studies that have carried out transcriptional profiling to look at the effect of neuroinflammation on multiple different cell types in the brain all within the same system. Most studies that have investigated gene expression in the brain in response to LPS have either used low-throughput approaches such as RT-qPCR or bulk RNA-seq that do not allow for an appreciation of genome-wide changes in gene expression across multiple different cell types[247,252,254–256], or have employed single-cell approaches but used reporter mouse lines and FACS sorting to isolate specific cell types rather than looking at gene expression across multiple different cell types in the brain[239,253,257,258]. Nevertheless, I did come across three papers that have looked at genome-wide profiling of transcription in three or more brain cell types in response to LPS[250,259,260]. One of the studies performed snRNAseq in mice either exposed to LPS systemically or to a saline injection and looked for cell-type-specific gene expression changes in a part of the hypothalamus involved in sickness responses[260]. However, this paper is less applicable to my work as it was focused on pathways mediating fever and appetite in a different brain region and did not either report extensively on distinct inflammatory changes between different cell types[260]. On the other hand, the other two studies bypassed single-cell RNA sequencing approaches by FACS sorting several cell types of interest from the mouse cortex and using RNA-seq to individually profile the gene expression of the different cell types in response to LPS[250,259]. These studies confirmed an upregulation of inflammatory gene expression in astrocytes, microglia, and neurons [250,259]. The study by Srinivasan et al. [245] also reported a large set of uniquely differentially expressed genes in astrocytes and microglia which my snRNAseq data corroborates. Moreover, as with my results, they identified sets of genes that were differentially regulated in both astrocytes and microglia but showed much higher average expression levels, much higher Log2FoldChanges, or even the opposite direction of change in one cell type relative to the other in response to LPS[250]. My data agrees with these findings and provides support that the *ex vivo* mouse hippocampal OBSC model system also induces specific transcriptional signatures in astrocytes and microglia in response to an inflammatory challenge.

4.3 LPS evoked inflammatory gene expression changes in neurons but had limited effects on the expression of genes that might mediate excitability in neurons.

In addition to having explored the transcriptional changes in microglia and astrocytes, I wanted to take advantage of the OBSC model system to explore the effect of LPS on neuronal gene expression when glial cells are present in the preparation. I found that the four coarse neuronal clusters primarily elicited upregulations in gene expression in response to LPS but had far fewer DEGs compared to the astrocyte and microglia clusters. This in accordance with findings from Srinivasan et al.[250] who carried out RNA-seq profiling separately on FACS sorted

astrocytes, microglia, and neurons and observed that systemic LPS resulted in a larger number of DEGs in both microglia and astrocytes than in neurons. Furthermore, they found that unsupervised clustering caused the astrocyte and microglia RNA-seq samples to naturally group into the treatment and control groups, whereas the neuron samples did not cluster into distinct treatment and control groups, suggesting that the brain's most pronounced transcriptional responses to LPS occurs within glial cell types[250]. As microglia are the resident immune cells of the brain, there is a common notion that they are the first-line responders to LPS via their expression of TLR4 which is the main receptor for LPS[246]. Moreover, there is support that microglia are necessary to evoke certain effects of LPS, including LPS-induced neurotoxicity as well as certain synaptic alterations[153,247,248,251,261]. Nonetheless, various other CNS cell types are known to express *Tlr4*, including astrocytes, neurons, and endothelial cells, suggesting that these cell types are likely capable of responding directly to LPS[245,246]. This was supported by my snRNAseq data showing that all major brain cell types had some expression of *Tlr4.* However, the non-neuronal cells were found to have a greater percentage of nuclei expressing *Tlr4* compared to neuronal cells, suggesting that it is primarily non-neuronal cells that respond directly to LPS. Further research would be needed to experimentally test whether astrocytes, neurons, and other brain cell types can respond directly to LPS in mouse hippocampal OBSCs or if they require microglia to initiate the inflammatory signalling cascade.

Looking at the functional pathways of the upregulated neuronal DEGs revealed that most terms were related to inflammatory pathways. This is comparable to other studies that have found an upregulation of inflammatory genes and pathways in neurons after LPS exposure[262,263]. The paper by Baxter et al.[262] explored the effect of LPS in the brain using a mixed-species RNA-seq approach consisting of a co-culture of purified neurons, astrocytes, and microglia from mouse, human, and rat, respectively. Individual cell-type transcriptomes could then be profiled using species-specific sorting of bulk RNA-seq data. Markedly, they found that many of the up- and downregulated LPS-induced DEGs in astrocytes and neurons were dependent on the presence of microglia[262]. However, they also showed that in turn, neurons and astrocytes act in combination to promote microglial homeostatic signalling in response to LPS via secreted factors such as transforming growth factor β2 (Tgf-β2). My data showed an LPS-induced increase in microglial expression of *Tgfbr1* which encodes a receptor for Tgf-β2. This opens the possibility that similar feedback mechanisms could function in mouse hippocampal OBSCs for astrocytes and neurons to regulate microglial signalling following immune activation. Notably, two previously discussed papers that carried out RNA-sequencing in glial and neuronal cells in the brain in response to LPS did not perform enrichment analyses on the neuronal DEGs[250,260]. Thus, this work offers a novel, unbiased

characterisation of transcriptional changes in various neuronal populations following an inflammatory challenge in the presence of other brain cell types from the same sample and belonging to the same species.

As this project is focused on understanding links between immune modulation and seizure mechanisms, I wanted to examine whether LPS induced changes in neurons that may mediate changes in excitability. I found that only 5 out of the 608 putative excitability genes were differentially expressed in the neuronal clusters. These included *Slc13a3*, *S100a6*, *S100a11*, *S100a13*, and *Npy2r* which were all upregulated in one or more of the neuronal clusters. As previously mentioned, not all genes in the curated list of potential excitability genes necessarily mediate neuronal excitability as relatively broad search terms were used to obtain the set of genes. This appeared to potentially be the case with these 5 genes as few neurotransmission-related terms were found to be enriched for the set of 5 putative excitability DEGs. I did nonetheless do some manual searching of these genes to see if there was literature suggesting a role for these genes in mediating neuronal function. I found that *Slc13a3*, which was upregulated in the excitatory neuron cluster, is a sodium-dependent dicarboxylate transporter that is involved in the transmembrane transport of the tricarboxylic acid (TCA) cycle intermediate, succinate[264]. To my knowledge, there is no literature implicating *Slc13a3* in altering neuronal excitability. However, neurons rely on extracellular sources of TCA cycle intermediates to replenish their intracellular neurotransmitter pools[264], and thus there is a possibility that *Slc13a3* could have an indirect effect on neurotransmission. This would still need to be tested. On the other hand, the S100 genes belong to a family of the genes which encode EF-hand calcium binding proteins and are known to play roles in buffering intracellular Ca^{2+} and modulating protein phosphorylation[265,266]. Additionally, S100 proteins have been found to function as cytokines and bind with different immune-related receptors including TLR4 and receptor for advanced glycation end-products (RAGE) which themselves bind to different pathogen associated molecular patterns (PAMPs) including LPS[266–268]. The binding of S100 proteins to these receptors activates a diverse set of pro-inflammatory signalling cascades. This is likely the main function explaining the upregulation of these genes in neurons secondary to LPS exposure. Individual roles for some of the S100 proteins have also been studied. In my dataset, *S100a6* was upregulated in the excitatory neurons, dentate gyrus cells, and inhibitory neurons. Upregulations of S100A6 have been reported in models of Alzheimer's disease and several other neurodegenerative conditions, as well as in sclerotic hippocampi of epilepsy patients[269]. Furthermore, increased levels of S100A6 mRNA have been reported following induced seizures in mouse models of epilepsy, and this upregulation was correlated with neurodegeneration[269]. In contrast, S100A11 and S100A13 have both been found to protect against neuronal apoptosis in ischemic stroke[270,271], suggesting a potential

neuroprotective function of these genes in response to LPS. There is no research indicating that *S100a11* or *S100a13* directly influences neuronal excitability. The *Npy2r* gene was also found to be upregulated in my dataset in response to LPS. NPY2R is a receptor for neuropeptide Y (NPY) and has been shown to inhibit the release of glutamate at CA3-CA1 pyramidal neuron synapses in rats by reducing pre-synaptic Ca^{2+} levels [272]. There are also reports of NPY inhibiting excitatory neurotransmission as well as having neuroprotective effects in a model of temporal lobe epilepsy[273]. While this is somewhat counterintuitive to the narrative of neuroinflammation potentially increasing neuronal excitability, there are some reports of pro-inflammatory molecules having an inhibitory effect in rodent brain slices[157,160,161]. It is therefore possible that *Npy2r* represents a gene that could mediate excitability changes in response to 24-hour LPS exposure, but this would need to be demonstrated electrophysiologically.

In addition to examining the expression of excitability genes, I performed an enrichment analysis on the neuronal DEGs to see if any enriched pathways were related to neurotransmission. The dentate gyrus cells were found to downregulate phosphorylation and kinase activity in response to LPS. While this is not directly linked to excitability, phosphorylation of receptors and ion channels is known to mediate synaptic function and thus this could be a potential way in which LPS affects neuronal function [274–278]. In addition, there was one upregulated pathway in inhibitory neurons termed “Purinergic nucleotide receptor signalling pathway”. I found no other significantly enriched terms for the neuronal DEGs that were related to neuronal excitability, synaptic activity, or neurotransmission. Thus, while a few putative DEGs and pathways were identified that could potentially mediate neuronal excitability in response to LPS, overall, 24-hour exposure to LPS in mouse hippocampal OBSCs had remarkably little effect on gene expression typically associated with changes in neuronal network excitability.

There are only a few studies that have investigated how changes in RNA or protein levels in the brain in response to LPS are associated with changes in neuronal excitability. Papageorgiou et al.[279] exposed rat hippocampal slice cultures to LPS for 72 hours and reported an increase in proinflammatory cytokines such as IL-1β, TNF-α, and IL-6 but no major changes in excitability nor any major neurotoxic effects when LPS was added by itself. My results seem to reproduce this, showing increases in inflammatory-related transcription in response to LPS but no distinct changes in the expression of genes that may mediate neuronal excitability. On the other hand, a study by Klawonn et al.[280] demonstrated that microglial activation, induced by 1 hour of systemic LPS administration in mice, resulted in an increase in the levels of IL-6 mRNA, and that this increase in IL-6 transcription was necessary for the negative affective state that followed LPS exposure. Markedly, the observed negative affective

state was accompanied with a decrease in firing rate of striatal neurons, providing indirect evidence that increased transcription of IL-6 alters excitability of neurons in the striatum[281]. Accompanying the decrease in excitability was a reduction in the membrane resistance and an increase in the fast after-hyperpolarisation, leading the authors to propose that an upregulation or increased opening of K^+ channels could be responsible[281]. However, the delayed rectifying K^+ channels which are the most likely K^+ channels responsible for these effects, did not show significantly altered mRNA levels in response to LPS[281]. This is an important finding in relation to my own work as it highlights that an inflammatory challenge can mediate neuronal excitability without necessarily altering the levels of expression of the implicated ion channels or receptors. Instead, it is possible that the gating properties of the ion channels may have been altered through structural or biochemical changes such as phosphorylation of subunits[277,278]. Another research group found an increase in excitatory neurotransmission in primary cultures of mouse hippocampal neurons in response to LPS which was dependent on TLR4 signalling without the levels of TLR4 protein changing between the control and LPS condition[60]. This is worth noting considering that I too found no statistically significant changes in the expression levels of *Tlr4* mRNA across the different clusters secondary to LPS exposure. In this way, these studies illustrate that it is possible for changes in neuronal excitability to occur in response to LPS without all implicated molecules necessarily changing in their levels of expression.

4.4 *Taenia crassiceps* had little effect on gene expression when compared to control conditions.

The snRNAseq analysis comparing the *T. crassiceps* homogenate to control conditions revealed very few changes in gene expression across the different clusters. Although there were more downregulated genes, there were no enriched pathways associated with these genes. On the other hand, the upregulated DEGs in response to the homogenate were associated with several metabolic terms such as cellular polysaccharide and lipid catabolic processes. It is interesting to observe an upregulation of carbohydrate and lipid metabolism in response to the *Taenia* homogenate as *Taenia* cysticerci are known to absorb and consume large quantities of host substrates including glucose, fatty acids, and proteins which they metabolise using various energetic pathways to survive and develop in the brain[282–285]. Targeting larval metabolic pathways is in fact one of the ways in which anti-parasitic drugs are known to have their effect [282–286]. The upregulation of *Aoah* in host cells could be a potential way in which *Taenia* larvae manipulate host carbohydrate and lipid production to obtain sufficient in energy for their survival and growth. This is not improbable considering the relatively simple genomes and limited biosynthetic capabilities of cestodes[286]. However, this is very much speculation, and should be deemed as such especially considering that the

enriched catabolic pathways in question were associated with only a single gene which was differentially expressed in only one neuronal sub-population.

In addition to these findings, I noted that the *Taenia* homogenate resulted in a downregulation of the Substance P receptor in microglia. This is an interesting finding as Substance P has previously been implicated in NCC seizurogenesis[57]. Early-stage granuloma extracts associated with dying *T. crassiceps* larvae from wild-type rodents with the precursor for Substance P have been found to trigger seizures when injected intrahippocampally into another rat or mouse and this effect was dependent on the presence of Substance P receptors in the animal receiving the injection[57]. Furthermore, in the same model system, Substance P signalling was found to contribute to the release of pro-inflammatory cytokines[58]. The *Tacr1* gene, which was downregulated in my dataset, encodes the tachykinin receptor 1 (also known as neurokinin-1 receptor) and is the receptor that Substance P binds to in the CNS. Activation of the neurokinin-1 receptor by Substance P in human microglial and astrocyte primary cultures has been found to augment inflammatory and/or neurotoxic responses by these cells[287]. Considering that our *Taenia* homogenate was primarily made from larvae that were frozen at a viable stage and appears to block pro-inflammatory activity[288], I have theorised that treatment with this whole-cyst homogenate reflects the viable cyst stage of NCC. This would align with the observed downregulation of the *Tacr1* gene in microglia which could even represent a possible mechanism by which the *T. crassiceps* homogenate partially suppresses pro-inflammatory activity. Furthermore, this fits with the report that there are few seizures and symptoms during the viable cyst stage of NCC as the receptors for Substance P could be actively downregulated during this stage by viable *Taenia* larval cysts in the brain. Again, this remains to be demonstrated experimentally. It was also worth noting that the Lamp5 interneurons had the greatest percentage of nuclei expressing the *Tacr1* gene, suggesting that the main effects of Substance P may occur through the Lamp5 cells. In addition to the Substance P receptor, I examined the expression of the gene encoding the precursor for Substance P, *Tac1*. Counter to what might be predicted from previous reports of the effects of *T. crassiceps* granulomatous extracts in the brain[57,58], *Tac1* was not differentially expressed between the control and Hom conditions. This can potentially be attributed to the other studies using granulomatous extracts from dying *T. crassiceps* larvae, while this research utilised a homogenate made from viable *T. crassiceps* larvae which may have a different effect on Substance P production.

4.5 *Taenia crassiceps* demonstrated ubiquitous immunosuppressive transcriptional changes when added to LPS.

To better appreciate the full effects of the *T. crassiceps* homogenate, I looked at how the addition of the homogenate affected cell-type-specific gene expression in the presence of a pro-inflammatory stimulant, namely, LPS. This DE analysis was done by running a pairwise comparison between the LPS (baseline) group and the LPS+Hom (treated) group. The analysis revealed broad global downregulations of pro-inflammatory genes and upregulations of anti-inflammatory genes following the addition of the *T. crassiceps* homogenate to LPS. The homogenate appeared to block/counteract the effect of LPS with many of the exact same genes and pathways that were upregulated or downregulated by LPS being found to act in the opposite direction when the homogenate was added to LPS. In this way, the transcriptional data very much corroborated the immunosuppressive effects we were expecting to see based on previous observations in the model system using ELISAs and immunohistochemistry. However, I now had the advantage of being able to decipher which cell types and gene networks the *Taenia* homogenate may be acting on to suppress the induction of inflammation by LPS. Although transcriptional changes were seen in all cell types, the astrocytes, OPCs, and microglia had the largest numbers of DEGs. This was especially true for the astrocytes which had as many as 525 downregulated genes and 207 upregulated genes. Microglia were also found to have fewer DEGs than astrocytes but both microglia and astrocytes showed the same trend to each other with a larger number of downregulated genes compared to upregulated genes in response to the homogenate being added to LPS. The large transcriptional responses to both pro-inflammatory and immunosuppressive stimuli in astrocytes suggests that they may play an important part in amplifying immunomodulatory signals in the brain.

Extensive research into the immunological effects of *Taenia* larvae has demonstrated that both *T. solium* and *T. crassiceps* infection are associated with mixed Th1 and Th2 responses in hosts[178,289,290]. The induction of the Th2 response appears to be permissive to the survival of the parasite and is therefore considered as an immunoregulatory strategy that the cestodes use to survive in host organisms[178,289]. The *Taenia*-induced Th2 immune responses is characterised by the secretion of high levels of anti-inflammatory cytokines including interleukin-4 (IL-4), IL-1, IL-6, interleukin-9, interleukin-10 (IL-10), interleukin-25, interleukin-33, and TGF-β[178,289]. This anti-inflammatory milieu is accompanied with cellular and humoral immune responses including high levels of CD4+ T lymphocytes becoming alternatively activated into Th2 and T regulatory subsets, as well as an increase in immunoglobulin G1- and IgE-producing B cells, eosinophilia, basophilia, and mast cells[178,289,291]. It is an established notion that most of these alterations in the cellular inflammatory response and leukocyte

activation occur in response to *Taenia* larvae releasing excretory/secretory antigens which have immunoregulatory properties[291]. In addition to this, histological and immunological analysis of craniotomy specimens containing *T. solium* cysts surrounded by granulomas from NCC patients have found the presence of plasma cells, B and T lymphocytes, macrophages, and mast cells to be associated with degenerating or calcified larval cysts[190,290]. Additionally, various cytokines were associated with dying larval cysts, including the Th1 cytokines IFN-γ, IL-18, and TGFβ and the Th2 cytokines IL-4, IL-13, and IL-10[190,290]. In summary, viable *Taenia* larvae induce a Th2 immune response in hosts to survive, while the host's Th1 immune response predominates the degenerating cyst stages. Presumably, this induction of the Th2 response requires *Taenia* larval modulation of lymphocytes directly and not via modulation of antigen presenting cells such as microglia. My justification for this is that in my model, *T. crassiceps* homogenate alone did not induce classic IL-4-mediated alternative activation in microglia, with no changes in gene expression associated with the M2 phenotype (Mao-A, CD36, Dusp1)[292]. Placing my findings in the context of these immunological studies, I hypothesise that treatment with our lab's *T. crassiceps* whole-cyst homogenate mimics what might be seen in the brain during the vesicular/viable cyst stages of NCC. My data provides support that extracts of *Taenia* larvae can prevent pro-inflammatory responses across all main resident brain cell types. Importantly, this research was done *ex vivo*, indicating that this immunosuppressive activity can occur without requiring infiltrating peripheral immune cells.

It is intriguing to speculate whether *Taenia* larvae elicit specific effects on different cell types in the brain or if, instead, LPS triggers cell-type-specific transcriptional changes, and the *Taenia* homogenate simply acts upstream on receptors such as TLR4 to block LPS from having its effect. The latter scenario seems most plausible considering that the homogenate appeared to have almost no effect on gene expression when compared to control conditions, suggesting that it is not actively downregulating pro-inflammatory genes or upregulating anti-inflammatory genes so much as blocking LPS from having its effect. This hypothesis is further substantiated by the wide-spread way in which the homogenate counteracted the effects of LPS across multiple genes and multiple cell types. It seems more likely, therefore, that such global opposing changes in gene expression would have their target upstream at a particular receptor that LPS acts on or a few pathways downstream of the initial site where LPS has its effect rather than the homogenate acting at numerous downstream targets of different cell types. However, the homogenate did not perfectly counteract the effects of LPS as we can see the trend was for the average expression levels of genes in the LPS+Hom condition to fall somewhere between what is seen in the control and LPS conditions, implying that the homogenate can partially restore gene expression levels back to control levels when it is added to LPS but not entirely. This could be explained by the homogenate competing with

LPS for binding to TLR4 or a related upstream receptor, and while mostly outcompeting LPS, there may be instances where LPS is still able to bind such that its effects are not completely blocked by the homogenate (See Figure 4.1 for an outline of LPS initial targets and signalling pathways). Alternatively, LPS may act on other receptors that the homogenate does not block, which would account for some effects of LPS still occurring despite the presence of the homogenate. Looking at the LPS signalling pathways that have previously been described[246,293,294] (See Figure 4.1 for a visual representation), I propose that the *T. crassiceps* homogenate acts at the level of the receptor for TLR4 and potentially other toll-like receptors but that there are some LPS receptors it fails to block or only blocks partially.

Of course, in NCC there is not a single pro-inflammatory stimulant such as LPS acting but rather the host's immune response at play which could have multiple targets other than the pathways that LPS activates. However, as discussed in the introduction, TLR4 polymorphisms have been implicated not only in susceptibility to NCC infection but also susceptibility to symptomatic NCC[33]. The authors of this study proposed that, in cases of symptomatic NCC, TLR4 variants may play a role in driving an immune response towards the Th1 phenotype, and that this could contribute to seizures[33]. Thus, there is evidence to suggest that at least a component of the host's immune responses to *Taenia* larvae likely acts through toll-like receptor signalling pathways including TLR4. My data further supports this by showing that in the presence of an inflammatory stimulant, material from mostly viable *Taenia* larvae suppresses several TLR4 downstream signalling cascades in the brain. Moreover, both *Cd14* and *Lbp* which encode proteins that assist with binding LPS to TLR4 were upregulated in astrocytes and/or microglia in response to LPS. In contrast, these genes were downregulated between the LPS vs LPS+Hom groups, suggesting that the *Taenia* homogenate may interfere with the LPS-induced upregulation of these two genes, thereby impeding the binding of LPS to TLR4.

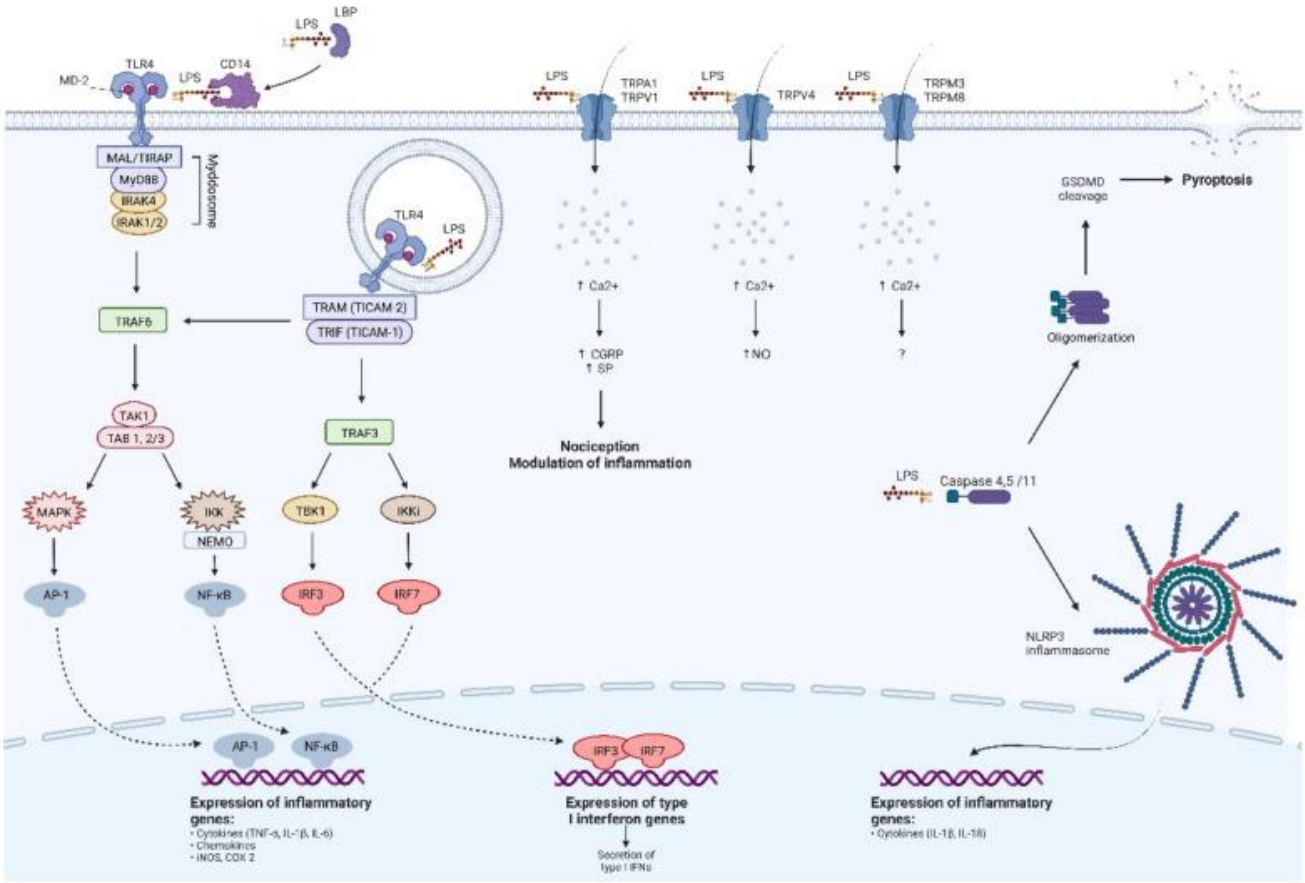

Figure 4.1 Mechanisms of molecular response to LPS (Taken from Figure 2 Skrzypczak-Wiercioch et al.[246], accessed March 2023). LPS binds several receptors and binding proteins, including LPS-binding protein (LBP), CD14, Toll like receptor 4 (TLR4), TRPA1, TRPV1, TRPV4, TRPM3, and TRPM8. Downstream of the TLR4 signalling cascade are the My88-dependent (Left) and My88-independent (Right) pathways. Together, these pathways lead to changes in inflammatory gene expression including the expression of various cytokines and chemokines as well as changes in the expression of type I interferon genes such as IFN-γ.

4.5 *Taenia crassiceps* had minimal effects on neuronal excitability genes when added to LPS.

I also decided to explore gene expression changes in the neuronal clusters between the LPS and LPS+Hom groups. Each of the neuronal clusters had more downregulated DEGs than upregulated DEGs for the LPS versus LPS+Hom DE comparison. The downregulated DEGs were associated with various inflammatory functions, suggesting that the immunosuppressive activity of the homogenate also affects neurons. In addition to this, I found that the addition of the homogenate to LPS had a statistically significant effect on the neuronal expression of 9 genes that belonged to my curated list of excitability genes. An enrichment analysis of these 9 excitability DEGs revealed an increase in GABAergic transmission by the dentate gyrus cells and a decrease in glutamatergic transmission by the excitatory neurons as well as changes associated with in sodium, calcium, and potassium transport. It is interesting to note that there

was an upregulation of GABAergic activity and a downregulation of glutamatergic activity, suggesting overall inhibitory effects of the homogenate in the presence of LPS. This fits well with the immunosuppressive effects of the homogenate which we hypothesised might play a role in seizure suppressing activity. However, as I have shown that LPS by itself had very little effect on neuronal excitability genes, it remains somewhat of a puzzle to understand how the homogenate would mediate the expression of genes involved in neuronal excitability. These findings are especially challenging to interpret considering that none of the differentially expressed excitability genes between the LPS vs LPS+Hom conditions were significantly differentially expressed in the control versus LPS or the control versus Hom comparisons. This implies that these differentially expressed excitability genes reflect neither the homogenate counteracting the effects of LPS nor an intrinsic effect of the homogenate alone. Either these identified DEGs are a spurious result (i.e., a false positive) or they are genes that are differentially expressed specifically when both the homogenate and LPS act in combination. This idea could be tested as we would expect that if LPS and the *T. crassiceps* homogenate acting together (rather than either one by itself) results in changes in the expression of these excitability genes, then the same excitability genes that are differentially expressed between the LPS versus LPS+Hom condition should also be differentially expressed between the control and LPS+Hom condition. This idea was thus refuted by the finding that the LPS vs LPS+Hom excitability DEGs were not differentially expressed in the control vs LPS+Hom condition. In this way, the analysis of the LPS vs LPS+Hom excitability DEGs showed little comparability to the effects of either LPS alone, the homogenate alone, or LPS and the homogenate acting together. Therefore, the biological significance of these results becomes hard to decipher, and caution is warranted in over-interpreting these results. Moreover, the vast majority of genes from the list of excitability genes were not significantly differentially expressed in neurons in response to the conditions where the *Taenia* homogenate was present (i.e., LPS versus LPS+Hom; controls versus Hom; and control versus LPS+Hom). Thus, it appears that the *T. crassiceps* homogenate has only minor effects on the transcription of genes that may mediate excitability. All in all, the snRNAseq findings for our *Taenia* homogenate treatments is purportedly comparable to a viable cestode model of NCC. In the presence of LPS, the homogenate demonstrated immunosuppressive activity most likely through the blockade of the TLR4 signalling pathway. In addition, the relative scarcity of convincing changes in excitability-related gene expression in response to the homogenate, or at most a slight shift towards inhibitory signalling, suggests that the main transcriptional signalling in neurons required for their normal functioning is conserved in the presence of the viable *T. crassiceps* homogenate whether alone or together with an inflammatory challenge.

4.6 LPS had no effect on the intrinsic electrical properties of pyramidal neurons.

The snRNAseq findings indicated that there were no major changes in excitability-related transcription in neurons following LPS exposure except for a few genes that could potentially mediate neurotransmission. These results were corroborated by the whole-cell patch-clamp data which found no changes in the intrinsic electrical properties of pyramidal neurons in response to 24-hour LPS treatment relative to control conditions. This suggests that short-term LPS exposure has little effect on the fundamental functioning of neurons *ex vivo*. As outlined in the introduction, there are numerous studies that have experimentally investigated the effects of LPS or other inflammatory challenges on neuronal excitability or seizure-related activity in the brain. Based on the experimental set-up used and main findings, these studies can be divided into categories to determine which studies are best to compare my results to. The first category of study includes those that have used a pro-convulsant agent to induce seizures and found that pro-inflammatory stimuli or immune activation can either exacerbate[108,110,111,115–126,133–139] or impede seizure activity and/or seizure susceptibility[155,156,165,295]. Most of these papers have found support for a role of inflammation in augmenting seizure activity but do not definitively show that inflammation alone is sufficient to alter network excitability or trigger seizures[108,110,111,115–126,133–139]. The second category of study consists of papers demonstrating a capacity for some components of the immune response to induce seizure-like activity without requiring pro-convulsant stimuli[145,151,152]. Then there are studies showing that immune activation by itself increases neuronal excitability but does not necessarily elicit seizure-like events by itself[60,152]. Finally, there are studies showing that certain inflammatory mediators either inhibit neuronal excitability or have no effect on neuronal function[157,160,161,279].

My experimental setup is best compared to the studies investigating the effects of inflammation alone on seizure activity or neuronal excitability. It is interesting to compare to studies that reported an increase in seizure activity or neuronal excitability as this is what I had initially predicted I might see. Two studies performed *in vivo* intracortical or intrahippocampal injections of either LPS or components of the complement system in rats and demonstrated that these pro-inflammatory stimuli elicited focal epileptiform discharges and/or seizures[145,146]. A key difference between these two studies and my own is that I was working with *ex vivo* hippocampal brain slices that lack adaptive immune responses. There is some support that adaptive immune responses, including the infiltration of leukocytes and serum albumin associated with BBB breakdown can play an important role in the relationship between inflammation and seizureogenesis[296]. Thus, the differences between my own

negative results and the findings of these two studies could potentially be attributed to a lack of adaptive immunity in my model system.

Nonetheless, there have also been several *in vitro* studies showing effects of LPS on seizure activity and neuronal excitability. Both Gullo et al.[152] and Giansante et al.[60] carried out work in primary cultures of mixed neuron, astrocyte, and microglial cells from mice and used *in vitro* multi-electrode arrays to measure reverberating activity of hundreds of neurons after LPS exposure[152]. Gullo et al.[152] found that approximately 5 hours of LPS exposure resulted in a net increase in the average number of spikes elicited which was reminiscent of seizure-like activity[152], while Giansante et al.[60] also demonstrated network hyperexcitability after 48 hours of LPS exposure. The preparation and recording methods of these studies are very different to my own, including the preparation of primary cultures that involved a tissue dissociation prior to culturing the cells as well as the use of multi-electrode arrays which record the field potential electrical activity from the extracellular space of a population of neurons. In contrast, I took recordings from individual neurons in intact organotypic brain slices using whole-cell patch-clamp electrophysiology. Consequently, while they were looking at overall excitability of the tissue in response to LPS, I was examining the effect of LPS on the intrinsic functioning of neurons, making it difficult to compare the two types of experiments.

However, Giansante et al.[60] did in fact also carry out patch-clamp experiments at 24, 48, 72, and 96 hours after LPS exposure to measure its effect on evoked excitatory and inhibitory postsynaptic currents (eEPSCs/eIPSCs) of hippocampal neurons. They reported that longer exposure to LPS resulted in a twofold increase in the eEPSC amplitude which was mostly absent when the cultures were only exposed to LPS for 5 mins [60]. No effect of LPS was found on eIPSC amplitude[60]. Additionally, the effect of LPS on excitatory neurotransmission was found to be dependent on TLR4 and the expression of L-type voltage-gated Ca21 channels at pre-synaptic terminals[60]. In support of these findings, Gao et al.[151] observed an increase in the amplitude of eEPSCs after 30 minutes of LPS exposure in acute mouse hippocampal slices but no effect on eIPSCs. Additionally, they found that LPS exposure increased the frequency of epileptiform discharges and spikes per burst induced by administration of 4-AP added to Mg^{2+}-free artificial cerebrospinal fluid[151]. Similarly, Pascual et al.[153] bath applied LPS to mouse acute hippocampal slices while taking whole-cell patch-clamp recordings. Interestingly, they observed an increase in the frequency of spontaneous EPSCs but no change in their amplitude, which differs to the two previous studies[60,152]. On the other hand, as with the two previous studies, Pascual et al.[153] also reported no effect on inhibitory neurotransmission in response to LPS[153]. Furthermore, the effect on EPSC frequency was found to be dependent on AMPAergic transmission, the presence of TLR4, as well as the purinergic receptor P2Y1R located on astrocytes[153]. Importantly, these three studies all

measured synaptic transmission and used various pharmacological blocks to isolate EPSCs and IPSCs mediated by different receptors and channels[60,151,153]. In contrast, I only looked at the intrinsic electrical properties of neurons in response to LPS but did not measure any synaptic properties. This is a major gap that could explain why I did not observe any changes in excitability in my setup. Future work can look to address this by exploring the effect of 24-hour LPS exposure on excitatory and inhibitory postsynaptic currents in mouse hippocampal OBSCs.

On the other hand, the paper by Hellstrom et al.[157] examined the effect of several day exposure to LPS on the intrinsic electrical properties of CA1 pyramidal neurons in rat hippocampal OBSCs. They reported that chronic exposure to LPS resulted in neurons having a significantly lower membrane resistance, a more elevated action potential threshold, and a slower frequency of action potential discharge compared to control slices exposed to regular growth media[157]. Additionally, the study found that the amplitude of inhibitory postsynaptic GABAergic potentials, but not excitatory glutamatergic postsynaptic potentials was significantly larger following chronic LPS exposure[157]. These results stand in contrast to the previous studies as they suggest that chronic LPS exposure modifies the intrinsic electrical properties of neurons and synaptic activity in such a way as to increase inhibitory neurotransmission[157]. There are a few differences in my model system compared to the Hellstrom et al.[157] paper, including that I used postnatal day 6-8 mice, whilst they used postnatal day 8-10 rats; I exposed brain slices to 10 ng/ml LPS for 24 hours, whereas they treated brain slices with 100 ng/ml LPS for 7 days; and finally, they also recorded changes in post-synaptic potentials, whilst I only measured the intrinsic electrical properties of cells. It is possible that factors such as species, age of the animal, dose, and period of exposure to LPS could also result in differences in neuronal responses to the treatment. On the other hand, Papageogriou et al.[279] found that LPS by itself had very little effects on neuronal excitability in rat hippocampal OBSCs but that exposure to IFN-γ together with LPS resulted in considerable neuronal dysfunction and death. This finding suggests that under some conditions, LPS alone may not be sufficient to alter excitability, but that the combination of immune mediators can play an important role in the effect that an inflammatory challenge has on brain function. My own work suggests that 24-hour exposure to 10 ng/ml of LPS in mouse hippocampal OBSCs does not affect the intrinsic excitability of pyramidal neurons.

These results serve as an important reminder that neuronal networks may be able to maintain normal function in the face of short-term innate immune activation. It is interesting that this narrative of the brain's resilience to inflammation is not prevalent in the literature, with most studies demonstrating how innate and adaptive immune responses can be detrimental to neuronal survival and/or alter neuronal function[60,145,146,151–153,157,245,246,251,261]. This may in part

be attributed to a publication bias towards studies that have found some effect of immune signalling in altering neuronal excitability and/or seizure activity. However, this is not to say that inflammation does not cause damage when unchecked nor to say that it does not play a role in seizure processes. It is evident from the sheer volume of literature available that there are numerous mechanisms by which neuroinflammation can contribute to seizures and epileptogenic processes. However, few studies have be able to produce models of epilepsy in which seizures are generated by inflammation in the absence of pharmacological interventions that facilitate epileptiform discharges. While there are examples of this[145,146,152], the scarcity of such a model system suggests that the conditions required for immune mediators to trigger seizures are specific and multifactorial. For example, the ability of an inflammatory challenge to alter neuronal excitability and/or trigger seizures may, in many cases, require involvement of the adaptive immune system or other precipitating conditions to be met such as dose, timing, developmental age, and choice of immune mediator(s).

4.7 The *Taenia crassiceps* homogenate had no effect on the intrinsic electrical properties of pyramidal neurons.

To explore whether *Taenia* larvae modulate neuronal excitability, I also performed whole-cell patch-clamp experiments on brain slices exposed to the *T. crassiceps* homogenate by itself and in the presence of LPS. I showed that neither of these treatments resulted in significant differences in the intrinsic electrical properties of pyramidal neurons when compared to control conditions, LPS, or to each other. These results corroborated the snRNAseq data in which there were few convincing changes in the expression of genes that might mediate neuronal excitability. There is limited research that has experimentally explored the electrophysiological effects of *Taenia* larvae on brain tissue. As described earlier, one research group has demonstrated that the release of Substance P from granulomas associated with dying *T. crassiceps* larvae has a seizurogenic effect in mice and rats injected intracranially with the granuloma extracts [55–57]. Some differences between this research and my own is that these studies were carried out *in vivo* and used observation and electroencephalogram monitoring to record seizure activity[55–57]. Additionally, while the early-stage granuloma extracts were found to contain parasite remnants, they did not test the effects of larvae directly on the brain without the presence of the granulomas. To my knowledge, there is only one other study published by members of the Raimondo lab and colleagues that explored electrophysiological effects of the *T. crassiceps* larvae using whole-cell patch-clamp[196]. They were able to demonstrate that AChEs derived from heat-activated secretory/excretory extracts of *T. crassiceps* larvae have sufficient activity to break down ACh at a concentration which induces changes in neuronal signalling[196]. In particular, the study involved puffing ACh directly onto neurons along with either heat-inactivated or heat-activated extracts of the *T. crassiceps*

homogenate shown to contain AChE[196]. They found that depolarisations and action potentials triggered when ACh was puffed together with heat-inactive *T. crassiceps* extracts were abolished when this was swapped for heat-activated extracts[196]. While these results do not show a direct effect of the *T. crassiceps* extracts altering neuronal excitability by themself, they do provide support that certain heat-labile components of *T. crassiceps* larvae have the potential to alter neurotransmission in the presence of relevant neurotransmitter signalling such as cholinergic signalling[196]. Markedly, the effect that they observed was suggestive of acute inhibitory activity by the heat-activated *Taenia* secretory/extracts which supports our hypothesis that the *T. crassiceps* homogenate which has immunosuppressive activity may have inhibitory effects on neurons. However, my data indicated that longer exposure to the *T. crassiceps* homogenate did not have any inhibitory effect on fundamental neuronal properties when acting alone or together with LPS. Arguably, this finding still aligns with the proposition that our whole-cyst homogenate represents the viable cestode stage of NCC. When both LPS and the *T. crassiceps* homogenate were administered, there were no effects on neuronal function, implying that neurons can maintain normal function despite being exposed to these mediators. This may reflect what happens in the brain of asymptomatic NCC patients: rather than *Taenia* larvae actively exerting chronic inhibitory or seizure-suppressing effects on neurons, it may simply be the absence of mediators that would increase excitability, such as Substance P, which accounts for the lack of neuronal excitability changes and scarcity of seizures during the vesicular stage of the disease. My data suggests that viable *Taenia* larvae drive immunosuppressive activity by blocking key inflammatory pathways in the brain which may allow them to survive in the viable state for some time. At a later point, when cysts start to degenerate, Substance P or other mediators which were not released during the viable cestode stage may begin to modify neuronal excitability and contribute to the onset of seizures. This project has therefore provided some possible insights into brain function during the asymptomatic stage of NCC during which the host immune response is generally suppressed. To gain more insight into the exact mechanisms by which seizures might occur in NCC, similar whole-cell patch-clamp experiments can be performed but instead use dead/dying *T. crassiceps* larvae and associated granulomas as described by Robinson et al.[57].

4.8 Limitations and directions for future work

There are various limitations to consider about this research project. Firstly, there are some considerations regarding the model system for both immune activation and *Taenia* infection. The hippocampal OBSCs are an *ex vivo* preparation which lacks adaptive immunity and associated invasion of peripheral immune cells with possible accompanying changes in BBB permeability as well as albumin extravasation[297]. Thus, it is possible that certain changes in gene expression or even neuronal excitability would be seen *in vivo* in response to LPS or the

Taenia larvae that we do not see in *ex vivo* conditions. Nonetheless, this *ex vivo* preparation offers its own advantage in providing a reduced system to isolate the effects of the innate immune response in response to these immunoregulatory stimuli. Another limitation of the model system is that it is only from one region in the brain, and therefore does not represent transcriptional and electrophysiological changes that occur across other parts of the brain following exposure to LPS or *Taenia* larvae. Arguably, focusing on just one brain region may be valuable as it reduces variability across samples and in turn increases the power of the analysis when it comes to understanding the effects of the treatments on transcription and neuronal excitability. Furthermore, the hippocampus is a well-established brain area for modelling epileptogenesis, and therefore was an appropriate region to focus on for this study[298]. Nevertheless, it is likely that different brain regions would have different responses to these treatments. For example, a specific subset of neurons in the hypothalamus have been shown to control fever and changes in appetite in response to LPS[260]. Additionally, the age and sex of the animals used in the experiments is also a factor worth considering, as there is evidence that treatment with LPS has varied effects on inflammatory transcription in the brain depending on the developmental period during which the exposure took place as well as the sex of the animal[144,299].

Other considerations include the agents used to model immune activation and *Taenia* infection. To stimulate immune activation, I chose to work with LPS as this is a commonly used mediator to activate an inflammatory response in the brain and other tissues[246]. However, it is worth acknowledging that exposure to LPS represents only one form of immune activation as there are other ways of evoking immune responses such using other PAMPs or DAMPs or by using pro-inflammatory cytokines such as TNF-α and IL-1β[300]. As a result, some of the findings could present differently in the presence of a different inflammatory stimulant. Likewise, to model *Taenia* infection in the brain, I chose to work with a homogenate made from *T. crassiceps* larvae. While several studies have provided support for *T. crassiceps* being very similar to *T.* solium[174–176,301], there are some differences between these two cestodes, including their natural life cycle as well as enzymatic activity which are important to keep in mind when using *T. crassiceps* to model human NCC as not all effects of *T. crassiceps* will necessarily extrapolate to *T. solium*[185,196]. Nonetheless, as there is reasonable similarity between these two cestodes, the insights gained from research on *T. crassiceps* can add to our knowledge and understanding about possible pathophysiological changes in NCC whilst avoiding some of the challenges involved in obtaining and working with *T. solium.* In addition to the species used, the viability of the *Taenia* larvae is a crucial aspect of the design as it will determine which stage of NCC is likely being modelled. Our whole-cyst *Taenia* larval homogenate was prepared from *T. crassiceps* larvae that were mostly viable at the point of

freezing. This, as well as the data demonstrating robust immunosuppressive activity and no effect on excitability of neurons, indicates that the homogenate likely models the early, viable stage of NCC during which patients are usually asymptomatic. Treating tissue with this *T. crassiceps* homogenate has provided some further understandings about how viable *Taenia* larvae modulate the host immune response in the brain. However, to understand mechanisms underlying seizure occurrence in NCC, it may be worth replicating some of these experiments with dead or dying granulomas associated with *T. crassiceps* larvae, as previously described[56,57].

Additionally, with regards to modelling neuroinflammation and *Taenia* infection in the brain, the dose and timing of exposure to LPS and the *Taenia* larval homogenate are variables that could mediate both transcriptional and electrophysiological responses to these agents. There has been quite a lot of heterogeneity in studies in terms of the concentrations of LPS used to incite an inflammatory challenge in the brain. Interestingly, several of the papers that found changes in excitatory neurotransmission in response to LPS used different concentrations of LPS and different periods of exposure but found similar results[60,151,153]. However, the study using the longest period of exposure found the opposite effect, reporting an increase in inhibitory neurotransmission which suggests that chronicity could determine the effect that molecules such as LPS have on neuronal excitability[157]. Both immune activation and *Taenia* infection are phenomena that occur over months to years in human patients. This chronic alteration in the brain's immune response may be a key component of the effect of these stimuli on neuronal network function. While it is not possible or feasible to model such long periods in culture, the 24-hour exposure was chosen to simulate slightly longer exposure times that would allow for changes in gene expression to occur. Nonetheless, it very possible that certain changes which occur over much longer time periods in NCC patients or patients with chronic inflammatory conditions that lead to epilepsy would not be reproduced in our model system.

Other limitations of this work relate to the snRNAseq experiments. For the transcriptional component of this study, I was specifically measuring levels of nuclear transcript in response to the different treatment conditions. Importantly, mRNA levels can change after transcripts get exported into the cytoplasm and transported to distal part of the cell such as the dendrites and axons due to RNA degradation and other regulatory processes[302,303]. As a result, any changes to mRNA levels occurring after translocation out of the nucleus in response to LPS or to the *T. crassiceps* homogenate would not have been detected. Furthermore, the snRNAseq platform that we used is not sensitive to splicing events which have previously been shown to take place in response to LPS exposure[250,304]. This is also a level of transcriptional regulation that *Taenia* larvae may modify which could be studied in future work.

Another limitation of looking at transcriptional changes is that post-translational modifications can occur to modify protein function which would not be reflected when measuring levels of mRNA[305]. This is especially relevant when it comes to molecular changes that may mediate excitability of neurons as some of the main changes that alter neuronal function are structural or biochemical changes to receptors and ion channels such as the phosphorylation of different neurotransmitter receptors which can modify their conductance or permeability to different ions[274–276]. My snRNAseq data indicated some changes in phosphorylation activity in response to LPS. However, whether this is linked to synaptic function would need to be studied further. While there are limitations of using a transcriptional approach to interpret changes in excitability, it is worth emphasising that this high-throughput transcriptional method offers the key advantage of being able to sequence essentially all relevant genes across all cell types, thereby enabling a relatively unbiased overview of the main molecular pathways that change in response to a treatment of interest[203]. In this way, any transcriptional changes occurring within different cell types can be used to generate new hypotheses about which genes networks are involved in regulating a cell's response to LPS or *T. crassiceps* larvae. However, functional studies with specific protein targets may be required to understand other regulatory effects of LPS and the homogenate, and this is particularly applicable for identifying alterations in synaptic properties and the excitability of neurons. Lastly, the label transfer method, which was used in conjunction with other approaches to annotate the snRNAseq clusters, may have been limited by the decision to improve computational efficiency by excluding nuclei from the Allen reference dataset that expressed more than 7500 genes. Arguably, this decision was justified in that, even with the high-performance computing facilities, it would not have been computationally feasible to use the Allen reference dataset in the analysis without first processing it to be smaller. Furthermore, as there was relatively good consensus between the annotations obtained using this method and other approaches, it is unlikely that the chosen filtering step significantly compromised the annotations obtained using the Label Transfer approach.

In addition, there were some limitations inherent to the whole-cell patch-clamp experiments that I carried out. For one, I only recorded from pyramidal neurons in the CA1 and CA3 areas of the hippocampus. It is possible that other neuronal populations such as various inhibitory neuronal sub-types or neurons in the dentate gyrus may respond to LPS or to the *Taenia* homogenate. However, once again, this comes down to the weigh up between gathering more information across different cell types versus introducing unwanted variability in the data. Choosing to record from diverse cell types would come with the challenge of acquiring sufficient cells to be sampled per cell type to be able to trust that any observed effects are a result of the treatment group rather than variation affected by the relative cell type

representation in each treatment group. As the set of conditions and technicality required to obtain even a single successful patch-clamp recording from a neuron can be very finicky and time-intensive, obtaining a large enough sample size can be difficult. In the case of my experimental design, this was heightened by the fact that there were four different treatment groups that each required a sufficient number of recordings from different cells. Thus, the choice to only focus on pyramidal neurons was justified by the decision to prioritise having a large enough number of datapoints per treatment group that would allow me to be confident in any effects observed. Another limitation of my electrophysiology experiments that I have mentioned prior to this is that only the intrinsic electrical properties of neurons were measured, but other relevant measures of neuronal excitability such as excitatory and inhibitory post-synaptic currents/potentials as well as bursting activity or seizure-like events were not examined. Several studies have found effects of LPS on synaptic properties of neurons and/or on the overall excitability of brain tissue[60,151,153,157]. Therefore, exploring these other measures of neuronal excitability in response to LPS and the *Taenia* larval homogenate in mouse hippocampal OBSCs would strengthen the existing analysis.

4.9 Conclusion

In summary, this project provides support that innate immune activation drives large transcriptional changes across all major brain cell types. The main transcriptional changes were associated with genes known to mediate inflammatory regulatory networks. Remarkably, very few changes were observed in the expression of genes that may mediate neuronal excitability. This was corroborated by whole-cell patch-clamp data showing no changes in the intrinsic electrical properties of neurons in response to short-term innate immune activation. In addition to this, *Taenia* larvae demonstrated a capacity to prevent the upregulation of proinflammatory transcriptional activity in the presence of LPS. The extent of this immunosuppression and associated downregulated pathways suggests that the *T. crassiceps* homogenate may exert its immunosuppressive effect by blocking the TLR4 signalling pathway. Few convincing changes in the expression of neuronal excitability genes were seen in response to the *T. crassiceps* homogenate. Additionally, the whole-cell patch-clamp experiments indicated no effect of the *T. crassiceps* homogenate on the intrinsic electrical properties of pyramidal neurons. Overall, it is proposed that the effects of the whole-cyst *T. crassiceps* homogenate best reflects what might be seen during the viable cyst stage of NCC, characterised by suppression of the host immune response but normal neuronal function remaining intact.

Acknowledgement

Several figures in this thesis included images that were generated using Biorender.

Supplementary data

https://drive.google.com/drive/folders/1UxkXk-8xTPn0xOThoHUelwdXPaYEu9j0?usp=sharing

References

1. Del Brutto OH. Neurocysticercosis. Published online 2014. doi:10.1177/1941874414533351
2. Garcia HH, Nash TE, Del Brutto OH. Clinical symptoms, diagnosis, and treatment of neurocysticercosis. *Lancet Neurol*. 2014;13(12):1202-1215. doi:10.1016/S1474-4422(14)70094-8
3. Ndimubanzi PC, Carabin H, Budke CM, et al. A systematic review of the frequency of neurocyticercosis with a focus on people with epilepsy. *PLoS Negl Trop Dis*. 2010;4(11). doi:10.1371/journal.pntd.0000870
4. Gripper LB, Welburn SC. The causal relationship between neurocysticercosis infection and the development of epilepsy - a systematic review. *Infect Dis Poverty*. 2017;6(1). doi:10.1186/s40249-017-0245-y
5. Carabin H, Ndimubanzi PC, Budke CM, et al. Clinical manifestations associated with neurocysticercosis: A systematic review. *PLoS Negl Trop Dis*. 2011;5(5). doi:10.1371/journal.pntd.0001152
6. Fabiani S, Bruschi F. Neurocysticercosis in Europe: Still a public health concern not only for imported cases. *Acta Trop*. 2013;128(1):18-26. doi:10.1016/J.ACTATROPICA.2013.06.020
7. WHO. Preventable epilepsy: Taenia solium infection burdens economies, societies and individuals: a rationale for investment and action. *Preventable epilepsy: Taenia solium infection burdens economies, societies and individuals: a rationale for investment and action*. Published online 2016.
8. White AC. Neurocysticercosis: A major cause of neurological disease worldwide. *Clinical Infectious Diseases*. 1997;24(2):101-115. doi:10.1093/clinids/24.2.101
9. Román G, Sotelo J, Del Brutto O, et al. A proposal to declare neurocysticercosis an international reportable disease. *Bull World Health Organ*. 2000;78(3):399-406.
10. Kerr MP. The impact of epilepsy on patients' lives. *Acta Neurol Scand*. 2012;126(S194). doi:10.1111/ane.12014
11. World Health Organisation. Epilepsy. Epilepsy Fact Sheet. Published 2019. Accessed April 1, 2023. https://www.who.int/news-room/fact-sheets/detail/epilepsy

12. Roma G, Sotelo J, Brutto O Del, et al. Policy and Practice A proposal to declare neurocysticercosis an international reportable disease.

13. Bhattarai R, Budke CM, Carabin H, et al. Quality of Life in Patients with Neurocysticercosis in Mexico. *Am J Trop Med Hyg*. 2011;84(5):782-786. doi:10.4269/AJTMH.2011.10-0646

14. De Lange A, Mahanty S, Raimondo J V. Model systems for investigating disease processes in neurocysticercosis. *Parasitology*. 2019;146(5):553-562. doi:10.1017/S0031182018001932

15. White AC, Baig S, Robinson P. Taenia saginata oncosphere excretory/secretory peptidases. *Journal of Parasitology*. 1996;82(1). doi:10.2307/3284107

16. García HH, Gonzalez AE, Evans CAW, Gilman RH, Working C. Taenia solium cysticercosis. *The Lancet*. 2003;361:547-556.

17. Arturo Carpio. Neurocysticercosis: an update. *Lancet Infect Disease*. 2002;2(12):751-762.

18. Steyn TJS, Awala AN, de Lange A, Raimondo JV. What Causes Seizures in Neurocysticercosis? *Epilepsy Curr*. 2022;0(0). doi:10.1177/15357597221137418

19. Carpio A, Romo ML. The relationship between neurocysticercosis and epilepsy: An endless debate. *Arq Neuropsiquiatr*. 2014;72(5). doi:10.1590/0004-282X20140024

20. Fleury A, Escobar A, Fragoso G, Sciutto E, Larralde C. Clinical heterogeneity of human neurocysticercosis results from complex interactions among parasite, host and environmental factors. *Trans R Soc Trop Med Hyg*. 2010;104(4):243-250. doi:10.1016/J.TRSTMH.2010.01.005

21. Flisser A, Espinoza B, Tovar A, Plancarte A, Correa D. Host-parasite relationship in cysticercosis: Immunologic study in different compartments of the host. *Vet Parasitol*. 1986;20(1-3). doi:10.1016/0304-4017(86)90094-4

22. Singh AK, Prasad KN, Prasad A, Tripathi M, Gupta RK, Husain N. Immune responses to viable and degenerative metacestodes of Taenia solium in naturally infected swine. *Int J Parasitol*. 2013;43(14):1101-1107. doi:10.1016/j.ijpara.2013.07.009

23. Fleury A, Cardenas G, Adalid-Peralta L, Fragoso G, Sciutto E. Immunopathology in Taenia solium neurocysticercosis. *Parasite Immunol*. 2016;38(3):147-157. doi:10.1111/pim.12299

24. Prasad A, Gupta RK, Pradhan S, Tripathi M, Pandey CM, Prasad KN. What triggers seizures in neurocysticercosis? A MRI-based study in pig farming community from a district of North India. *Parasitol Int*. 2008;57(2). doi:10.1016/j.parint.2007.12.001

25. Prasad KN, Verma A, Srivastava S, Gupta RK, Pandey CM, Paliwal VK. An epidemiological study of asymptomatic neurocysticercosis in a pig farming community in northern India. *Trans R Soc Trop Med Hyg*. 2011;105(9). doi:10.1016/j.trstmh.2011.06.001

26. Ndimubanzi PC, Carabin H, Budke CM, et al. A systematic review of the frequency of neurocyticercosis with a focus on people with epilepsy. *PLoS Negl Trop Dis*. 2010;4(11). doi:10.1371/journal.pntd.0000870

27. Restrepo BI, Llaguno P, Sandoval MA, Enciso JA, Teale JM. Analysis of immune lesions in neurocysticercosis patients: Central nervous system response to helminth appears Th1-like instead of Th2. *J Neuroimmunol*. 1998;89(1-2):64-72. doi:10.1016/S0165-5728(98)00112-X

28. Garcia HH, Del Brutto OH. Antiparasitic treatment of neurocysticercosis - The effect of cyst destruction in seizure evolution. *Epilepsy and Behavior*. 2017;76:158-162. doi:10.1016/j.yebeh.2017.03.013

29. Verma A, Prasad KN, Cheekatla SS, Nyati KK, Paliwal VK, Gupta RK. Immune response in symptomatic and asymptomatic neurocysticercosis. *Med Microbiol Immunol*. 2011;200(4). doi:10.1007/s00430-011-0198-x

30. Prasad A, Prasad KN, Gupta RK, Pradhan S. Increased expression of ICAM-1 among symptomatic neurocysticercosis. *J Neuroimmunol*. 2009;206(1-2):118-120. doi:10.1016/j.jneuroim.2008.09.015

31. Carpio A, Romo ML, Hauser WA, Kelvin EA. New understanding about the relationship among neurocysticercosis, seizures, and epilepsy. *Seizure*. 2021;90. doi:10.1016/j.seizure.2021.02.019

32. Amit P, Prasad KN, Kumar GR, et al. Immune response to different fractions of Taenia solium cyst fluid antigens in patients with neurocysticercosis. *Exp Parasitol*. 2011;127(3):687-692. doi:10.1016/j.exppara.2010.11.006

33. Verma A, Prasad KN, Gupta RK, et al. Toll-Like Receptor 4 Polymorphism and Its Association with Symptomatic Neurocysticercosis. *J Infect Dis*. 2010;202(8):1219-1225. doi:10.1086/656395

34. Galea I. The blood–brain barrier in systemic infection and inflammation. *Cell Mol Immunol*. 2021;18(11). doi:10.1038/s41423-021-00757-x

35. Alvarez JI, Teale JM. Breakdown of the blood brain barrier and blood-cerebrospinal fluid barrier is associated with differential leukocyte migration in distinct compartments of the CNS during the course of murine NCC. *J Neuroimmunol*. 2006;173(1-2):45-55. doi:10.1016/j.jneuroim.2005.11.020

36. Guerra-Giraldez C, Marzal M, Cangalaya C, et al. Disruption of the blood-brain barrier in pigs naturally infected with Taenia solium, untreated and after anthelmintic treatment. *Exp Parasitol*. 2013;134(4). doi:10.1016/j.exppara.2013.05.005

37. Verma A, Prasad KN, Nyati KK, et al. Association of MMP-2 and MMP-9 with clinical outcome of neurocysticercosis. *Parasitology*. 2011;138(11). doi:10.1017/S0031182011001259

38. David Y, Cacheaux LP, Ivens S, et al. Astrocytic dysfunction in epileptogenesis: Consequence of altered potassium and glutamate homeostasis? *Journal of Neuroscience*. 2009;29(34). doi:10.1523/JNEUROSCI.2323-09.2009

39. Noé FM, Bellistri E, Colciaghi F, et al. Kainic acid–induced albumin leak across the blood–brain barrier facilitates epileptiform hyperexcitability in limbic regions. *Epilepsia*. 2016;57(6):967-976. doi:10.1111/EPI.13394

40. Weissberg I, Wood L, Kamintsky L, et al. Albumin induces excitatory synaptogenesis through astrocytic TGF-β/ALK5 signaling in a model of acquired epilepsy following

blood-brain barrier dysfunction. *Neurobiol Dis*. 2016;78:115-125. doi:10.1016/j.nbd.2015.02.029.Albumin

41. Nash TE, Pretell EJ, Lescano AG, et al. Perilesional brain oedema and seizure activity in patients with calcified neurocysticercosis: a prospective cohort and nested case-control study. *Lancet Neurol*. 2008;7(12):1099-1105. doi:10.1016/S1474-4422(08)70243-6

42. McKeever PE. Immunohistology of the Nervous System. In: *Diagnostic Immunohistochemistry*. ; 2010. doi:10.1016/B978-1-4160-5766-6.00024-8

43. Messam CA, Hou J, Janabi N, Monaco MC, Gravell M, Major EO. Glial Cell Types. In: *Encyclopedia of the Human Brain*. ; 2002. doi:10.1016/b0-12-227210-2/00152-7

44. Jha SK. Cerebral edema and its management. *Med J Armed Forces India*. 2003;59(4). doi:10.1016/S0377-1237(03)80147-8

45. Pradhan S, Kathuria MK, Gupta RK. Perilesional gliosis and seizure outcome: a study based on magnetization transfer magnetic resonance imaging in patients with neurocysticercosis. *Ann Neurol*. 2000;48(2):181-187. Accessed August 19, 2019. http://www.ncbi.nlm.nih.gov/pubmed/10939568

46. Nash TE, Garcia HH. Perilesional brain oedema and seizure activity: cause or effect? - Authors' reply. *Lancet Neurol*. 2009;8(3). doi:10.1016/S1474-4422(09)70029-8

47. Losi G, Cammarota M, Carmignoto G. The role of astroglia in the epileptic brain. *Front Pharmacol*. 2012;3 JUL. doi:10.3389/fphar.2012.00132

48. Loewen JL, Barker-Haliski ML, Jill Dahle E, Steve White H, Wilcox KS. Neuronal injury, gliosis, and glial proliferation in two models of temporal lobe epilepsy. *J Neuropathol Exp Neurol*. 2016;75(4). doi:10.1093/jnen/nlw008

49. Lassmann H, Petsche U, Kitz K, et al. The role of brain edema in epileptic brain damage induced by systemic kainic acid injection. *Neuroscience*. 1984;13(3). doi:10.1016/0306-4522(84)90089-7

50. Iffland PH, Grant GA, Janigro D. Mechanisms of cerebral edema leading to early seizures after traumatic brain injury. In: *Vascular Mechanisms in CNS Trauma*. ; 2014. doi:10.1007/978-1-4614-8690-9_2

51. Hüttmann K, Sadgrove M, Wallraff A, et al. Seizures preferentially stimulate proliferation of radial glia-like astrocytes in the adult dentate gyrus: Functional and immunocytochemical analysis. *European Journal of Neuroscience*. 2003;18(10). doi:10.1111/j.1460-9568.2003.03002.x

52. Represa A, Niquet J, Pollard H, Ben-Ari Y. Cell death, gliosis, and synaptic remodeling in the hippocampus of epileptic rats. *J Neurobiol*. 1995;26(3). doi:10.1002/neu.480260313

53. Vezzani A, Auvin S, Ravizza T, Aronica E. *Glia-Neuronal Interactions in Ictogenesis and Epileptogenesis: Role of Inflammatory Mediators*.; 2012.

54. Vezzani A, Auvin S, Ravizza T, Aronica E. *Glia-Neuronal Interactions in Ictogenesis and Epileptogenesis: Role of Inflammatory Mediators*.; 2012.

55. Matos-Silva H, Reciputti BP, de Paula ÉC, et al. Experimental encephalitis caused by Taenia crassiceps cysticerci in mice. *Arq Neuropsiquiatr*. 2012;70(4). doi:10.1590/S0004-282X2012005000010

56. Stringer JL, Marks LM, White AC, Robinson P. Epileptogenic activity of granulomas associated with murine cysticercosis. *Exp Neurol*. 2003;183(2):532-536. doi:10.1016/S0014-4886(03)00179-1

57. Robinson P, Garza A, Weinstock J, Serpa JA, Goodman JC. Substance P Causes Seizures in Neurocysticercosis. *PLoS Pathog*. 2012;8(2):1002489. doi:10.1371/journal.ppat.1002489

58. Garza A, Tweardy DJ, Weinstock J, Viswanathan B, Robinson P. Substance P signaling contributes to granuloma formation in taenia crassiceps infection, a murine model of cysticercosis. *J Biomed Biotechnol*. 2010;2010. doi:10.1155/2010/597086

59. Mashaghi A, Marmalidou A, Tehrani M, Grace PM, Pothoulakis C, Dana R. Neuropeptide substance P and the immune response. *Cellular and Molecular Life Sciences*. 2016;73(22). doi:10.1007/s00018-016-2293-z

60. Giansante G, Marte A, Romei A, et al. Presynaptic L-Type Ca21 channels increase glutamate release probability and excitatory strength in the hippocampus during chronic neuroinflammation. *Journal of Neuroscience*. 2020;40(36):6825-6841. doi:10.1523/JNEUROSCI.2981-19.2020

61. Herrick JA, Bustos JA, Clapham P, Garcia HH, Loeb JA. Unique characteristics of epilepsy development in neurocysticercosis. *American Journal of Tropical Medicine and Hygiene*. 2020;103(2). doi:10.4269/ajtmh.19-0485

62. De Taveira MO, Morita ME, Yasuda CL, et al. Neurocysticercotic calcifications and hippocampal sclerosis: A case-control study. *PLoS One*. 2015;10(7). doi:10.1371/journal.pone.0131180

63. Thom M. Review: Hippocampal sclerosis in epilepsy: A neuropathology review. *Neuropathol Appl Neurobiol*. 2014;40(5). doi:10.1111/nan.12150

64. Neto AR, Centeno RS, Ferraz F. Tratamento cirúrgico da epilepsia associada à neurocisticercose. *JBNC - JORNAL BRASILEIRO DE NEUROCIRURGIA*. 2018;9(3). doi:10.22290/jbnc.v9i3.287

65. Rathore C, Thomas B, Kesavadas C, Abraham M, Radhakrishnan K. Calcified neurocysticercosis lesions and antiepileptic drug-resistant epilepsy: A surgically remediable syndrome? *Epilepsia*. 2013;54(10). doi:10.1111/epi.12349

66. Carpio A, Romo ML. Should calcified neurocysticercosis lesions be surgically removed? *Epilepsia*. 2014;55(2). doi:10.1111/epi.12510

67. García HH, Evans CAW, Nash TE, et al. Current Consensus Guidelines for Treatment of Neurocysticercosis. *Clin Microbiol Rev*. 2002;15(4):747-756. doi:10.1128/CMR.15.4.747-756.2002

68. White AC, Coyle CM, Rajshekhar V, et al. Diagnosis and Treatment of Neurocysticercosis: 2017 Clinical Practice Guidelines by the Infectious Diseases Society of America (IDSA) and the American Society of Tropical Medicine and Hygiene (ASTMH). *Clinical Infectious Diseases*. 2018;66(8). doi:10.1093/cid/cix1084

69. H. Garcia, T. Nash, O. Del Brutto O. Clinical symptoms, diagnosis, and treatment of neurocysticercosis. *Physiol Behav*. 2017;176(3):139-148. doi:10.1016/S1474-4422(14)70094-8.Clinical

70. Cuddapah VA, Robel S, Watkins S, Sontheimer H. A neurocentric perspective on glioma invasion. *Nat Rev Neurosci*. 2014;15(7). doi:10.1038/nrn3765

71. Bustos J, Gonzales I, Saavedra H, Handali S, Garcia HH. Neurocysticercosis. A frequent cause of seizures, epilepsy, and other neurological morbidity in most of the world. *J Neurol Sci*. 2021;427. doi:10.1016/j.jns.2021.117527

72. Abba K, Ranganathan LN, Ramaratnam S. Anthelmintics for people with neurocysticercosis. *Cochrane Database of Systematic Reviews*. 2021;(4). doi:10.1002/14651858.CD006200

73. Baranwal AK, Singhi PD, Khandelwal N, Singhi SC. Albendazole therapy in children with focal seizures and single small enhancing computerized tomographic lesions: A randomized, placebo-controlled, double blind trial. *Pediatric Infectious Disease Journal*. 1998;17(8):696-700. doi:10.1097/00006454-199808000-00007

74. Garcia HH, Pretell EJ, Gilman RH, et al. A Trial of Antiparasitic Treatment to Reduce the Rate of Seizures Due to Cerebral Cysticercosis. *New England Journal of Medicine*. 2004;350(3):249-258. doi:10.1056/NEJMoa031294

75. Baird RA, Wiebe S, Zunt JR, Halperin JJ, Gronseth G, Roos KL. Evidence-based guideline: Treatment of parenchymal neurocysticercosis: Report of the guideline development subcommittee of the American Academy of Neurology. *Neurology*. 2013;80(15):1424-1429. doi:10.1212/WNL.0b013e31828c2f3e

76. Sharma M, Singh T, Mathew A. Antiepileptic drugs for seizure control in people with neurocysticercosis. *Cochrane Database of Systematic Reviews*. Published online October 12, 2015. doi:10.1002/14651858.CD009027.pub2

77. Garcia HH, Gonzales I, Lescano AG, et al. Efficacy of combined antiparasitic therapy with praziquantel and albendazole for neurocysticercosis: A double-blind, randomised controlled trial. *Lancet Infect Dis*. 2014;14(8). doi:10.1016/S1473-3099(14)70779-0

78. Romo ML, Wyka K, Carpio A, et al. The effect of albendazole treatment on seizure outcomes in patients with symptomatic neurocysticercosis. *Trans R Soc Trop Med Hyg*. 2015;109(11). doi:10.1093/trstmh/trv078

79. Otte WM, Singla M, Sander JW, Singh G. Drug therapy for solitary cysticercus granuloma: A systematic review and meta-analysis. *Neurology*. 2013;80(2). doi:10.1212/WNL.0b013e31827b90a8

80. Zhao BC, Jiang HY, Ma WY, et al. Albendazole and Corticosteroids for the Treatment of Solitary Cysticercus Granuloma: A Network Meta-analysis. *PLoS Negl Trop Dis*. 2016;10(2). doi:10.1371/journal.pntd.0004418

81. Garcia HH, Gonzales I, Lescano AG, et al. Enhanced steroid dosing reduces seizures during antiparasitic treatment for cysticercosis and early after. *Epilepsia*. 2014;55(9):1452-1459. doi:10.1111/epi.12739

82. Del Brutto OH, Sotelo J. Neurocysticercosis: An update. *Clinical Infectious Diseases*. 1988;10(6). doi:10.1093/clinids/10.6.1075

83. Nash TE, Mahanty S, Garcia HH. Corticosteroid use in neurocysticercosis. *Expert Rev Neurother*. 2011;11(8). doi:10.1586/ern.11.86

84. de Kinderen R, Evers S, Rinkens R, et al. Side-effects of antiepileptic drugs: the economic burden. *Seizure*. 2014;23(3):184-190. doi:10.1016/J.SEIZURE.2013.11.009

85. Vazquez V, Sotelo J. The Course of Seizures after Treatment for Cerebral Cysticercosis. *New England Journal of Medicine*. 1992;327(10):696-701. doi:10.1056/nejm199209033271005

86. Garcia HH, Pretell EJ, Gilman RH, et al. A Trial of Antiparasitic Treatment to Reduce the Rate of Seizures Due to Cerebral Cysticercosis. *New England Journal of Medicine*. 2004;350(3):249-258. doi:10.1056/NEJMoa031294

87. World Health Organization. *WHO | Epilepsy: A Public Health Imperative*.; 2019.

88. Chen Z, Brodie MJ, Liew D, Kwan P. Treatment outcomes in patients with newly diagnosed epilepsy treated with established and new antiepileptic drugs a 30-year longitudinal cohort study. *JAMA Neurol*. 2018;75(3). doi:10.1001/jamaneurol.2017.3949

89. Vezzani A, French J, Bartfai T, Baram TZ. The role of inflammation in epilepsy. *Nat Rev Neurol*. 2011;7(1):31-40. doi:10.1038/nrneurol.2010.178

90. Rana A, Musto AE. The role of inflammation in the development of epilepsy. *J Neuroinflammation*. 2018;15(1). doi:10.1186/S12974-018-1192-7

91. Balosso S, Vezzani A, Ravizza T. Emerging Molecular Mechanisms of Neuroinflammation in Seizure Disorders. In: Springer, Cham; 2021:21-43. doi:10.1007/978-3-030-67403-8_2

92. Riikonen R. Infantile spasms: Therapy and outcome. *J Child Neurol*. 2004;19(6). doi:10.1177/088307380401900601

93. Wheless JW, Clarke DF, Arzimanoglou A, Carpenter D. Treatment of pediatric epilepsy: European expert opinion, 2007. *Epileptic Disorders*. 2007;9(4). doi:10.1684/epd.2007.0144

94. Wirrell E, Farrell K, Whiting S. The epileptic encephalopathies of infancy and childhood. *Canadian Journal of Neurological Sciences*. 2005;32(4). doi:10.1017/S0317167100004388

95. Schorner A, Weissert R. Patients with epileptic seizures and multiple sclerosis in a multiple sclerosis center in Southern Germany between 2003-2015. *Front Neurol*. 2019;10(JUN). doi:10.3389/fneur.2019.00613

96. Bien CG, Urbach H, Schramm J, et al. Limbic encephalitis as a precipitating event in adult-onset temporal lobe epilepsy. *Neurology*. 2007;69(12). doi:10.1212/01.wnl.0000276946.08412.ef

97. Vincent A, Bien CG. Anti-NMDA-receptor encephalitis: a cause of psychiatric, seizure, and movement disorders in young adults. *Lancet Neurol*. 2008;7(12). doi:10.1016/S1474-4422(08)70225-4

98. Dalmau J, Gleichman AJ, Hughes EG, et al. Anti-NMDA-receptor encephalitis: case series and analysis of the effects of antibodies. *Lancet Neurol*. 2008;7(12). doi:10.1016/S1474-4422(08)70224-2

99. Choi J, Nordli DR, Alden TD, et al. Cellular injury and neuroinflammation in children with chronic intractable epilepsy. *J Neuroinflammation*. 2009;6. doi:10.1186/1742-2094-6-38

100. Crespel A, Coubes P, Rousset MC, et al. Inflammatory reactions in human medial temporal lobe epilepsy with hippocampal sclerosis. *Brain Res*. 2002;952(2). doi:10.1016/S0006-8993(02)03050-0

101. Aronica E, Boer K, van Vliet EA, et al. Complement activation in experimental and human temporal lobe epilepsy. *Neurobiol Dis*. 2007;26(3). doi:10.1016/j.nbd.2007.01.015

102. Maldonado M, Baybis M, Newman D, et al. Expression of ICAM-1, TNF-α, NFκB, and MAP kinase in tubers of the tuberous sclerosis complex. *Neurobiol Dis*. 2003;14(2). doi:10.1016/S0969-9961(03)00127-X

103. Boer K, Crino PB, Gorter JA, et al. Gene expression analysis of tuberous sclerosis complex cortical tubers reveals increased expression of adhesion and inflammatory factors. *Brain Pathology*. 2010;20(4). doi:10.1111/j.1750-3639.2009.00341.x

104. Iyer AM, Zurolo E, Boer K, et al. Tissue plasminogen activator and urokinase plasminogen activator in human epileptogenic pathologies. *Neuroscience*. 2010;167(3). doi:10.1016/j.neuroscience.2010.02.047

105. Shao LR, Habela CW, Stafstrom CE. Pediatric epilepsy mechanisms: Expanding the paradigm of excitation/inhibition imbalance. *Children*. 2019;6(2). doi:10.3390/children6020023

106. Raimondo J V., Kay L, Ellender TJ, Akerman CJ. Optogenetic silencing strategies differ in their effects on inhibitory synaptic transmission. *Nat Neurosci*. 2012;15(8). doi:10.1038/nn.3143

107. Patel M. A metabolic paradigm for epilepsy. *Epilepsy Curr*. 2018;18(5). doi:10.5698/1535-7597.18.5.318

108. Vezzani A, Moneta D, Conti M, et al. Powerful anticonvulsant action of IL-1 receptor antagonist on intracerebral injection and astrocytic overexpression in mice. *Proc Natl Acad Sci U S A*. 2000;97(21). doi:10.1073/pnas.190206797

109. Minami M, Kuraishi Y, Satoh M. Effects of kainic acid on messenger RNA levels of IL-1β, IL-6, TNFα and LIF in the rat brain. *Biochem Biophys Res Commun*. 1991;176(2). doi:10.1016/S0006-291X(05)80225-6

110. Vezzani A, Conti M, De Luigi A, et al. Interleukin-1β immunoreactivity and microglia are enhanced in the rat hippocampus by focal kainate application: Functional evidence for enhancement of electrographic seizures. *Journal of Neuroscience*. 1999;19(12). doi:10.1523/jneurosci.19-12-05054.1999

111. De Simoni MG, Perego C, Ravizza T, et al. Inflammatory cytokines and related genes are induced in the rat hippocampus by limbic status epilepticus. *European Journal of Neuroscience*. 2000;12(7):2623-2633. doi:10.1046/j.1460-9568.2000.00140.x

112. Eriksson C, Tehranian R, Iverfeldt K, Winblad B, Schultzberg M. Increased expression of mRNA encoding interleukin-1β and caspase-1 and the secreted isoform of interleukin-1 receptor antagonist in the rat brain following systemic kainic acid

administration. *J Neurosci Res*. 2000;60(2). doi:10.1002/(SICI)1097-4547(20000415)60:2<266::AID-JNR16>3.0.CO;2-P

113. Voutsinos-Porche B, Koning E, Kaplan H, et al. Temporal patterns of the cerebral inflammatory response in the rat lithium-pilocarpine model of temporal lobe epilepsy. *Neurobiol Dis*. 2004;17(3). doi:10.1016/j.nbd.2004.07.023

114. Vezzani A, French J, Bartfai T, Baram TZ. The role of inflammation in epilepsy. *Nat Rev Neurol*. 2011;7(1):31-40. doi:10.1038/nrneurol.2010.178

115. Marchi N, Fan Q, Ghosh C, et al. Antagonism of peripheral inflammation reduces the severity of status epilepticus. *Neurobiol Dis*. 2009;33(2). doi:10.1016/j.nbd.2008.10.002

116. Ravizza T, Lucas SM, Balosso S, et al. Inactivation of caspase-1 in rodent brain: A novel anticonvulsive strategy. *Epilepsia*. 2006;47(7). doi:10.1111/j.1528-1167.2006.00590.x

117. Balosso S, Maroso ÃM, Sanchez-alavez ÃM, et al. A novel non-transcriptional pathway mediates the proconvulsive effects of interleukin-1. *Brain*. 2008;131(November):3256-3265. doi:10.1093/brain/awn271

118. Maroso M, Balosso S, Ravizza T, et al. Toll-like receptor 4 and high-mobility group box-1 are involved in ictogenesis and can be targeted to reduce seizures. *Nat Med*. 2010;16(4). doi:10.1038/nm.2127

119. Oliveira MS, Furian AF, Royes LFF, et al. Cyclooxygenase-2/PGE2 pathway facilitates pentylenetetrazol-induced seizures. *Epilepsy Res*. 2008;79(1). doi:10.1016/j.eplepsyres.2007.12.008

120. Huang X, Zhang H, Yang J, et al. Pharmacological inhibition of the mammalian target of rapamycin pathway suppresses acquired epilepsy. *Neurobiol Dis*. 2010;40(1). doi:10.1016/j.nbd.2010.05.024

121. Fabene PF, Mora GN, Martinello M, et al. A role for leukocyte-endothelial adhesion mechanisms in epilepsy. *Nat Med*. 2008;14(12). doi:10.1038/nm.1878

122. Jung KH, Chu K, Lee ST, et al. Cyclooxygenase-2 inhibitor, celecoxib, inhibits the altered hippocampal neurogenesis with attenuation of spontaneous recurrent seizures following pilocarpine-induced status epilepticus. *Neurobiol Dis*. 2006;23(2). doi:10.1016/j.nbd.2006.02.016

123. Galic MA, Riazi K, Heida JG, et al. Postnatal inflammation increases seizure susceptibility in adult rats. *Journal of Neuroscience*. 2008;28(27):6904-6913. doi:10.1523/JNEUROSCI.1901-08.2008

124. Ho YH, Lin Y Te, Wu CWJ, Chao YM, Chang AYW, Chan JYH. Peripheral inflammation increases seizure susceptibility via the induction of neuroinflammation and oxidative stress in the hippocampus. *J Biomed Sci*. 2015;22(1):1-14. doi:10.1186/s12929-015-0157-8

125. Librizzi L, Noè F, Vezzani A, De Curtis M, Ravizza T. Seizure-induced brain-borne inflammation sustains seizure recurrence and blood-brain barrier damage. *Ann Neurol*. 2012;72(1):82-90. doi:10.1002/ANA.23567

126. Wang A, Si Z, Li X, Lu L, Pan Y, Liu J. FK506 Attenuated Pilocarpine-Induced Epilepsy by Reducing Inflammation in Rats. *Front Neurol*. 2019;10. doi:10.3389/fneur.2019.00971

127. Lukasiuk K. Epileptogenesis. *Encyclopedia of the Neurological Sciences*. Published online January 1, 2014:196-199. doi:10.1016/B978-0-12-385157-4.00297-9

128. Vezzani A, French J, Bartfai T, Baram TZ. The role of inflammation in epilepsy. *Nat Rev Neurol*. 2011;7(1):31-40. doi:10.1038/nrneurol.2010.178

129. Shimada T, Takemiya T, Sugiura H, Yamagata K. Role of inflammatory mediators in the pathogenesis of epilepsy. *Mediators Inflamm*. 2014;2014. doi:10.1155/2014/901902

130. Librizzi L, Regondi MC, Pastori C, Frigerio S, Frassoni C, De Curtis M. Expression of adhesion factors induced by epileptiform activity in the endothelium of the isolated guinea pig brain in vitro. *Epilepsia*. 2007;48(4):743-751. doi:10.1111/J.1528-1167.2007.01047.X

131. Vila Verde D, de Curtis M, Librizzi L. Seizure-Induced Acute Glial Activation in the in vitro Isolated Guinea Pig Brain. *Front Neurol*. 2021;12. doi:10.3389/FNEUR.2021.607603

132. Shimada T, Takemiya T, Sugiura H, Yamagata K. Role of inflammatory mediators in the pathogenesis of epilepsy. *Mediators Inflamm*. 2014;2014. doi:10.1155/2014/901902

133. Zeng LH, Rensing NR, Wong M. The mammalian target of rapamycin signaling pathway mediates epileptogenesis in a model of temporal lobe epilepsy. *Journal of Neuroscience*. 2009;29(21). doi:10.1523/JNEUROSCI.0066-09.2009

134. Ravizza T, Noé F, Zardoni D, Vaghi V, Sifringer M, Vezzani A. Interleukin Converting Enzyme inhibition impairs kindling epileptogenesis in rats by blocking astrocytic IL-1β production. *Neurobiol Dis*. 2008;31(3). doi:10.1016/j.nbd.2008.05.007

135. Dubé C, Vezzani A, Behrens M, Bartfai T, Baram TZ. Interleukin-1β contributes to the generation of experimental febrile seizures. *Ann Neurol*. 2005;57(1). doi:10.1002/ana.20358

136. Dubé CM, Ravizza T, Hamamura M, et al. Epileptogenesis provoked by prolonged experimental febrile seizures: Mechanisms and biomarkers. *Journal of Neuroscience*. 2010;30(22). doi:10.1523/JNEUROSCI.0551-10.2010

137. Heida JG, Pittman QJ. Causal Links between Brain Cytokines and Experimental Febrile Convulsions in the Rat. *Epilepsia*. 2005;46(12):1906-1913. doi:10.1111/J.1528-1167.2005.00294.X

138. Sayyah M, Javad-Pour M, Ghazi-Khansari M. The bacterial endotoxin lipopolysaccharide enhances seizure susceptibility in mice: involvement of proinflammatory factors: nitric oxide and prostaglandins. *Neuroscience*. 2003;122(4):1073-1080. doi:10.1016/J.NEUROSCIENCE.2003.08.043

139. Galic MA, Riazi K, Henderson AK, Tsutsui S, Pittman QJ. Viral-like brain inflammation during development causes increased seizure susceptibility in adult rats. *Neurobiol Dis*. 2009;36(2). doi:10.1016/j.nbd.2009.07.025

140. Lipopolysaccharide - an overview | ScienceDirect Topics. Accessed September 16, 2022. https://www.sciencedirect.com/topics/neuroscience/lipopolysaccharide

141. Auvin S, Porta N, Nehlig A, Lecointe C, Vallée L, Bordet R. Inflammation in rat pups subjected to short hyperthermic seizures enhances brain long-term excitability. *Epilepsy Res*. 2009;86(2-3). doi:10.1016/j.eplepsyres.2009.05.010

142. Auvin S, Mazarati A, Shin D, Sankar R. Inflammation enhances epileptogenesis in the developing rat brain. *Neurobiol Dis*. 2010;40(1). doi:10.1016/j.nbd.2010.06.004

143. Kovács Z, Kékesi KA, Szilágyi N, et al. Facilitation of spike-wave discharge activity by lipopolysaccharides in Wistar Albino Glaxo/Rijswijk rats. *Neuroscience*. 2006;140(2). doi:10.1016/j.neuroscience.2006.02.023

144. Harré EM, Galic MA, Mouihate A, Noorbakhsh F, Pittman QJ. Neonatal inflammation produces selective behavioural deficits and alters N-methyl-D-aspartate receptor subunit mRNA in the adult rat brain (European Journal of Neuroscience (2007) 27, (644-653)). *European Journal of Neuroscience*. 2008;27(8):2210. doi:10.1111/j.1460-9568.2008.06185.x

145. Rodgers KM, Hutchinson MR, Northcutt A, Maier SF, Watkins LR, Barth DS. The cortical innate immune response increases local neuronal excitability leading to seizures. *A JOURNAL OF NEUROLOGY*. doi:10.1093/brain/awp177

146. Xiong ZQ, Qian W, Suzuki K, McNamara JO. Formation of complement membrane attack complex in mammalian cerebral cortex evokes seizures and neurodegeneration. *Journal of Neuroscience*. 2003;23(3). doi:10.1523/jneurosci.23-03-00955.2003

147. Rus H, Cudrici C, Niculescu F. The role of the complement system in innate immunity. *Immunol Res*. 2005;33(2). doi:10.1385/IR:33:2:103

148. Libbey JE, Kirkman NJ, Wilcox KS, White HS, Fujinami RS. Role for Complement in the Development of Seizures following Acute Viral Infection. *J Virol*. 2010;84(13). doi:10.1128/jvi.00422-10

149. Libbey JE, Kirkman NJ, Smith MCP, et al. Seizures following picornavirus infection. *Epilepsia*. 2008;49(6). doi:10.1111/j.1528-1167.2008.01535.x

150. Kirkman NJ, Libbey JE, Wilcox KS, White HS, Fujinami RS. Innate but not adaptive immune responses contribute to behavioral seizures following viral infection. *Epilepsia*. 2010;51(3). doi:10.1111/j.1528-1167.2009.02390.x

151. Gao F, Liu Z, Ren W, Jiang W. Acute lipopolysaccharide exposure facilitates epileptiform activity via enhanced excitatory synaptic transmission and neuronal excitability in vitro. *Neuropsychiatr Dis Treat*. 2014;10:1489-1495. doi:10.2147/NDT.S65695

152. Gullo F, Amadeo A, Donvito G, et al. Atypical “seizure-like” activity in cortical reverberating networks in vitro can be caused by LPS-induced inflammation: A multi-electrode array study from a hundred neurons. *Front Cell Neurosci*. 2014;8(November):1-18. doi:10.3389/fncel.2014.00361

153. Pascual O, Achour S Ben, Rostaing P, Triller A, Bessis A. Microglia activation triggers astrocyte-mediated modulation of excitatory neurotransmission. doi:10.1073/pnas.1111098109

154. Sayyah M, Beheshti S, Shokrgozar MA, et al. Antiepileptogenic and anticonvulsant activity of interleukin-1 beta in amygdala-kindled rats. *Exp Neurol*. 2005;191(1):145-153. doi:10.1016/J.EXPNEUROL.2004.08.032

155. Sayyah M, Najafabadi IT, Beheshti S, Majzoob S. Lipopolysaccharide retards development of amygdala kindling but does not affect fully-kindled seizures in rats. *Epilepsy Res*. 2003;57(2-3):175-180. doi:10.1016/J.EPLEPSYRES.2003.11.002

156. Ahmadi A, Sayyah M, Khoshkholgh-Sima B, et al. Intra-hippocampal injection of lipopolysaccharide inhibits kindled seizures and retards kindling rate in adult rats. *Exp Brain Res*. 2013;226(1):107-120. doi:10.1007/S00221-013-3415-6

157. Hellstrom IC, Danik M, Luheshi GN, Williams S. Chronic LPS exposure produces changes in intrinsic membrane properties and a sustained IL-β-dependent increase in GABAergic inhibition in hippocampal CA1 pyramidal neurons. *Hippocampus*. 2005;15(5):656-664. doi:10.1002/hipo.20086

158. Holtman L, van Vliet EA, van Schaik R, Queiroz CM, Aronica E, Gorter JA. Effects of SC58236, a selective COX-2 inhibitor, on epileptogenesis and spontaneous seizures in a rat model for temporal lobe epilepsy. *Epilepsy Res*. 2009;84(1):56-66. doi:10.1016/J.EPLEPSYRES.2008.12.006

159. Polascheck N, Bankstahl M, Löscher W. The COX-2 inhibitor parecoxib is neuroprotective but not antiepileptogenic in the pilocarpine model of temporal lobe epilepsy. *Exp Neurol*. 2010;224(1):219-233. doi:10.1016/J.EXPNEUROL.2010.03.014

160. Luk WP, Zhang Y, White TD, et al. Adenosine: a Mediator of Interleukin-1β-Induced Hippocampal Synaptic Inhibition. *The Journal of Neuroscience*. 1999;19(11):4238-4244. doi:10.1523/JNEUROSCI.19-11-04238.1999

161. Jo JH, Park EJ, Lee JK, Jung MW, Lee CJ. Lipopolysaccharide inhibits induction of long-term potentiation and depression in the rat hippocampal CA1 area. *Eur J Pharmacol*. 2001;422(1-3). doi:10.1016/S0014-2999(01)01075-5

162. Park KI, Dzhala V, Saponjian Y, Staley KJ. What Elements of the Inflammatory System Are Necessary for Epileptogenesis In Vitro? *eNeuro*. 2015;2(2):e0027-e0038. doi:10.1523/ENEURO.0027-14.2015

163. Hellstrom IC, Danik M, Luheshi GN, Williams S. Chronic LPS Exposure Produces Changes in Intrinsic Membrane Properties and a Sustained IL-b-Dependent Increase in GABAergic Inhibition in Hippocampal CA1 Pyramidal Neurons. doi:10.1002/hipo.20086

164. Balosso S, Ravizza T, Perego C, et al. Tumor necrosis factor-alpha inhibits seizures in mice via p75 receptors. *Ann Neurol*. 2005;57(6):804-812. doi:10.1002/ANA.20480

165. Chen W, Sheng J, Guo J, et al. Tumor necrosis factor-α enhances voltage-gated Na+ currents in primary culture of mouse cortical neurons. *J Neuroinflammation*. 2015;12(1). doi:10.1186/s12974-015-0349-x

166. Kim HJ, Chung JI, Lee SH, Jung YS, Moon CH, Baik EJ. Involvement of endogenous prostaglandin F2α on kainic acid-induced seizure activity through FP receptor: The mechanism of proconvulsant effects of COX-2 inhibitors. *Brain Res*. 2008;1193:153-161. doi:10.1016/J.BRAINRES.2007.12.017

167. Verastegui MR, Mejia A, Clark T, et al. Novel Rat Model for Neurocysticercosis Using Taenia solium. *Am J Pathol*. 2015;185(8):2259. doi:10.1016/J.AJPATH.2015.04.015

168. De Aluja AS, Villalobos ANM, Plancarte A, Rodarte LF, Hernández M, Sciutto E. Experimental Taenia solium cysticercosis in pigs: Characteristics of the infection and antibody response. *Vet Parasitol*. 1996;61(1-2). doi:10.1016/0304-4017(95)00817-9

169. Santamaría E, Plancarte A, De Aluja AS. The experimental infection of pigs with different numbers of Taenia solium eggs: Immune response and efficiency of establishment. *Journal of Parasitology*. 2002;88(1). doi:10.1645/0022-3395(2002)088[0069:TEIOPW]2.0.CO;2

170. Nguekam A, Zoli AP, Vondou L, et al. Kinetics of circulating antigens in pigs experimentally infected with Taenia solium eggs. *Vet Parasitol*. 2003;111(4):323-332. doi:10.1016/S0304-4017(02)00391-6

171. Lange A De, Mahanty S, Raimondo J V. Model systems for investigating disease processes in neurocysticercosis. *Parasitology*. 2018;146(5):553-562. doi:10.1017/S0031182018001932

172. Arora N, Tripathi S, Kumar P, Mondal P, Mishra A, Prasad A. Recent advancements and new perspectives in animal models for Neurocysticercosis immunopathogenesis. *Parasite Immunol*. 2017;39(7). doi:10.1111/pim.12439

173. Liu YJ, Li QZ, Hao YH. Oncospheres of Taenia solium develop into cysticerci in normal mice. *Journal of Veterinary Medicine, Series B*. 2002;49(8). doi:10.1046/j.1439-0450.2002.00569.x

174. Larralde C, Montoya RM, Sciutto E, Diaz ML, Govezensky T, Coltorti E. Deciphering western blots of tapeworm antigens (Taenia solium, Echinococcus granulosus, and Taenia crassiceps) reacting with sera from neurocysticercosis and hydatid disease patients. *American Journal of Tropical Medicine and Hygiene*. 1989;40(3). doi:10.4269/ajtmh.1989.40.282

175. Kunz J, Kalinna B, Watschke V, Geyer E. Taenia crassiceps metacestode vesicular fluid antigens shared with the Taenia solium larval stage and reactive with serum antibodies from patients with neurocysticercosis. *Zentralbl Bakteriol*. 1989;271(4):510-520. doi:10.1016/S0934-8840(89)80113-6

176. Arruda GC, Da Silva ADT, Quagliato EMAB, Maretti MA, Rossi CL. Evaluation of Taenia solium and Taenia crassiceps cysticercal antigens for the serodiagnosis of neurocysticercosis. *Tropical Medicine & International Health*. 2005;10(10):1005-1012. doi:10.1111/J.1365-3156.2005.01480.X

177. Sciutto E, Fragoso G, Trueba L, et al. Cysticercosis vaccine: cross protecting immunity with T. solium antigens against experimental murine T. crassiceps cysticercosis. *Parasite Immunol*. 1990;12(6):687-696. doi:10.1111/j.1365-3024.1990.tb00997.x

178. Díaz-Zaragoza M, Jiménez LL, Hernández M, et al. Protein expression profile of Taenia crassiceps cysticerci related to Th1- and Th2-type responses in the mouse cysticercosis model. *Acta Trop*. 2020;212:105696. doi:10.1016/J.ACTATROPICA.2020.105696

179. Landa A, Navarro L, Ochoa-Sánchez A, Jiménez L. Taenia solium and Taenia crassiceps: miRNomes of the larvae and effects of miR-10-5p and let-7-5p on murine peritoneal macrophages. *Biosci Rep*. 2019;39(11). doi:10.1042/BSR20190152

180. Willms K, Zurabian R. Taenia crassiceps: in vivo and in vitro models. *Parasitology*. 2010;137(3):335-346. doi:10.1017/S0031182009991442

181. Willms K, Zurabian R. Taenia crassiceps: in vivo and in vitro models. *Parasitology*. 2010;137(3):335-346. doi:10.1017/S0031182009991442

182. Wünschmann A, Garlie V, Averbeck G, Kurtz H, Hoberg EP. Cerebral cysticercosis by Taenia crassiceps in a domestic cat. *Journal of Veterinary Diagnostic Investigation*. 2003;15(5):484-488. doi:10.1177/104063870301500517

183. Lightowlers MW. Fact or hypothesis: Taenia crassiceps as a model for Taenia solium, and the S3Pvac vaccine. *Parasite Immunol*. 2010;32(11-12):701. doi:10.1111/J.1365-3024.2010.01231.X

184. Lescano AG, Zunt J. Other cestodes: sparganosis, coenurosis and Taenia crassiceps cysticercosis. *Handb Clin Neurol*. 2013;114:335-345. doi:10.1016/B978-0-444-53490-3.00027-3

185. Lightowlers MW. Fact or hypothesis: Taenia crassiceps as a model for Taenia solium, and the S3Pvac vaccine. *Parasite Immunol*. 2010;32(11-12):701. doi:10.1111/J.1365-3024.2010.01231.X

186. Zurabian R, Aguilar L, Jiménez J a, Robert L, Willms K. Evagination and infectivity of Taenia crassiceps cysticerci in experimental animals. *J Parasitol*. 2008;94(1):1-6. doi:10.1645/GE-1239.1

187. Matos-Silva H, Reciputti BP, Paula ÉC de, et al. Experimental encephalitis caused by Taenia crassiceps cysticerci in mice. *Arq Neuropsiquiatr*. 2012;70(4):287-292. doi:10.1590/s0004-282x2012005000010

188. Alvarez JI, Mishra BB, Gundra UM, Mishra PK, Teale JM. Mesocestoides corti intracranial infection as a murine model for neurocysticercosis. *Parasitology*. 2010;137(3):359-372. doi:10.1017/S0031182009991971

189. Cardona A. E., Restrepo B. I. TJM. Development of an Animal Model for Neurocysticercosis: Immune Response in the Central Nervous System Is Characterized by a Predominance of γδ T Cells. *J Immunol*. 1999;162(2):995-1002. doi:10.4049/jimmunol.162.2.995

190. Prodjinotho UF, Lema J, Lacorcia M, et al. Host immune responses during Taenia solium Neurocysticercosis infection and treatment. *PLoS Negl Trop Dis*. 2020;14(4):1-16. doi:10.1371/JOURNAL.PNTD.0008005

191. Segev A, Garcia-Oscos F, Kourrich S. Whole-cell patch-clamp recordings in brain slices. *Journal of Visualized Experiments*. 2016;2016(112). doi:10.3791/54024

192. Wang Y, Liu YZ, Wang SY, Wang Z. In vivo whole-cell recording with high success rate in anaesthetized and awake mammalian brains. *Mol Brain*. 2016;9(1):1-14. doi:10.1186/S13041-016-0266-7/FIGURES/9

193. Arora T, Mehta A, Joshi V, et al. Substitute of Animals in Drug Research: An Approach Towards Fulfillment of 4R's. *Indian J Pharm Sci*. 2011;73(1):1. doi:10.4103/0250-474X.89750

194. The National Centre for the Replacement R& R of AR. The 3Rs.

195. Humpel C. Organotypic brain slice cultures: A review. *Neuroscience*. 2015;305:86-98. doi:10.1016/J.NEUROSCIENCE.2015.07.086

196. de Lange A, Prodjinotho UF, Tomes H, et al. Taenia larvae possess distinct acetylcholinesterase profiles with implications for host cholinergic signalling. *PLoS Negl Trop Dis*. 2020;14(12). doi:10.1371/journal.pntd.0008966

197. Stoppini L, Buchs PA, Muller D. A simple method for organotypic cultures of nervous tissue. *J Neurosci Methods*. 1991;37(2):173-182. doi:10.1016/0165-0270(91)90128-M

198. Opitz-Araya X, Barria A. Organotypic Hippocampal Slice Cultures. *J Vis Exp*. 2011;48(48). doi:10.3791/2462

199. De Simoni A, Yu LMY. Preparation of organotypic hippocampal slice cultures: interface method. *Nature Protocols 2006 1:3*. 2006;1(3):1439-1445. doi:10.1038/nprot.2006.228

200. Fuller L, Dailey ME. Preparation of Rodent Hippocampal Slice Cultures. *Cold Spring Harb Protoc*. 2007;2007(10):pdb.prot4848. doi:10.1101/PDB.PROT4848

201. Opitz-Araya X, Barria A. Organotypic Hippocampal Slice Cultures. *J Vis Exp*. 2011;48(48). doi:10.3791/2462

202. Grindberg R V., Yee-Greenbaum JL, McConnell MJ, et al. RNA-sequencing from single nuclei. *Proc Natl Acad Sci U S A*. 2013;110(49). doi:10.1073/pnas.1319700110

203. Whitley SK, Horne WT, Kolls JK. Research Techniques Made Simple: Methodology and Clinical Applications of RNA Sequencing. *Journal of Investigative Dermatology*. 2016;136(8). doi:10.1016/j.jid.2016.06.003

204. Chen G, Ning B, Shi T. Single-cell RNA-seq technologies and related computational data analysis. *Front Genet*. 2019;10(APR). doi:10.3389/fgene.2019.00317

205. Armand EJ, Li J, Xie F, Luo C, Mukamel EA. Single-Cell Sequencing of Brain Cell Transcriptomes and Epigenomes. *Neuron*. 2021;109(1). doi:10.1016/j.neuron.2020.12.010

206. Wang X, He Y, Zhang Q, Ren X, Zhang Z. Direct Comparative Analyses of 10X Genomics Chromium and Smart-seq2. *Genomics Proteomics Bioinformatics*. 2021;19(2). doi:10.1016/j.gpb.2020.02.005

207. Yi JJ, Ehlers MD. Ubiquitin and protein turnover in synapse function. *Neuron*. 2005;47(5). doi:10.1016/j.neuron.2005.07.008

208. Brockmann MM, Döngi M, Einsfelder U, Körber N, Refojo D, Stein V. Neddylation regulates excitatory synaptic transmission and plasticity. *Sci Rep*. 2019;9(1). doi:10.1038/s41598-019-54182-2

209. Kim KR, Jeong HJ, Kim Y, et al. Calbindin regulates Kv4.1 trafficking and excitability in dentate granule cells via CaMKII-dependent phosphorylation. *Exp Mol Med*. 2021;53(7). doi:10.1038/s12276-021-00645-4

210. Jiang J, Tang B, Wang L, et al. Systemic LPS-induced microglial activation results in increased GABAergic tone: A mechanism of protection against neuroinflammation in the medial prefrontal cortex in mice. *Brain Behav Immun*. 2022;99. doi:10.1016/j.bbi.2021.09.017

211. Harris RA, McCarthy GM, Bridges CR, Blednov YA. CNS cell-type localization and LPS response of TLR signaling pathways. *F1000Res*. 2017;6. doi:10.12688/f1000research.12036.1

212. Baxter PS, Dando O, Emelianova K, et al. Microglial identity and inflammatory responses are controlled by the combined effects of neurons and astrocytes. *Cell Rep*. 2021;34(12). doi:10.1016/j.celrep.2021.108882

213. Segev A, Garcia-Oscos F, Kourrich S. Whole-cell Patch-clamp Recordings in Brain Slices. *J Vis Exp*. 2016;2016(112). doi:10.3791/54024

214. de Lange A, Walters A, Hsu NJ, Jacobs M, Raimondo JV. Enzyme linked immunosorbent assays (ELISAs) for mouse IL-10, IL-6, IL-1β and TNF-α. *protocols.io*. Published online August 6, 2020.

215. 10x Genomics. *Chromium Single Cell V(D)J Reagent Kits with Feature Barcoding Technology for Cell Surface Protein, Document Number CG000186 Rev A*.; 2019.

216. Illumina Inc. 9885 Towne Centre Drive, San Diego, CA 92121, USA.

217. 10x Genomics Cell Ranger 7.1.0.

218. Hao Y, Hao S, Andersen-Nissen E, et al. Integrated analysis of multimodal single-cell data. *Cell*. 2021;184(13). doi:10.1016/j.cell.2021.04.048

219. R Core Team. R: A language and environment for statistical computing. . Published online 2022.

220. Amezquita RA, Lun ATL, Becht E, et al. Orchestrating single-cell analysis with Bioconductor. *Nat Methods*. 2020;17(2). doi:10.1038/s41592-019-0654-x

221. McGinnis CS, Murrow LM, Gartner ZJ. DoubletFinder: Doublet Detection in Single-Cell RNA Sequencing Data Using Artificial Nearest Neighbors. *Cell Syst*. 2019;8(4). doi:10.1016/j.cels.2019.03.003

222. Wolock SL, Lopez R, Klein AM. Scrublet: Computational Identification of Cell Doublets in Single-Cell Transcriptomic Data. *Cell Syst*. 2019;8(4). doi:10.1016/j.cels.2018.11.005

223. DePasquale EAK, Schnell DJ, Van Camp PJ, et al. DoubletDecon: Deconvoluting Doublets from Single-Cell RNA-Sequencing Data. *Cell Rep*. 2019;29(6). doi:10.1016/j.celrep.2019.09.082

224. Xi NM, Li JJ. Benchmarking Computational Doublet-Detection Methods for Single-Cell RNA Sequencing Data. *Cell Syst*. 2021;12(2). doi:10.1016/j.cels.2020.11.008

225. Cao Y, Wang X, Peng G. SCSA: A cell type annotation tool for single-cell RNA-seq data. *Front Genet*. 2020;11. doi:10.3389/fgene.2020.00490

226. Zhang X, Lan Y, Xu J, et al. CellMarker: A manually curated resource of cell markers in human and mouse. *Nucleic Acids Res*. 2019;47(D1). doi:10.1093/nar/gky900

227. Yuan H, Yan M, Zhang G, et al. CancerSEA: A cancer single-cell state atlas. *Nucleic Acids Res*. 2019;47(D1). doi:10.1093/nar/gky939

228. Zeisel A, Hochgerner H, Lönnerberg P, et al. Molecular Architecture of the Mouse Nervous System. *Cell*. 2018;174(4). doi:10.1016/j.cell.2018.06.021

229. Allen Cell Types Database -- Mouse Whole Cortex and Hippocampus - 10x Genomics [dataset]. Published online 2020.

230. Love MI, Huber W, Anders S. Moderated estimation of fold change and dispersion for RNA-seq data with DESeq2. *Genome Biol*. 2014;15(12). doi:10.1186/s13059-014-0550-8

231. Stephens M. False discovery rates: A new deal. *Biostatistics*. 2017;18(2). doi:10.1093/biostatistics/kxw041

232. Chen EY, Tan CM, Kou Y, et al. Enrichr: Interactive and collaborative HTML5 gene list enrichment analysis tool. *BMC Bioinformatics*. 2013;14. doi:10.1186/1471-2105-14-128

233. Xie Z, Bailey A, Kuleshov M V., et al. Gene Set Knowledge Discovery with Enrichr. *Curr Protoc*. 2021;1(3). doi:10.1002/cpz1.90

234. Molecular Instruments. HCR™ RNA-FISH protocol for sample on slide. Published online February 13, 2023:1-7.

235. Nicovich PR, Taormina MJ, Baker CA, et al. Multimodal cell type correspondence by intersectional mFISH in intact tissues. *bioRxiv*. Published online 2019.

236. University of Strathclyde. WinWCP Strathclyde Electrophysiology Software.

237. MATLAB, 2020. 9.9.0.1524771 (R2020b), Natick, Massachusetts: The MathWorks Inc. Published online 2020.

238. GraphPad Prism version 8.0.1. San Diego, California USA. Published online 2018.

239. Sousa C, Golebiewska A, Poovathingal SK, et al. Single-cell transcriptomics reveals distinct inflammation-induced microglia signatures. *EMBO Rep*. 2018;19(11). doi:10.15252/embr.201846171

240. Zöller T, Schneider A, Kleimeyer C, et al. Silencing of TGFβ signalling in microglia results in impaired homeostasis. *Nat Commun*. 2018;9(1). doi:10.1038/s41467-018-06224-y

241. Rainer J, Gatto L, Weichenberger CX. Ensembldb: An R package to create and use Ensembl-based annotation resources. *Bioinformatics*. 2019;35(17). doi:10.1093/bioinformatics/btz031

242. American Epilepsy Society. Basic Mechanisms Underlying Seizures and Epilepsy. In: Bromfield E, Cavazos J, Sirven. JI, editors, eds. *An Introduction to Epilepsy [Internet]*. ; 2006.

243. Wang J, Ou SW, Wang YJ. Distribution and function of voltage-gated sodium channels in the nervous system. *Channels*. 2017;11(6). doi:10.1080/19336950.2017.1380758

244. Vezzani A. Brain Inflammation and Seizures: Evolving Concepts and New Findings in the Last 2 Decades. *Epilepsy Curr*. 2020;20(6_suppl):40S-43S. doi:10.1177/1535759720948900

245. Batista CRA, Gomes GF, Candelario-Jalil E, Fiebich BL, de Oliveira ACP. Lipopolysaccharide-induced neuroinflammation as a bridge to understand neurodegeneration. *Int J Mol Sci*. 2019;20(9). doi:10.3390/ijms20092293

246. Skrzypczak-Wiercioch A, Sałat K. Lipopolysaccharide-Induced Model of Neuroinflammation: Mechanisms of Action, Research Application and Future Directions for Its Use. *Molecules*. 2022;27(17). doi:0.3390/molecules27175481

247. Sheppard O, Coleman MP, Durrant CS. Lipopolysaccharide-induced neuroinflammation induces presynaptic disruption through a direct action on brain tissue involving microglia-derived interleukin 1 beta. *J Neuroinflammation*. 2019;16(1). doi:10.1186/s12974-019-1490-8

248. Bonow RH, Aïd S, Zhang Y, Becker KG, Bosetti F. The brain expression of genes involved in inflammatory response, the ribosome, and learning and memory is altered by centrally injected lipopolysaccharide in mice. *Pharmacogenomics Journal*. 2009;9(2). doi:10.1038/tpj.2008.15

249. Pulido-Salgado M, Vidal-Taboada JM, Barriga GGD, Solà C, Saura J. RNA-Seq transcriptomic profiling of primary murine microglia treated with LPS or LPS + IFNγ. *Scientific Reports 2018 8:1*. 2018;8(1):1-21. doi:10.1038/s41598-018-34412-9

250. Srinivasan K, Friedman BA, Larson JL, et al. Untangling the brain's neuroinflammatory and neurodegenerative transcriptional responses. *Nat Commun*. 2016;7. doi:10.1038/NCOMMS11295

251. Block ML, Zecca L, Hong JS. Microglia-mediated neurotoxicity: Uncovering the molecular mechanisms. *Nat Rev Neurosci*. 2007;8(1). doi:10.1038/nrn2038

252. Diaz-Castro B, Bernstein AM, Coppola G, Sofroniew M V., Khakh BS. Molecular and functional properties of cortical astrocytes during peripherally induced neuroinflammation. *Cell Rep*. 2021;36(6). doi:10.1016/j.celrep.2021.109508

253. Hasel P, L Rose I V, Sadick JS, Kim RD, Liddelow SA. Neuroinflammatory astrocyte subtypes in the mouse brain. *Nat Neurosci*. doi:10.1038/s41593-021-00905-6

254. Das A, Kim SH, Arifuzzaman S, et al. Transcriptome sequencing reveals that LPS-triggered transcriptional responses in established microglia BV2 cell lines are poorly representative of primary microglia. *J Neuroinflammation*. 2016;13(1). doi:10.1186/s12974-016-0644-1

255. Coleman LG, Zou J, Crews FT. Microglial depletion and repopulation in brain slice culture normalizes sensitized proinflammatory signaling. *J Neuroinflammation*. 2020;17(1). doi:10.1186/s12974-019-1678-y

256. Bennett ML, Bennett FC, Liddelow SA, et al. New tools for studying microglia in the mouse and human CNS. *Proc Natl Acad Sci U S A*. 2016;113(12). doi:10.1073/pnas.1525528113

257. Delbridge ARD, Huh D, Brickelmaier M, et al. Organotypic Brain Slice Culture Microglia Exhibit Molecular Similarity to Acutely-Isolated Adult Microglia and Provide a Platform to Study Neuroinflammation. *Front Cell Neurosci*. 2020;14:444. doi:10.3389/FNCEL.2020.592005/BIBTEX

258. Ilanges A, Shiao R, Shaked J, Luo J, Yu X, Friedman J. Brainstem ADCYAP1+ neurons control multiple aspects of sickness behaviour. *Nature*. 2022;609(7928):761-771.

259. Swartzlander DB, Propson NE, Roy ER, et al. Concurrent cell type-specific isolation and profiling of mouse brains in inflammation and Alzheimer's disease. *JCI Insight*. 2018;3(13). doi:10.1172/jci.insight.121109

260. Osterhout JA, Kapoor V, Eichhorn SW, et al. A preoptic neuronal population controls fever and appetite during sickness. *Nature*. 2022;606:937-944. doi:10.1038/s41586-022-04793-z

261. Liddelow SA, Guttenplan KA, Clarke LE, et al. Neurotoxic reactive astrocytes are induced by activated microglia. *Nature*. 2017;541(7638):481-487. doi:10.1038/nature21029

262. Baxter PS, Dando O, Emelianova K, et al. Microglial identity and inflammatory responses are controlled by the combined effects of neurons and astrocytes. *Cell Rep*. 2021;34(12). doi:10.1016/j.celrep.2021.108882

263. Leow-Dyke S, Allen C, Denes A, et al. Neuronal toll-like receptor 4 signaling induces brain endothelial activation and neutrophil transmigration in vitro. *J Neuroinflammation*. 2012;9. doi:10.1186/1742-2094-9-230

264. Sárvári M, Kalló I, Hrabovszky E, et al. Estradiol replacement alters expression of genes related to neurotransmission and immune surveillance in the frontal cortex of middle-aged, ovariectomized rats. *Endocrinology*. 2010;151(8). doi:10.1210/en.2010-0375

265. Kelemen K, Szilágyi T. New approach for untangling the role of uncommon calcium-binding proteins in the central nervous system. *Brain Sci*. 2021;11(5). doi:10.3390/brainsci11050634

266. Hermann A, Donato R, Weiger TM, Chazin WJ. S100 calcium binding proteins and ion channels. *Front Pharmacol*. 2012;3 APR. doi:10.3389/fphar.2012.00067

267. Kim HJ, Jeong MS, Jang SB. Molecular characteristics of rage and advances in small-molecule inhibitors. *Int J Mol Sci*. 2021;22(13). doi:10.3390/ijms22136904

268. Singh P, Ali SA. Multifunctional Role of S100 Protein Family in the Immune System: An Update. *Cells*. 2022;11(15):2274. doi:10.3390/cells11152274

269. Filipek A, Leśniak W. S100A6 and its brain ligands in neurodegenerative disorders. *Int J Mol Sci*. 2020;21(11). doi:10.3390/ijms21113979

270. Xia Q, Li X, Zhou H, Zheng L, Shi J. S100A11 protects against neuronal cell apoptosis induced by cerebral ischemia via inhibiting the nuclear translocation of annexin A1 article. *Cell Death Dis*. 2018;9(6). doi:10.1038/s41419-018-0686-7

271. Matsunaga H, Ueda H. Stress-induced non-vesicular release of prothymosin-α initiated by an interaction with S100A13, and its blockade by caspase-3 cleavage. *Cell Death Differ*. 2010;17(11). doi:10.1038/cdd.2010.52

272. Qian J, Colmers WF, Saggau P. Inhibition of synaptic transmission by neuropeptide Y in rat hippocampal area CA1: Modulation of presynaptic Ca2+ entry. *Journal of Neuroscience*. 1997;17(21). doi:10.1523/jneurosci.17-21-08169.1997

273. Corvino V, Marchese E, Giannetti S, et al. The neuroprotective and neurogenic effects of neuropeptide y administration in an animal model of hippocampal neurodegeneration and temporal lobe epilepsy induced by trimethyltin. *J Neurochem*. 2012;122(2). doi:10.1111/j.1471-4159.2012.07770.x

274. Comenencia-Ortiz E, Moss SJ, Davies PA. Phosphorylation of GABAA receptors influences receptor trafficking and neurosteroid actions. *Psychopharmacology (Berl)*. 2014;231(17):3453-3465. doi:10.1007/s00213-014-3617-z

275. Zhang X, Tsuboi D, Funahashi Y, Yamahashi Y, Kaibuchi K, Nagai T. Phosphorylation Signals Downstream of Dopamine Receptors in Emotional Behaviors: Association with Preference and Avoidance. *Int J Mol Sci*. 2022;23(19):11643. doi:10.3390/ijms231911643

276. Wang JQ, Guo ML, Jin DZ, Xue B, Fibuch EE, Mao LM. Roles of subunit phosphorylation in regulating glutamate receptor function. *Eur J Pharmacol*. 2014;728:183-187. doi:10.1016/j.ejphar.2013.11.019

277. Ikematsu N, Dallas ML, Ross FA, et al. Phosphorylation of the voltage-gated potassium channel Kv2.1 by AMP-activated protein kinase regulates membrane excitability. *Proc Natl Acad Sci U S A*. 2011;108(44). doi:10.1073/pnas.1106201108

278. Ha SR, Rasband MN. The SIZ of Pain. *Neuron*. 2019;102(4). doi:10.1016/j.neuron.2019.04.040

279. Papageorgiou IE, Lewen A, Galow L V., et al. TLR4-activated microglia require IFN- γ to induce severe neuronal dysfunction and death in situ. *Proceedings of the National Academy of Sciences*. 2016;113(1):212-217. doi:10.1073/pnas.1513853113

280. Klawonn AM, Fritz M, Castany S, et al. Microglial activation elicits a negative affective state through prostaglandin-mediated modulation of striatal neurons. *Immunity*. 2021;54(2):225-234.e6. doi:10.1016/j.immuni.2020.12.016

281. Klawonn AM, Fritz M, Castany S, et al. Microglial activation elicits a negative affective state through prostaglandin-mediated modulation of striatal neurons. *Immunity*. 2021;54(2):225-234.e6. doi:10.1016/j.immuni.2020.12.016

282. de Andrade Picanço G, de Lima NF, Fraga CM, et al. A benzimidazole derivative (RCB15) in vitro induces the alternative energetic metabolism and glycolysis in Taenia crassiceps cysticerci. *Acta Trop*. 2017;176. doi:10.1016/j.actatropica.2017.08.022

283. Vinaud MC, Ferreira CS, Lino Junior R de S, Bezerra JCB. Taenia crassiceps: Fatty acids oxidation and alternative energy source in in vitro cysticerci exposed to anthelminthic drugs. *Exp Parasitol*. 2009;122(3). doi:10.1016/j.exppara.2009.03.015

284. Fraga CM, Costa TL, Bezerra JCB, De Souza Lino R, Vinaud MC. Taenia crassiceps: Host treatment alters glycolisis and tricarboxilic acid cycle in cysticerci. *Exp Parasitol*. 2012;130(2). doi:10.1016/j.exppara.2011.11.001

285. Picanço GDA, De Lima NF, Gomes TC, et al. Partial inhibition of the main energetic pathways and its metabolic consequences after in vivo treatment with benzimidazole derivatives in experimental neurocysticercosis. *Parasitology*. 2019;146(12). doi:10.1017/S0031182019000933

286. Flores-Bautista J, Navarrete-Perea J, Fragoso G, Flisser A, Soberón X, Laclette JP. Fate of uptaken host proteins in Taenia solium and Taenia crassiceps cysticerci. *Biosci Rep*. 2018;38(4):1-10. doi:10.1042/BSR20180636

287. Burmeister AR, Johnson MB, Chauhan VS, et al. Human microglia and astrocytes constitutively express the neurokinin-1 receptor and functionally respond to substance P. *J Neuroinflammation*. 2017;14(1). doi:10.1186/s12974-017-1012-5

288. Chen S, Lu M, Liu D, et al. Human substance P receptor binding mode of the antagonist drug aprepitant by NMR and crystallography. *Nat Commun*. 2019;10(1). doi:10.1038/s41467-019-08568-5

289. Peón AN, Ledesma-Soto Y, Terrazas LI. Regulation of immunity by Taeniids: Lessons from animal models and in vitro studies. *Parasite Immunol*. 2016;38(3):124-135. doi:10.1111/pim.12289

290. Restrepo BI, Alvarez JI, Castaño JA, et al. Brain granulomas in neurocysticercosis patients are associated with a Th1 and Th2 profile. *Infect Immun*. 2001;69(7):4554-4560. doi:10.1128/IAI.69.7.4554-4560.2001/ASSET/1BF55DEC-BCAB-43A8-BA36-502039D816AB/ASSETS/GRAPHIC/II0710143001.JPEG

291. Peón AN, Espinoza-Jiménez A, Terrazas LI. Immunoregulation by taenia crassiceps and its antigens. *Biomed Res Int*. 2013;2013. doi:10.1155/2013/498583

292. Bhattacharjee A, Shukla M, Yakubenko VP, Mulya A, Kundu S, Cathcart MK. IL-4 and IL-13 employ discrete signaling pathways for target gene expression in alternatively activated monocytes/macrophages. *Free Radic Biol Med*. 2013;54. doi:10.1016/j.freeradbiomed.2012.10.553

293. Watts C. Location, location, location: Identifying the neighborhoods of LPS signaling. *Nat Immunol*. 2008;9(4). doi:10.1038/ni0408-343

294. Lu YC, Yeh WC, Ohashi PS. LPS/TLR4 signal transduction pathway. *Cytokine*. 2008;42(2). doi:10.1016/j.cyto.2008.01.006

295. Sayyah M, Beheshti S, Shokrgozar MA, et al. Antiepileptogenic and anticonvulsant activity of interleukin-1β in amygdala-kindled rats. *Exp Neurol*. 2005;191(1). doi:10.1016/j.expneurol.2004.08.032

296. Rana A, Musto A. The role of inflammation in the development of epilepsy. *J Neuroinflammation*. 2018;15(144):1-12. doi:10.1186/s12974-018-1192-7

297. Yamanaka G, Morichi S, Takamatsu T, et al. Links between immune cells from the periphery and the brain in the pathogenesis of epilepsy: A narrative review. *Int J Mol Sci*. 2021;22(9). doi:10.3390/ijms22094395

298. Chatzikonstantinou A. Epilepsy and the Hippocampus. In: ; 2014:121-142. doi:10.1159/000356435

299. Gomez CD, Read J, Acharjee S, Pittman QJ. Early life inflammation increases CA1 pyramidal neuron excitability in a sex and age dependent manner through a chloride homeostasis disruption. *Journal of Neuroscience*. 2019;39(37). doi:10.1523/JNEUROSCI.2973-18.2019

300. Chen L, Deng H, Cui H, et al. Inflammatory responses and inflammation-associated diseases in organs. *Oncotarget*. 2018;9(6). doi:10.18632/oncotarget.23208

301. SCIUTTO E, FRAGOSO G, TRUEBA L, et al. Cysticercosis vaccine: cross protecting immunity with T. solium antigens against experimental murine T. crassiceps cysticercosis. *Parasite Immunol*. 1990;12(6). doi:10.1111/j.1365-3024.1990.tb00997.x

302. Heck AM, Wilusz J. The interplay between the RNA decay and translation machinery in eukaryotes. *Cold Spring Harb Perspect Biol*. 2018;10(5). doi:10.1101/cshperspect.a032839

303. Zaghlool A, Niazi A, Björklund ÅK, Westholm JO, Ameur A, Feuk L. Characterization of the nuclear and cytosolic transcriptomes in human brain tissue reveals new insights

into the subcellular distribution of RNA transcripts. *Sci Rep*. 2021;11(1). doi:10.1038/s41598-021-83541-1

304. Babenko VN, Shishkina GT, Lanshakov DA, Sukhareva E V., Dygalo NN. LPS Administration Impacts Glial Immune Programs by Alternative Splicing. *Biomolecules*. 2022;12(2). doi:10.3390/biom12020277

305. Tweedie-Cullen RY, Reck JM, Mansuy IM. Comprehensive mapping of post-translational modifications on synaptic, nuclear, and histone proteins in the adult mouse brain. *J Proteome Res*. 2009;8(11). doi:10.1021/pr9003739